Nanopattern-stimulated superconductor-insulator transition in thin TiN films

Tatyana I. Baturina
Aleksey Yu. Mironov
Dmitrii A. Nasimov
Alexander V. Latyshev

Institute of Semiconductor Physics, Novosibirsk, Russia

Christoph Strunk
Ante Bilušić
David Kalok

University of Regensburg, Germany

Nikolay M. Chtchelkatchev

L.D. Landau Institute for Theoretical Physics, Chernogolovka, Russia

Valerii M. Vinokur

Argonne National Laboratory, USA

Mikhail R. Baklanov
Alessandra Satta

IMEC, Belgium

Benjamin Sacépé
Claude Chapelier
Marc Sanquer

CEA Grenoble, France

MTI Workshop
Superconductor-Insulator Transition

16 November, 2010

Superconductor – Insulator transition

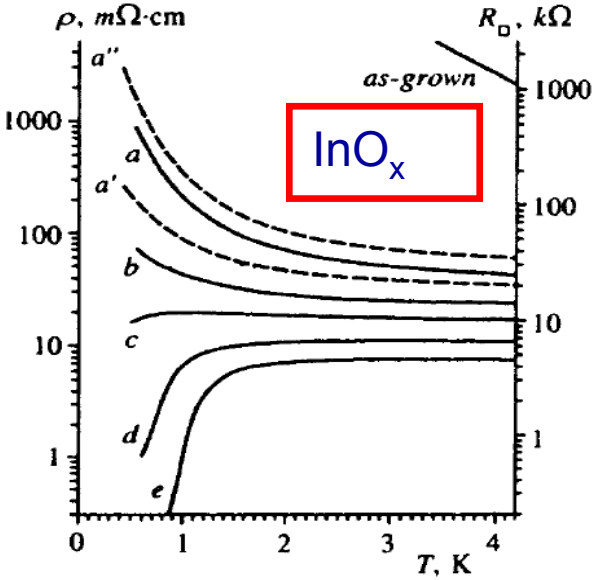

V.F. Gantmakher, M.V. Golubkov, J.G.S. Lok, and A.K. Geim, JETP 82, 951 (1996).

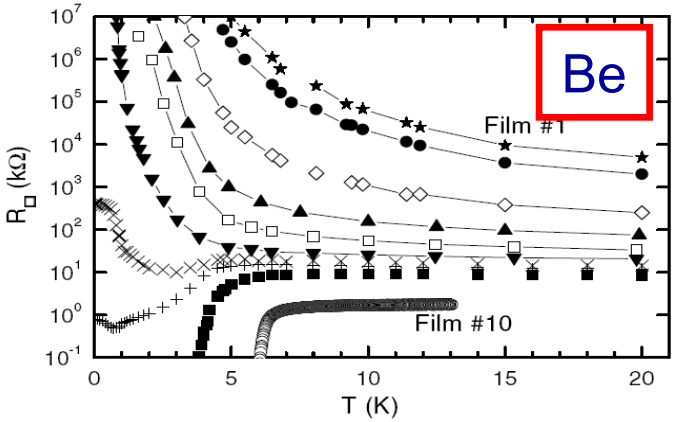

E. Bielejec, J. Ruan, and W. Wu PRL 87, 36801 (2001).

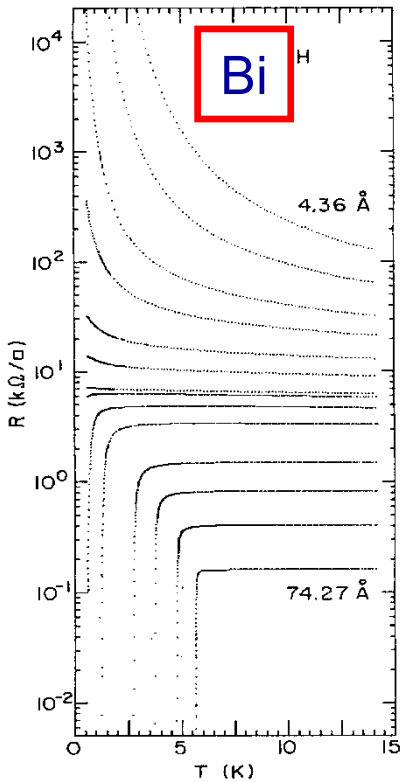

D.B. Haviland, Y. Liu, and A.M. Goldman (1989)

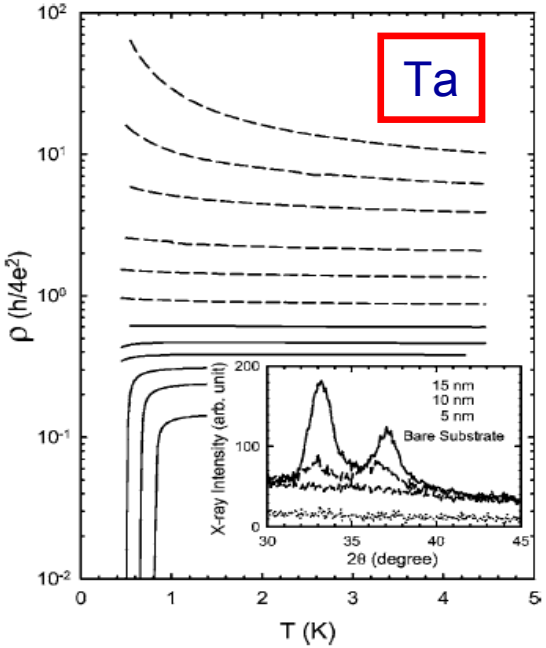

Y. Qin, C.L. Vicente, J. Yoon, PRB 73, 100505(R) (2006).

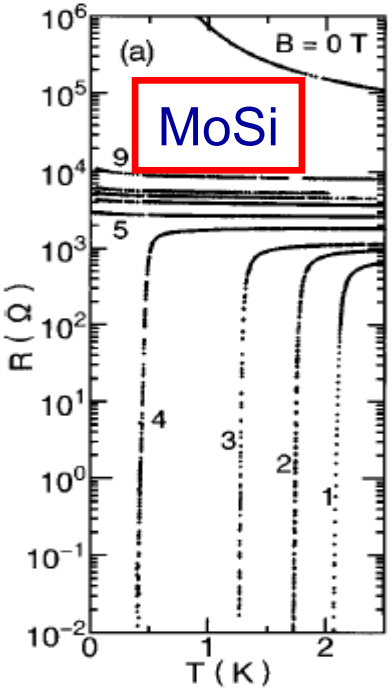

S. Okuma, T. Terashima, and N. Kokubo, PRB 58, 2816 (1998).

the effect of the restricted geometry

+

periodicity

T. I. Baturina, V.M. Vinokur, A.Yu. Mironov, N.M. Chtchelkatchev, D.A. Nasimov, A.V. Latyshev, preprint arXiv:1011.1592

Experiment

TiN films

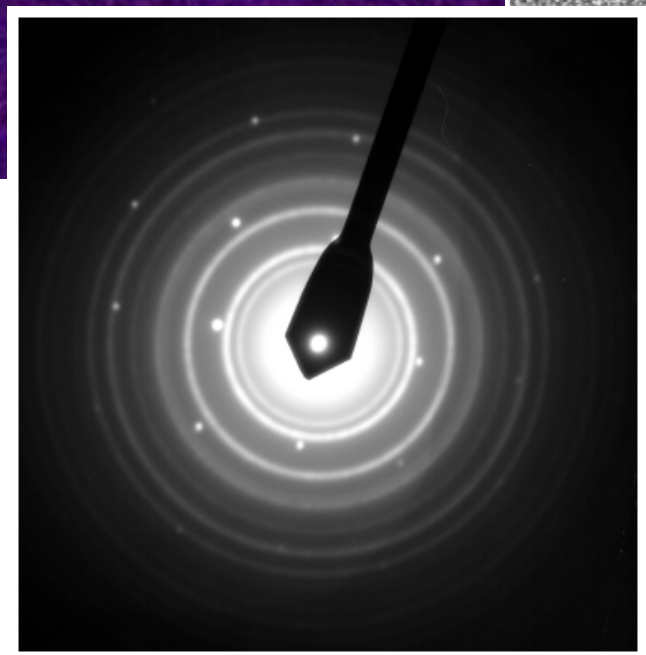

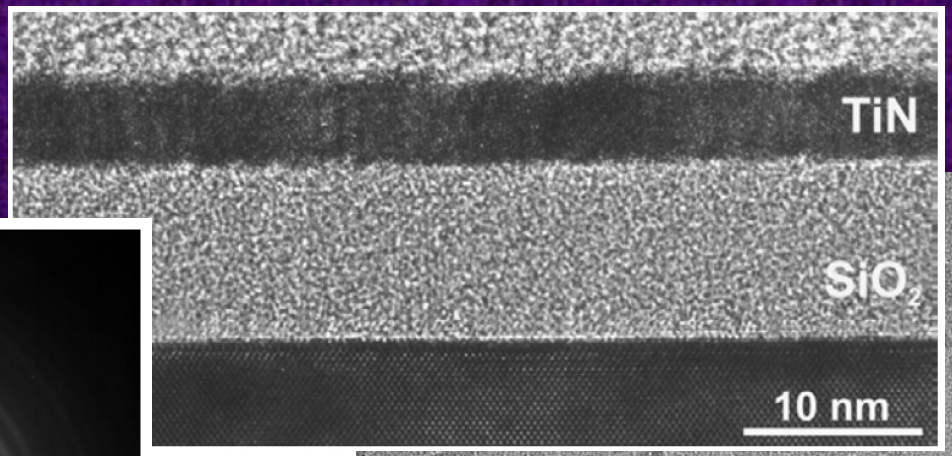

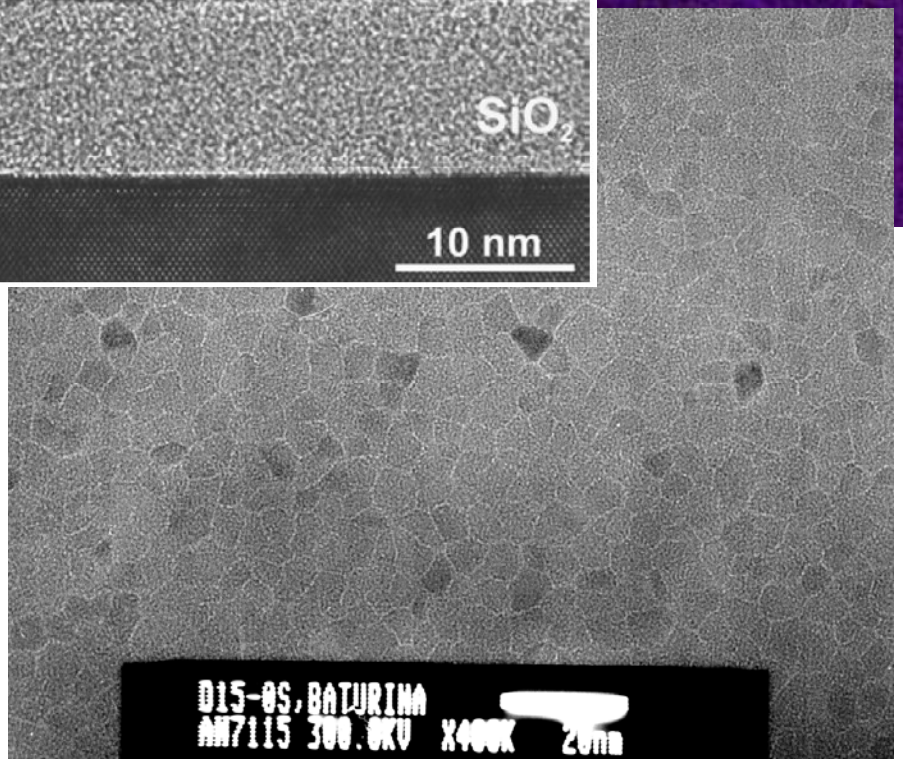

✓ TiN films were formed by atomic layer chemical vapor deposition onto a Si/SiO_2 substrate at 350 ^0C.

✓ Composition:

Ti	N	Cl
1	0.94	0.035

the thickness is 5 nm

ξ_d = 9.3 nm - the superconducting coherence length

Disorder-driven SIT in TiN films (B=0)

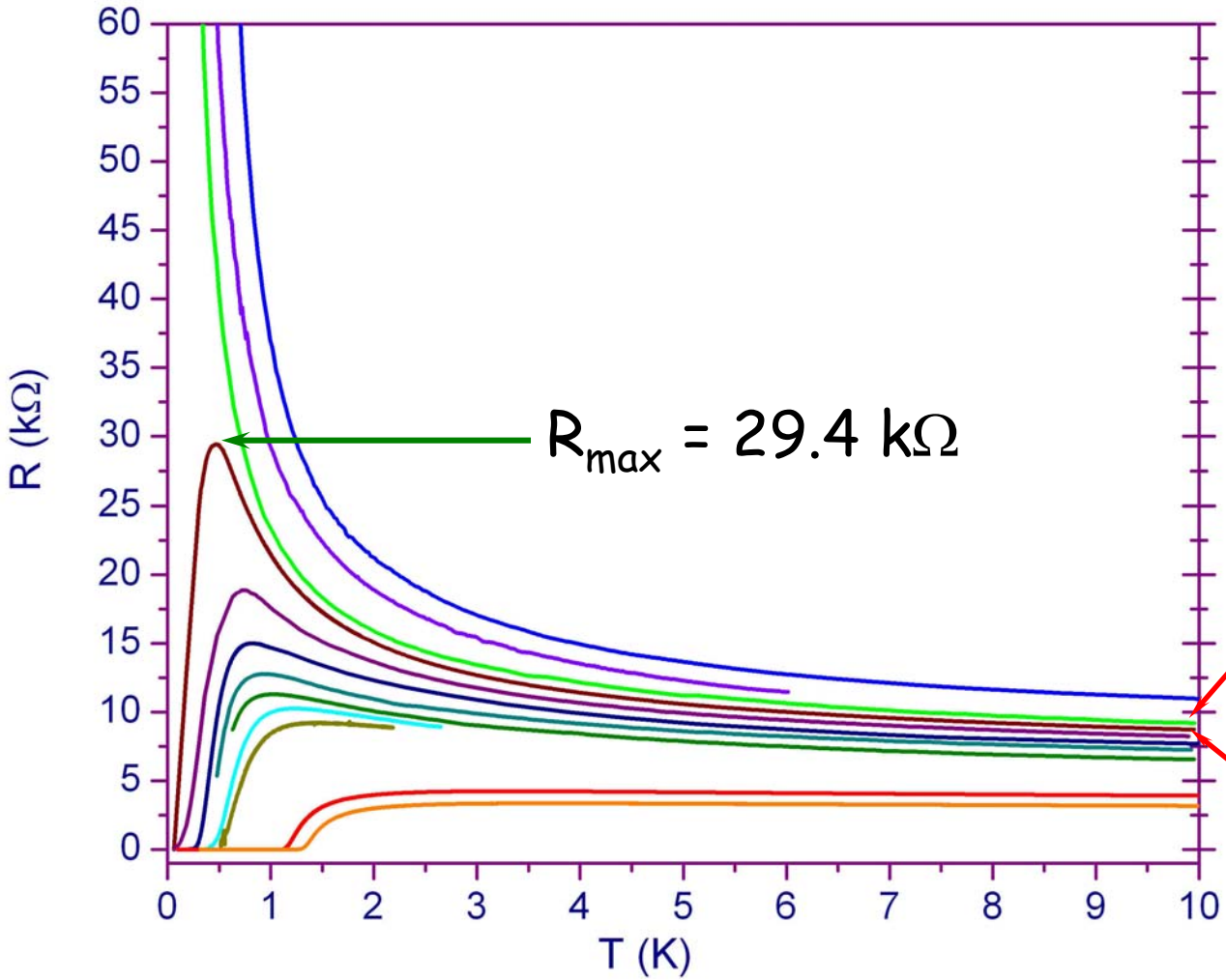

T = 300 K

4.73 kΩ – I3

4.48 kΩ - S1

5% (!)

T. Baturina, D.R. Islamov, J. Bentner, C. Strunk, M.R. Baklanov, A. Satta, JETP Lett. 79, 337 (2004)
T. Baturina, C. Strunk, M.R. Baklanov, A. Satta, PRL 98, 127003 (2007)
T. Baturina, A.Yu. Mironov, V. Vinokur, M.R. Baklanov, C. Strunk, PRL 99, 257003 (2007)
T. Baturina, A. Bilušic, A.Yu. Mironov, V. Vinokur, M.R. Baklanov, C. Strunk, Physica C 468, 316 (2008)

Disorder-driven SIT in TiN films (B=0)

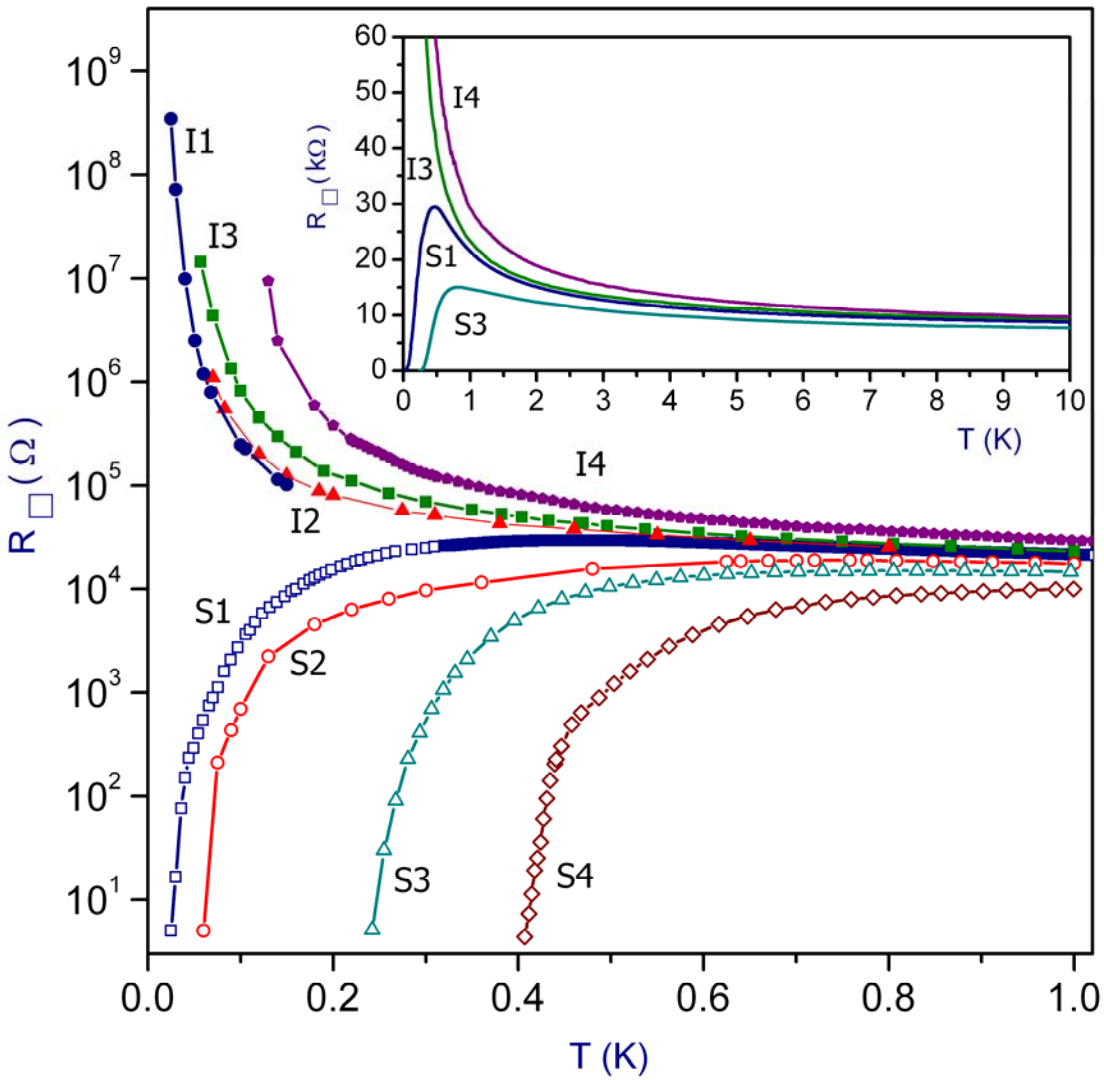

Rsq @ 300 K

4.60 kΩ – I1

4.48 kΩ - S1

<3% (!)

T. Baturina, A.Yu. Mironov, V. Vinokur, M.R. Baklanov, C. Strunk, PRL 99, 257003 (2007)
T. Baturina, A. Bilušic, A.Yu. Mironov, V. Vinokur, M.R. Baklanov, C. Strunk, Physica C 468, 316 (2008)

Experiment

TiN films

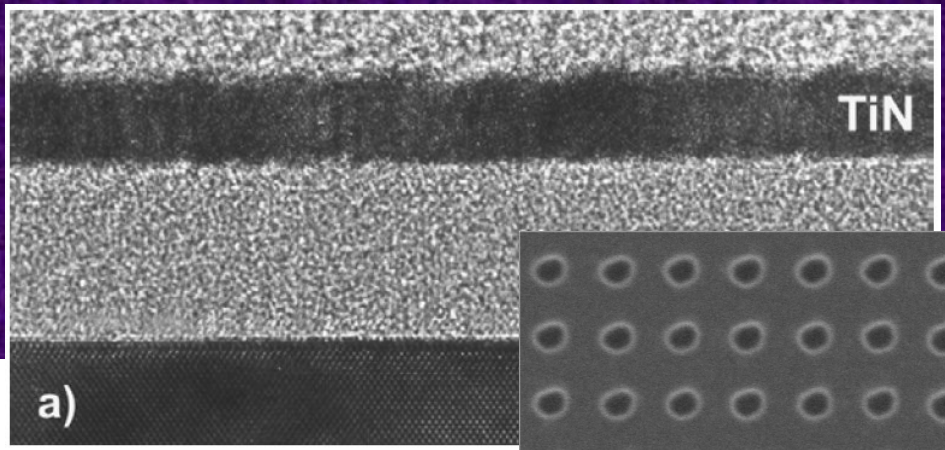

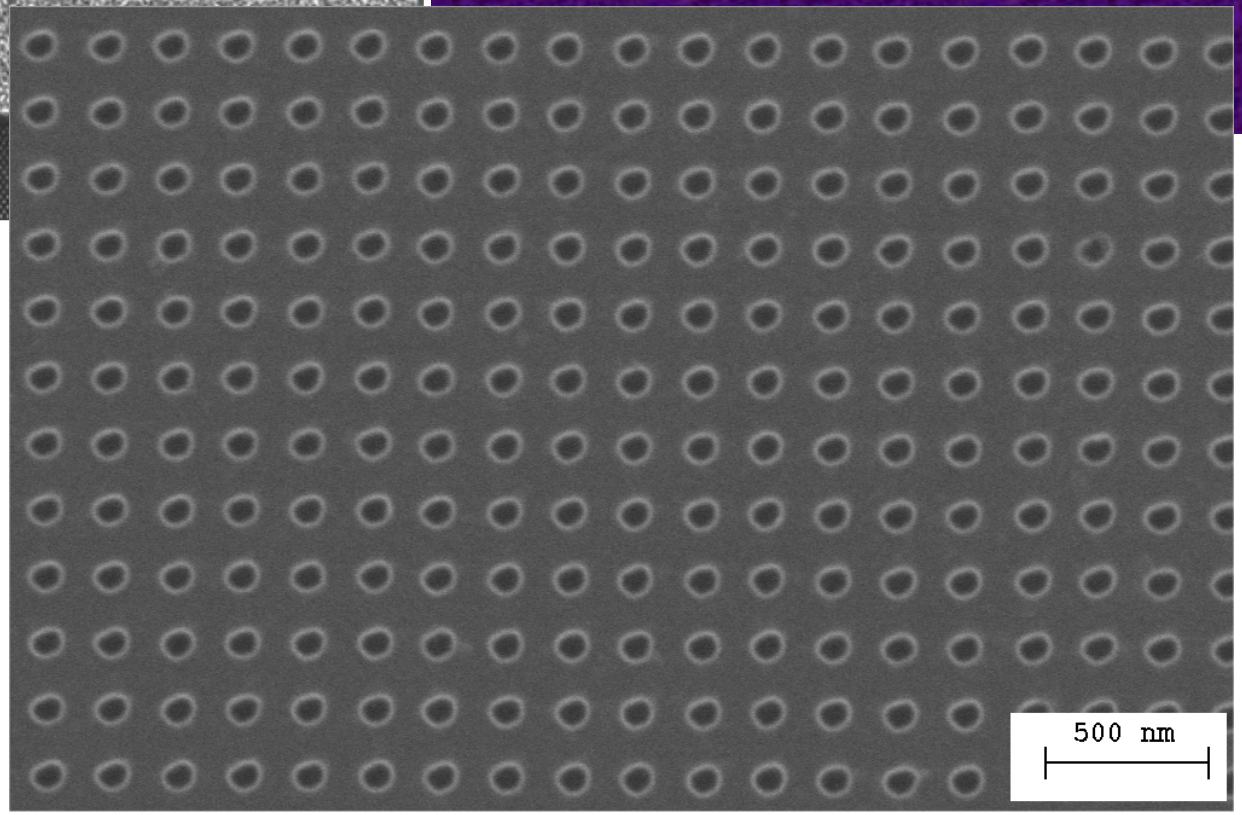

$$a = 200\ \text{nm}$$

$$d = 120\ \text{nm}$$

$$w \approx 80\ \text{nm}$$

SIT in continuous and nanoperforated TiN films

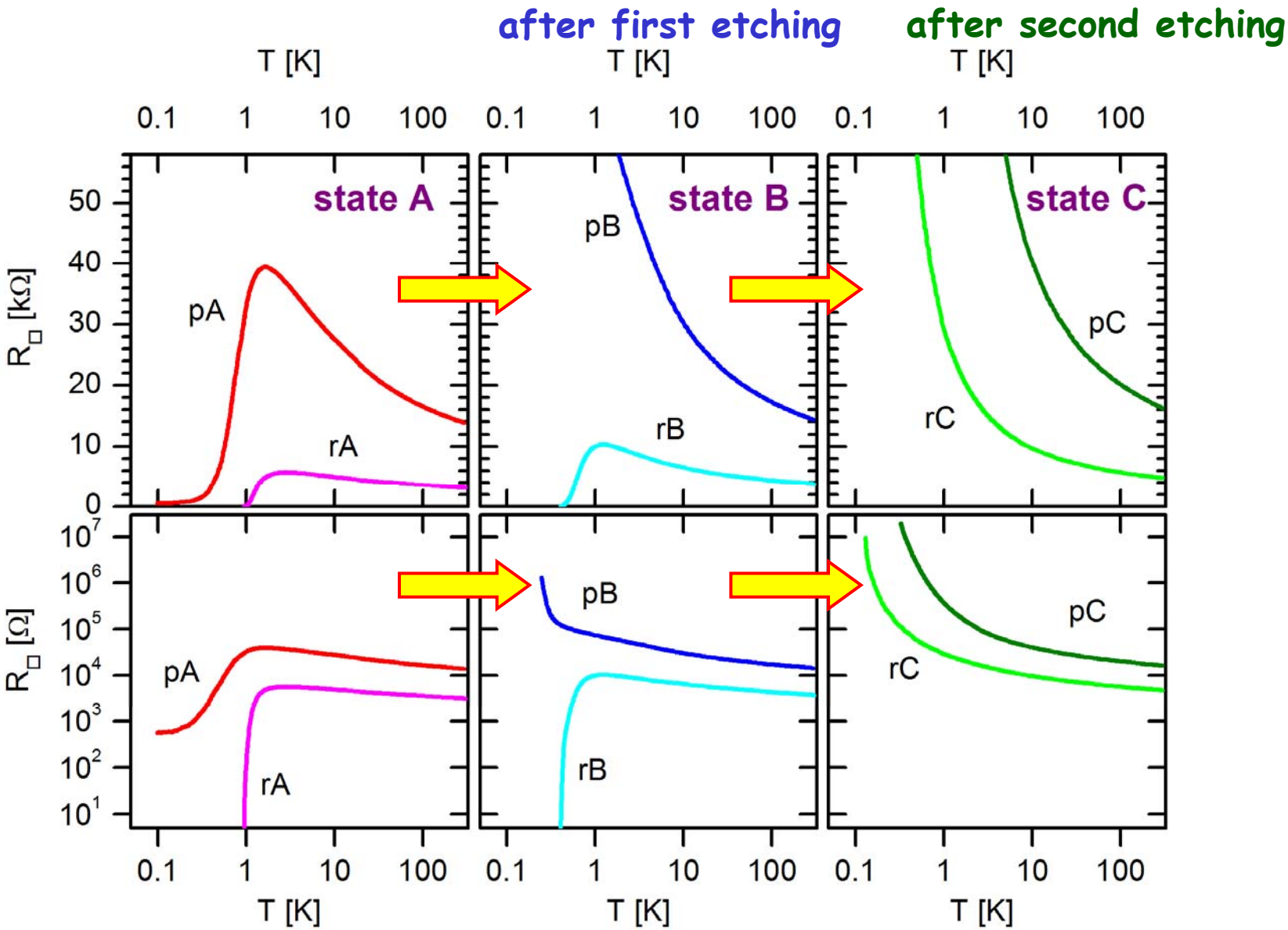

SIT in continuous and nanoperforated TiN films

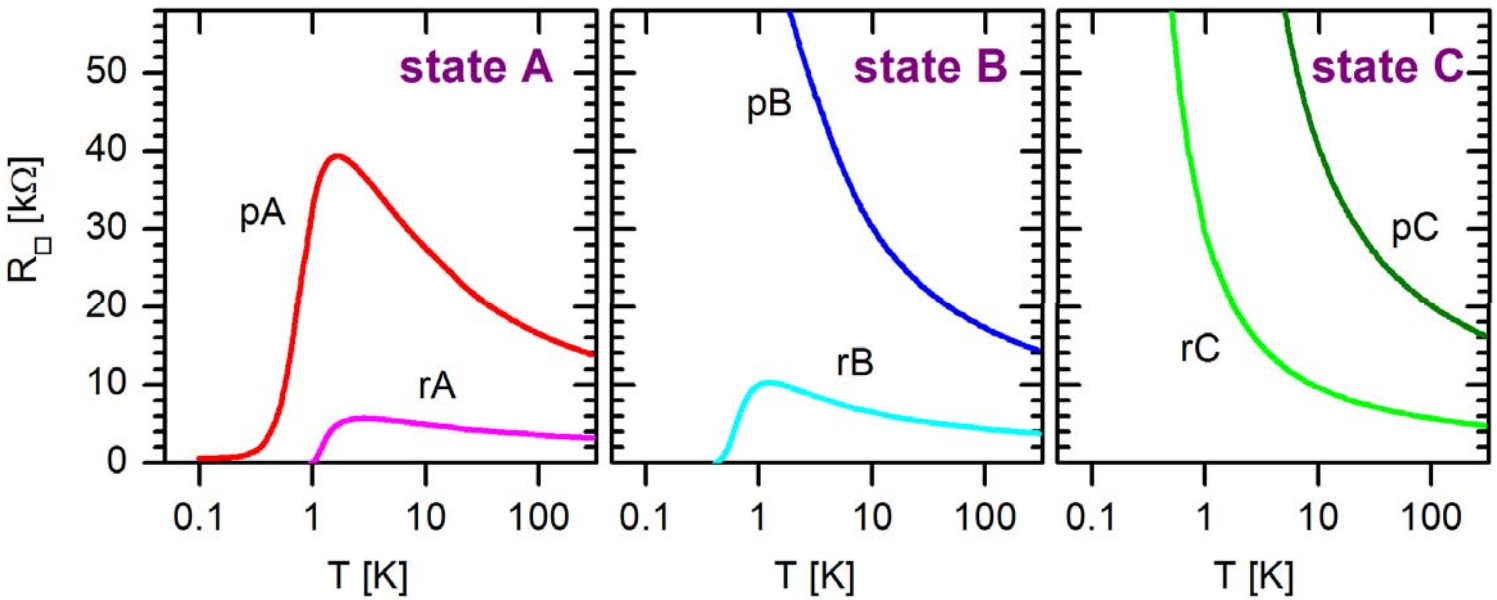

Resistance per square @ T = 300 K

	state A	state B	state C
continuous	3.17 kΩ	3.75 kΩ	4.76 kΩ
perforated	13.87 kΩ	14.45 kΩ	16.26 kΩ

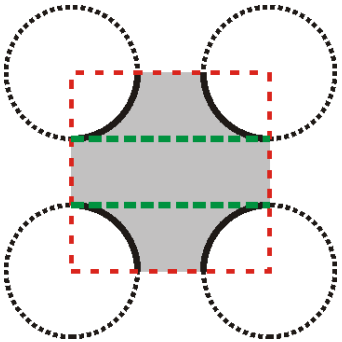

the ratios ~ 3 - 4, reflecting the reduction of the effective cross-section of the sample upon perforation

SIT in continuous and nanoperforated TiN films

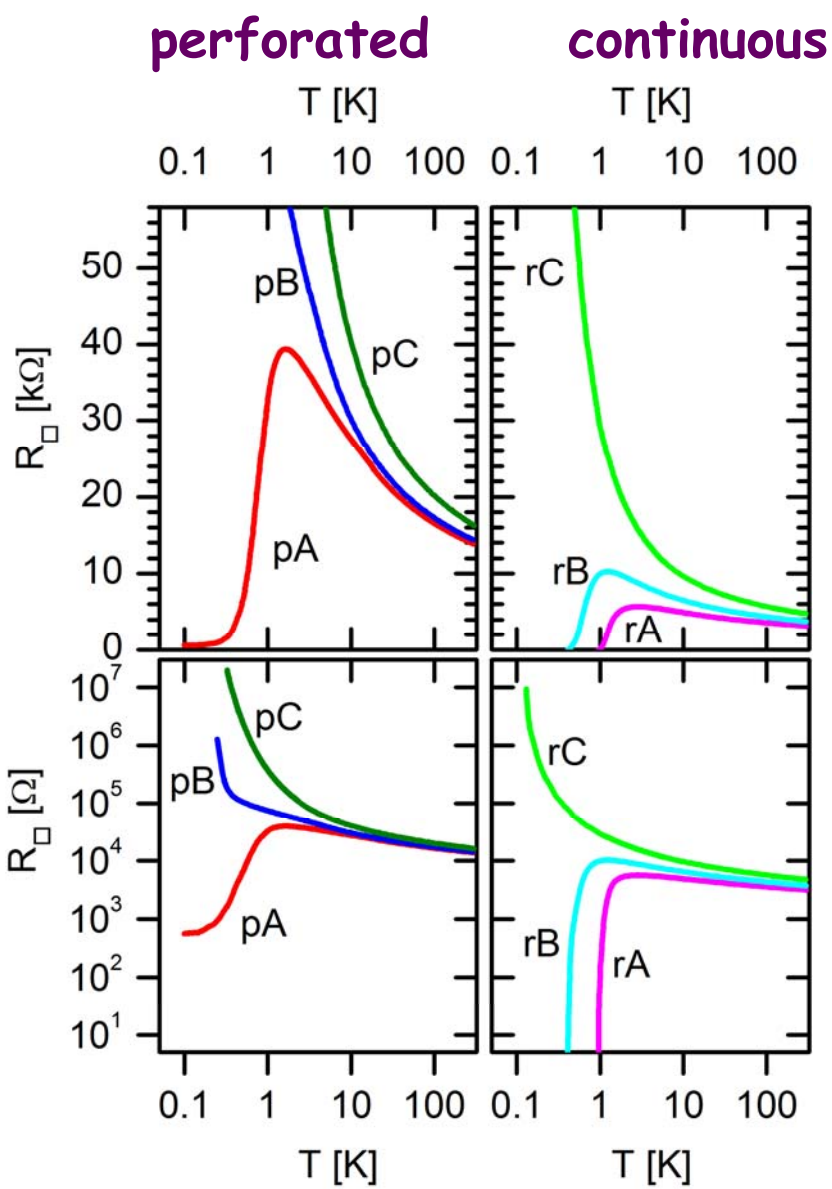

$$G = (R_\square)^{-1} = G_0 + G_{00} A \ln(T)$$

Drude conductivity
+
quantum corrections:
weak localization,
e-e interaction

$$G_{00} = e^2/(\pi h)$$

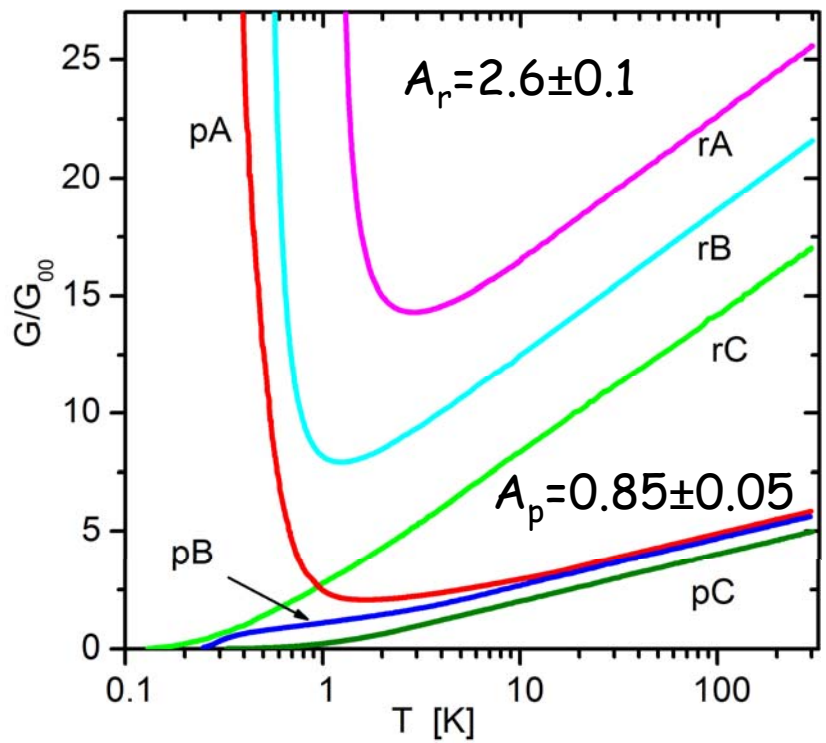

SIT in continuous and nanoperforated TiN films

the prefactors are different…
as they should

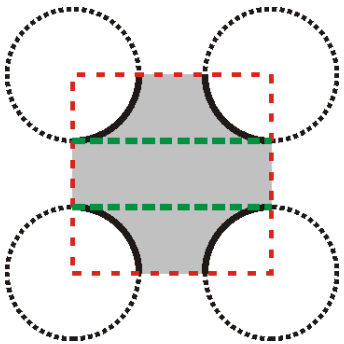

$A_r / A_p \approx 3$

continuous **perforated**

$R_\square \Rightarrow \alpha R_\square$

α - geometry factor

$$G = (\alpha R_\square)^{-1}$$

$$G = G_0/\alpha + G_{00}(A/\alpha)\ln(T)$$

$$G = (R_\square)^{-1} = G_0 + G_{00} A \ln(T)$$

Drude conductivity
+
quantum corrections:
weak localization,
e-e interaction

$$G_{00} = e^2/(\pi h)$$

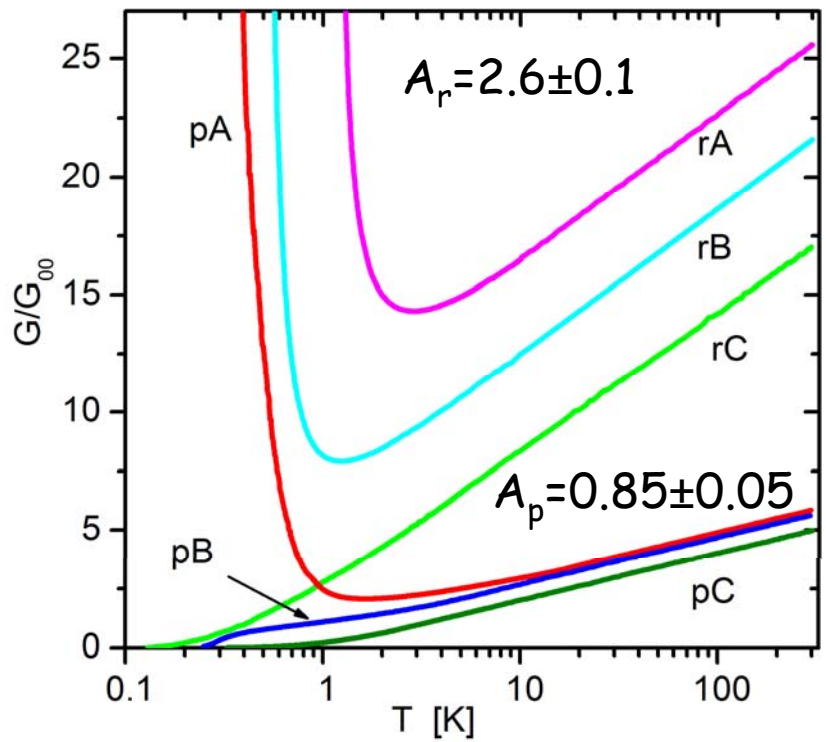

SIT in continuous and nanoperforated TiN films

At this point
we conclude that
the high temperature behavior of the conductance
is well explained merely by the geometry factor

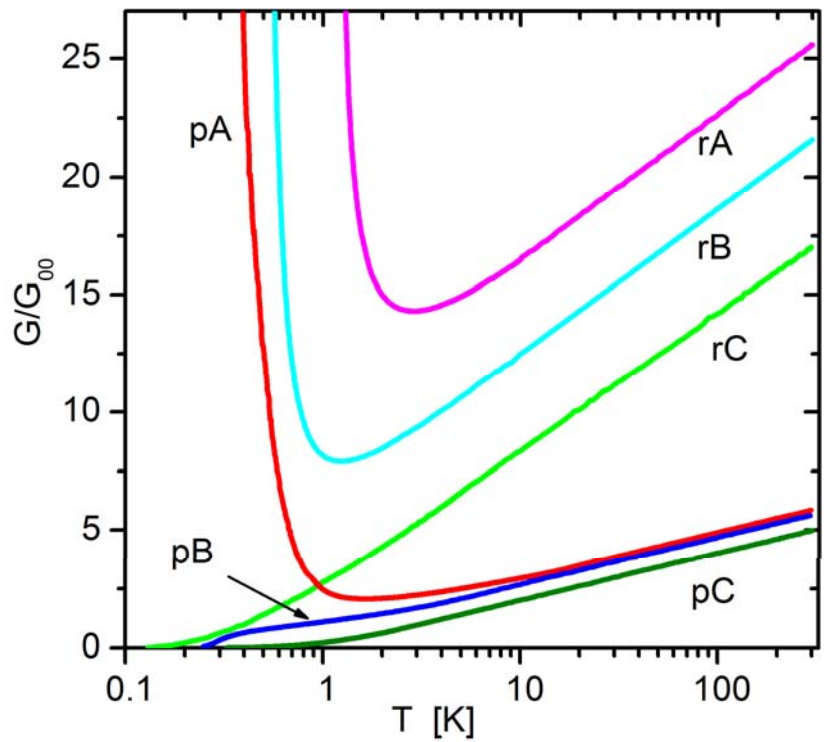

SIT in continuous and nanoperforated TiN films

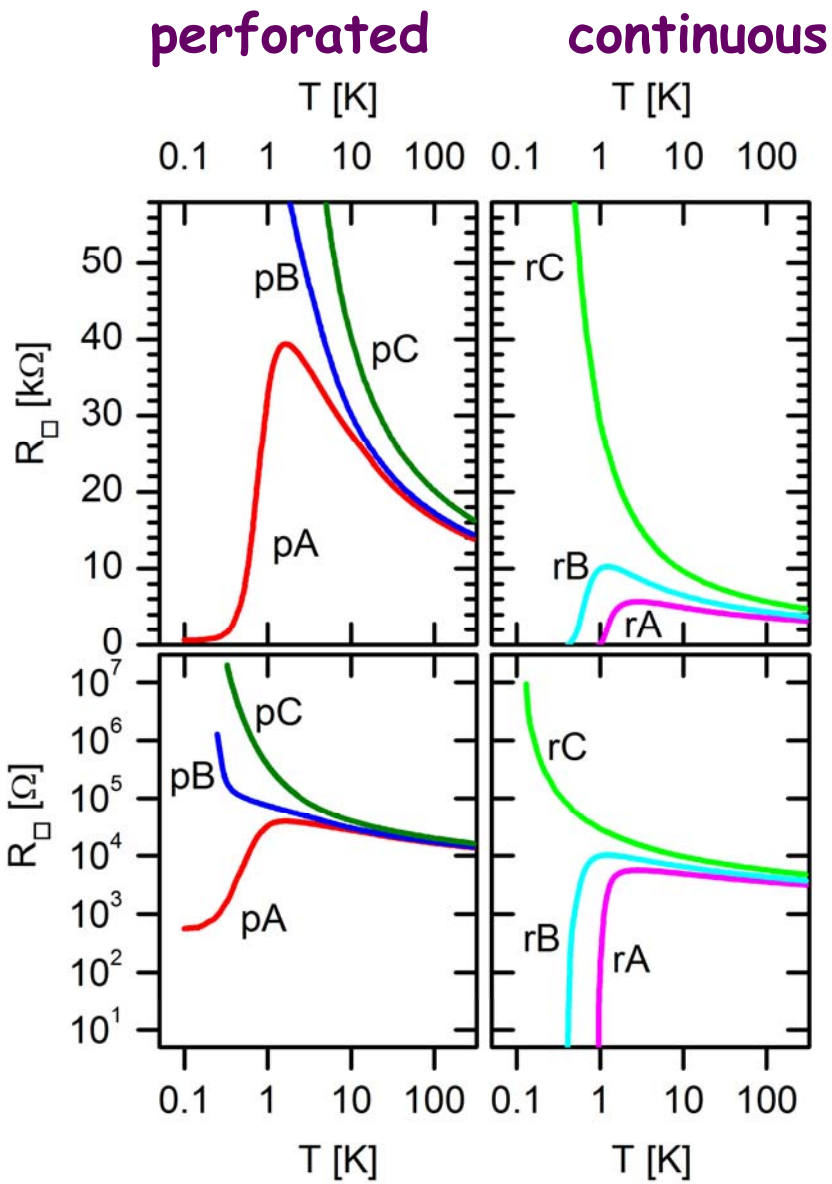

non-superconducting samples

$$R = R_0 \exp(T_0/T)$$

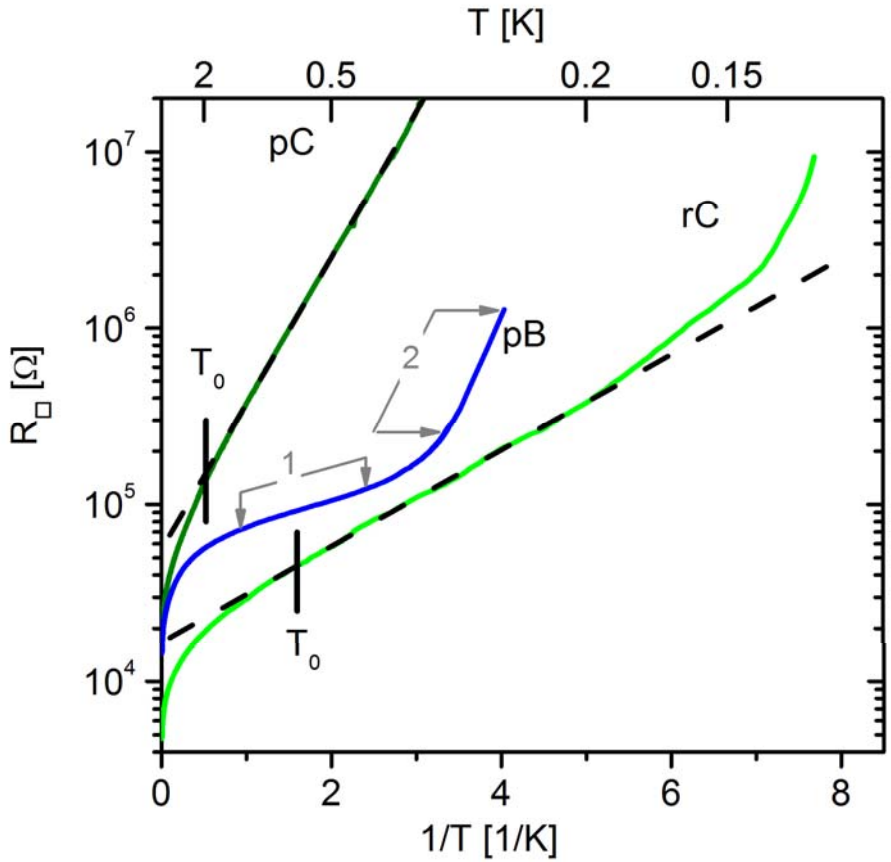

SIT in continuous and nanoperforated TiN films

perforated pB

	R_0	T_0
(1)	51.5 kΩ	0.35 K
(2)	0.15 kΩ	2.21 K

non-superconducting samples

$$R = R_0 \exp(T_0/T)$$

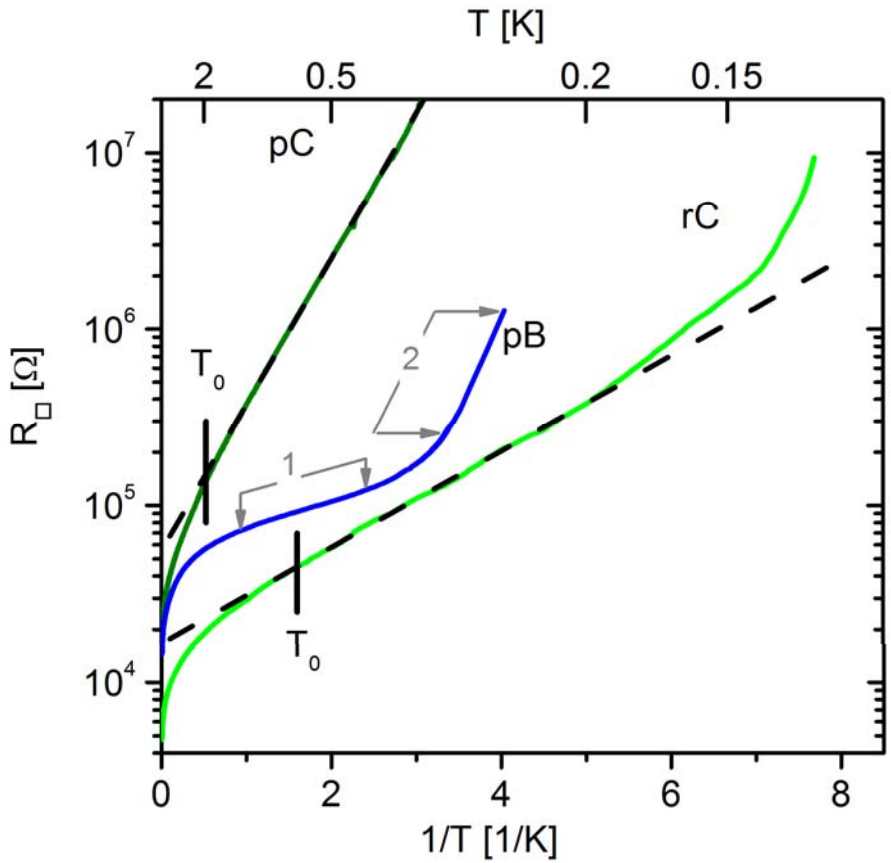

SIT in continuous and nanoperforated TiN films

non-superconducting samples

$$R = R_0 \exp(T_0/T)$$

	R_0	T_0
continuous rC	16.6 kΩ	0.63 K
perforated pC	55.6 kΩ	1.9 K

the ratio of R_0's = 3
= geometry factor

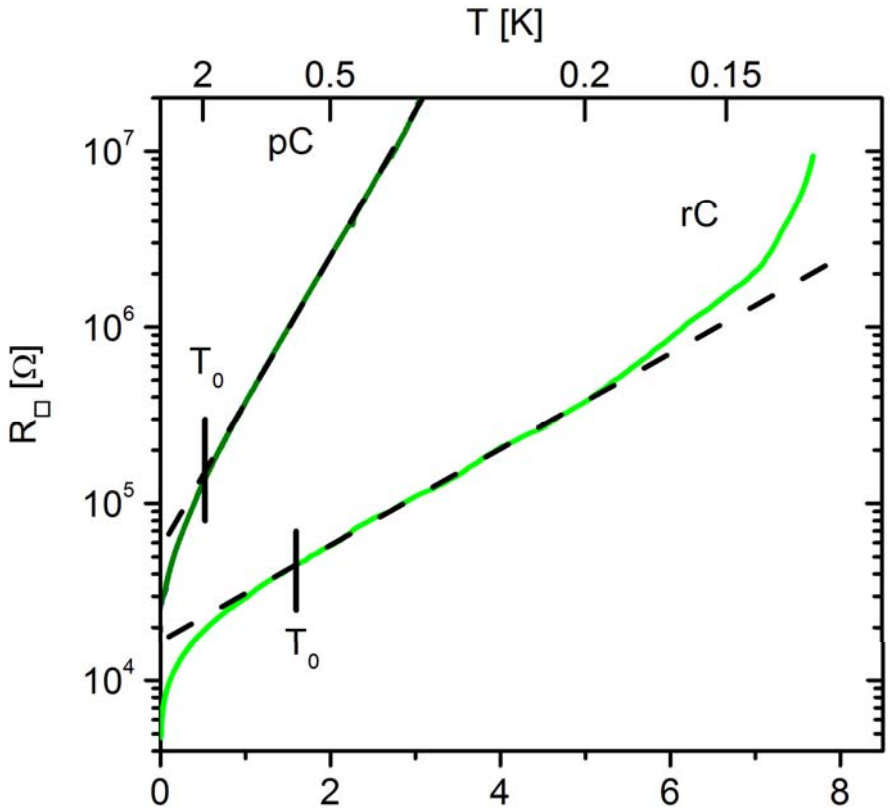

why are T_0's different

one would have expected
that had T_0 been formed over
the microscopic scale,
it would have remained the same
in both reference and perforated films

This suggests that T_0 is built on the macroscopic spatial scales, not less then 200 nm and is influenced by changes in geometric characteristics and the connectivity introduced by patterning.

Collective Cooper-Pair Transport in the Insulating State of Josephson-Junction Arrays

M. Fistul, V. Vinokur, T. Baturina, PRL **100**, 086805 (2008)
V. Vinokur, T. Baturina, M. Fistul, A. Mironov, M. Baklanov, C. Strunk, Nature 452, 613 (2008)

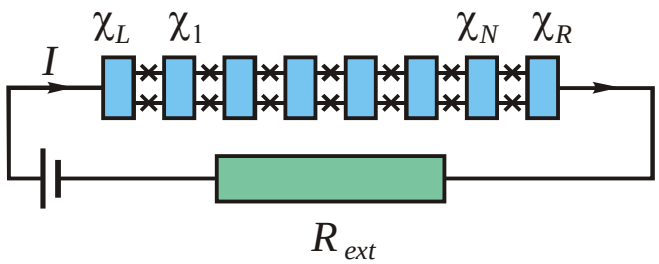

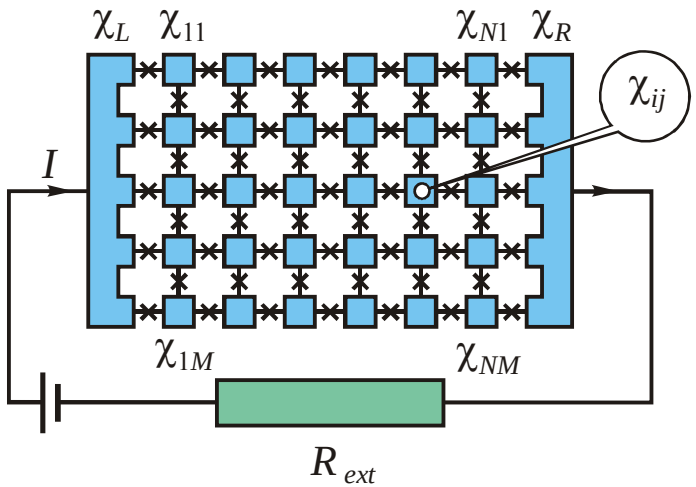

$$R \propto \exp\left[\frac{\Delta_c}{k_B T}\right]$$

1D JJA: $\Delta_c \cong E_c L / b$

2D JJA: $\Delta_c \cong E_c \ln(L/b)$

E_c is the charging energy

b is the size of the elemental cell of the array

L is the smaller quantity out of either the electrostatic screening length of JJA or its linear dimension

size-dependent activation-type behavior of the resistance !!

size-dependent activation-type behavior of the resistance !!

D. Kowal and Z. Ovadyahu, Physica C **468**, 322 (2008)

M. Fistul, V. Vinokur, T. Baturina, PRL **100**, 086805 (2008)

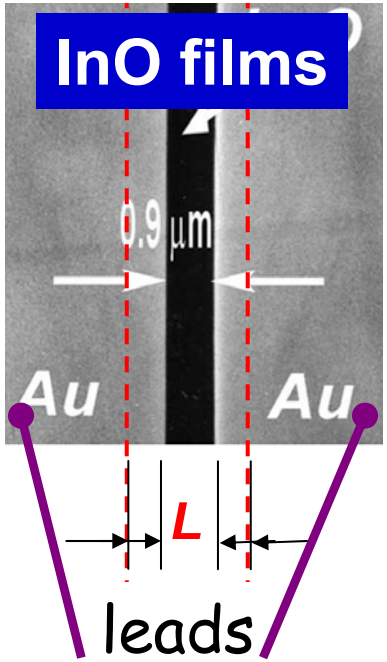

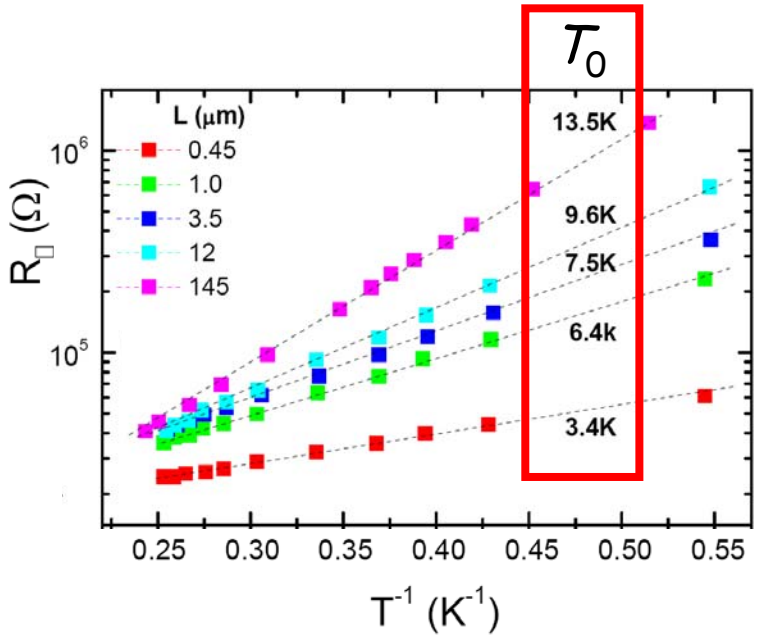

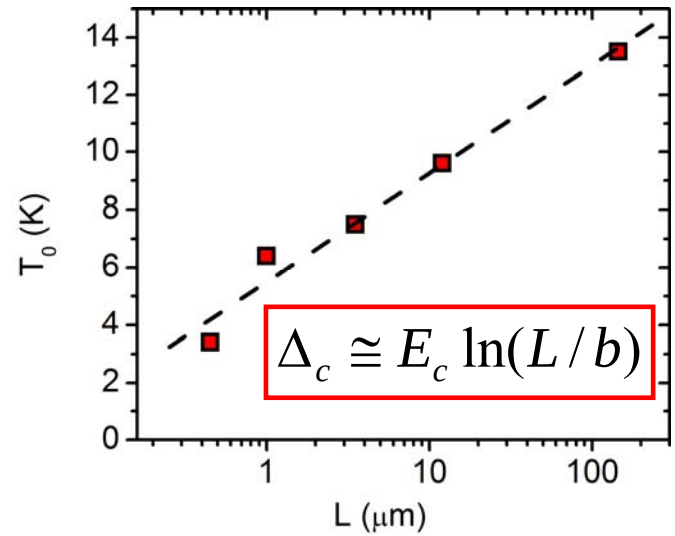

The activation energy T_0 appears to depend on the sample size: the larger the sample, the larger T_0

TiN films

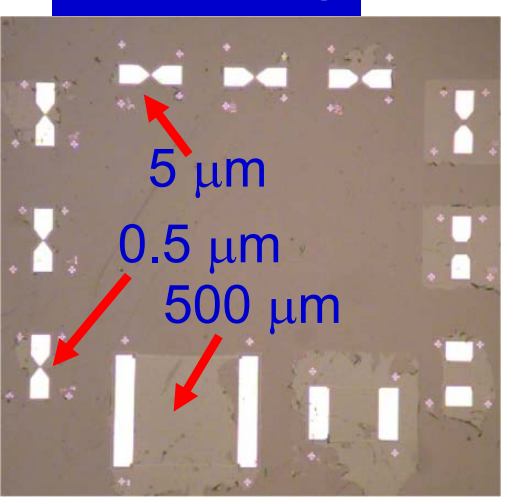

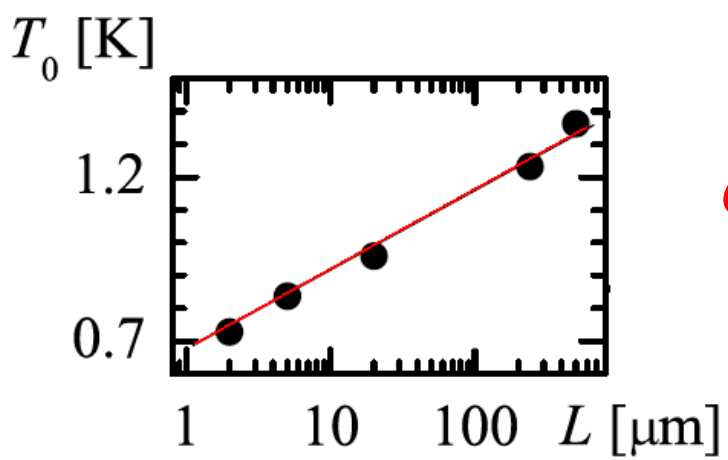

Next talk: Christoph Strunk

Collective Cooper-Pair Transport in the Insulating State of Josephson-Junction Arrays

M. Fistul, V. Vinokur, T. Baturina, PRL **100**, 086805 (2008)
V. Vinokur, T. Baturina, M. Fistul, A. Mironov, M. Baklanov, C. Strunk, Nature **452**, 613 (2008)

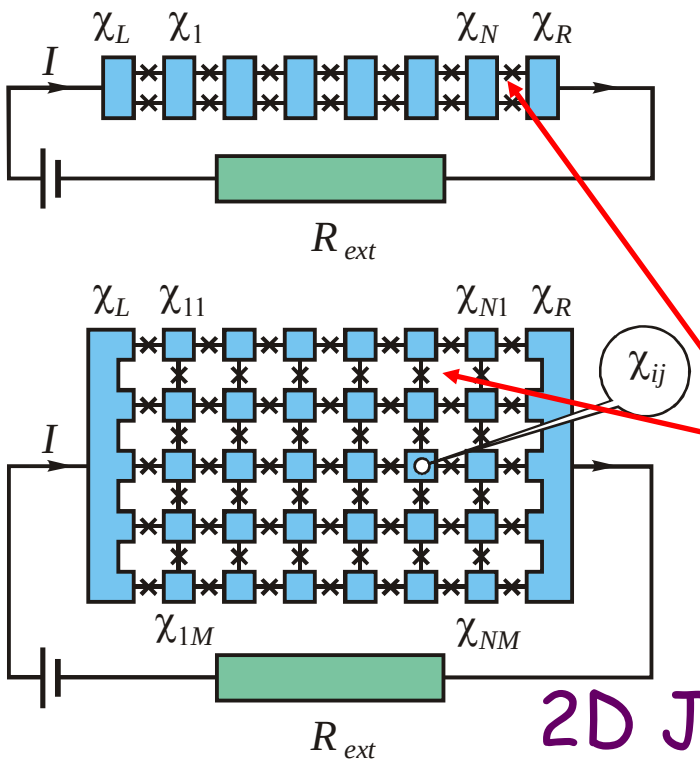

magnetic field dependence:

$$\Delta_c(B) = \Delta_c[1 - \alpha E_J(B)/E_c]$$

correction from Josephson coupling

$$f = eBA_{loop}/\pi h$$

1D JJA: $E_J^{1D} = E_{J0}|\cos(\pi f)|$

2D JJA: $E_J^{2D} = E_{J0}\{1 - 4f\sin^2[\pi(1-f)/4]\}$

M. Tinkham, D.W. Abraham, and C. J. Lobb, Phys. Rev. B **28**, 6578 (1983)

Threshold voltage
is size- and magnetic-field dependent

$$eV_T \simeq \Delta_c$$

More of experiment…

VOLUME 81, NUMBER 1 PHYSICAL REVIEW LETTERS 6 JULY 1998

Length-Scale Dependence of the Superconductor-to-Insulator Quantum Phase Transition in One Dimension

Edmond Chow* and Per Delsing
Department of Microelectronics and Nanoscience, Chalmers University of Technology and Göteborg University, S-412 96, Göteborg, Sweden

David B. Haviland
Department of Physics, Royal Institute of Technology, S-100 44 Stockholm, Sweden
(Received 16 September 1997)

One-dimensional (1D) arrays of small-capacitance Josephson junctions demonstrate a sharp transition, from Josephson-like behavior to the Coulomb blockade of Cooper-pair tunneling, as the effective Josephson coupling between nearest neighbors is tuned with an externally applied magnetic field. Comparing the zero-bias resistance of three arrays with 255, 127, and 63 junctions, we observe a critical behavior where the resistance, extrapolated to $T = 0$, is independent of length at a critical magnetic field. Comparison is made with a theory of this $T = 0$ quantum phase transition, which maps to the 2D classical XY model. [S0031-9007(98)06542-9]

1D JJA

E. Chow, P. Delsing, D.B. Haviland, PRL **81**, 204 (1998)

One-dimensional arrays of small-capacitance Josephson junctions (255, 127, and 63 junctions)

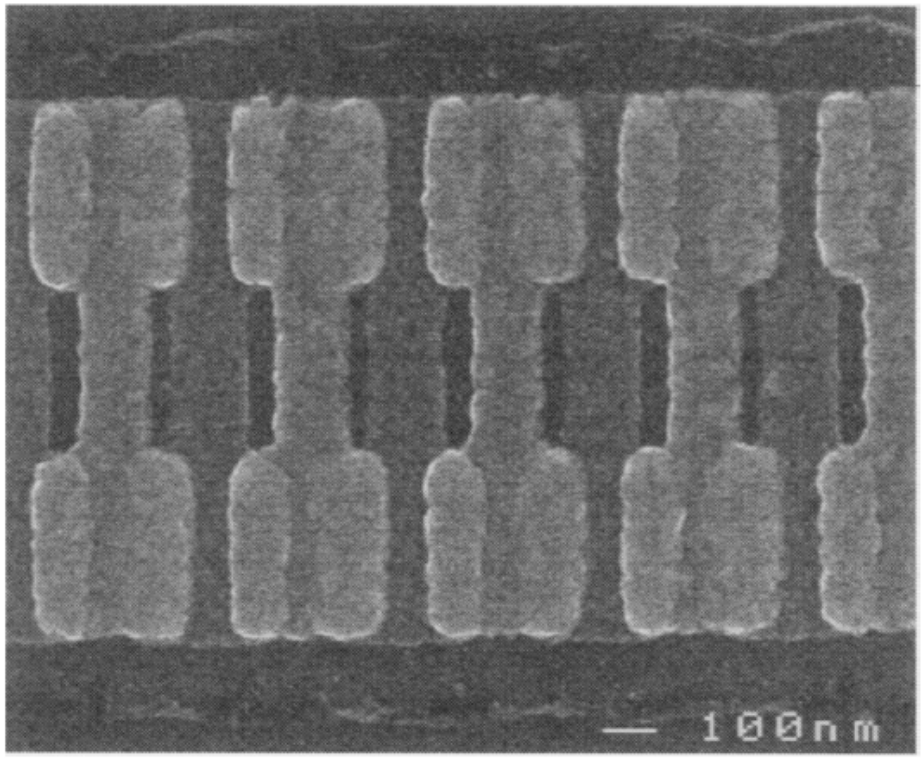

FIG. 1. A scanning electron micrograph of a section of the Josephson junction array. Tunnel junctions are formed at the overlap between the base electrode (darker gray) and the top electrode (lighter gray). The hole between neighboring electrodes forms the SQUID geometry.

$Al/Al_2O_3/Al$ tunnel junctions

$A_{loop} = 0.12\ \mu m^2$ is the effective area of the SQUID loop.

$A \simeq 0.039\ \mu m^2$ is junction area

$R_T = 4.9\ k\Omega \pm 6\%$

$C \simeq 3.5\ fF$

electrostatic screening length

$\Lambda \equiv (C/C_0)^{1/2} \simeq 10$

$E_{J0}/E_C \simeq 142\ \mu eV/23\ \mu eV = 6.1$

$$E_J = E_{J0} |\cos \pi B A_{loop}/\Phi_0|$$

1D JJA

E. Chow, P. Delsing, D.B. Haviland, PRL 81, 204 (1998)

One-dimensional arrays of small-capacitance Josephson junctions (255, 127, and 63 junctions)

$$\Delta_c(B) = \Delta_c[1 - \alpha E_J(B)/E_c]$$

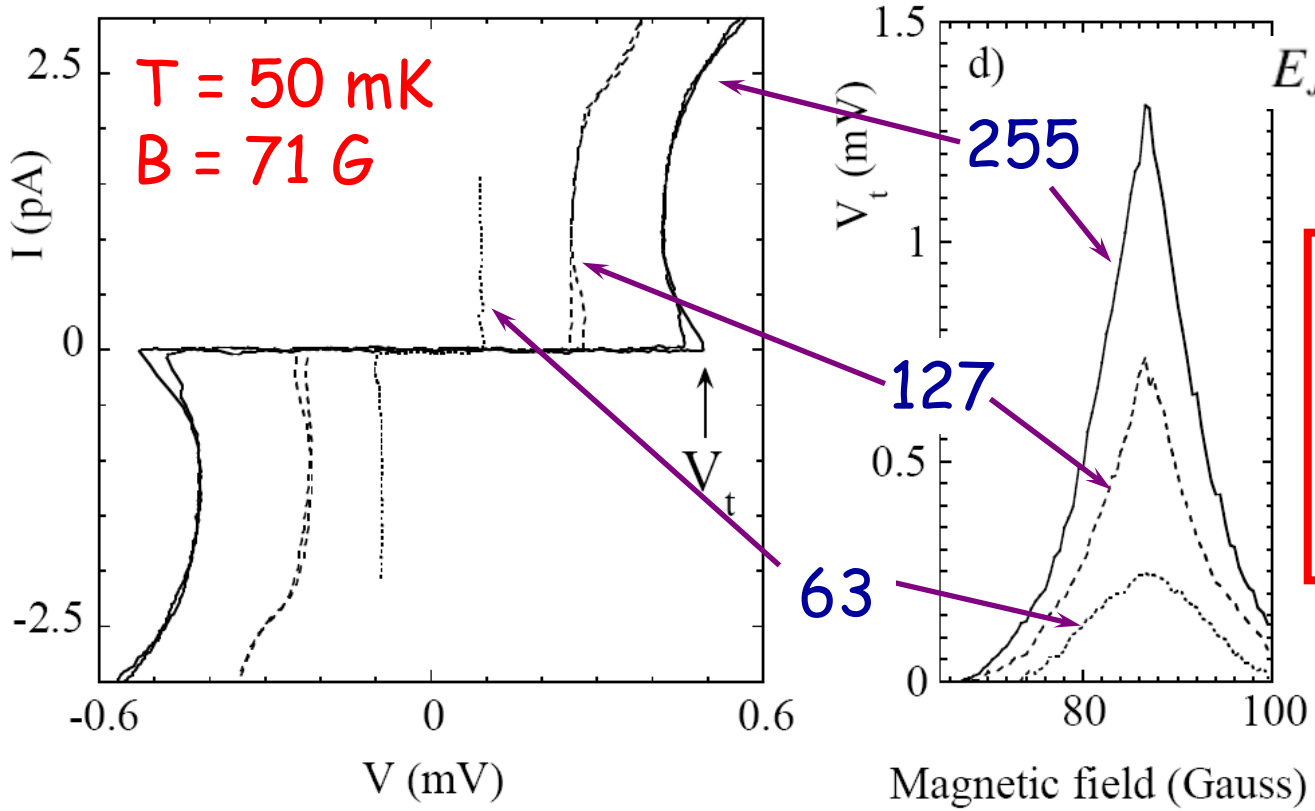

$$E_J = E_{J0}|\cos \pi B A_{\text{loop}}/\Phi_0|$$

$$A_{\text{loop}} = 0.12\ \mu\text{m}^2$$

$$\max V_T(B) \text{ at } E_J = 0$$

$$B = \frac{\Phi_0}{2A_{loop}} = 86\,\text{G}$$

$$eV_T \cong E_c N$$

Threshold voltage
is size- and magnetic-field dependent

$$eV_T \simeq \Delta_c$$

Collective Cooper-Pair Transport in the Insulating State of Josephson-Junction Arrays

M. Fistul, V. Vinokur, T. Baturina, PRL **100**, 086805 (2008)
V. Vinokur, T. Baturina, M. Fistul, A. Mironov, M. Baklanov, C. Strunk, Nature **452**, 613 (2008)

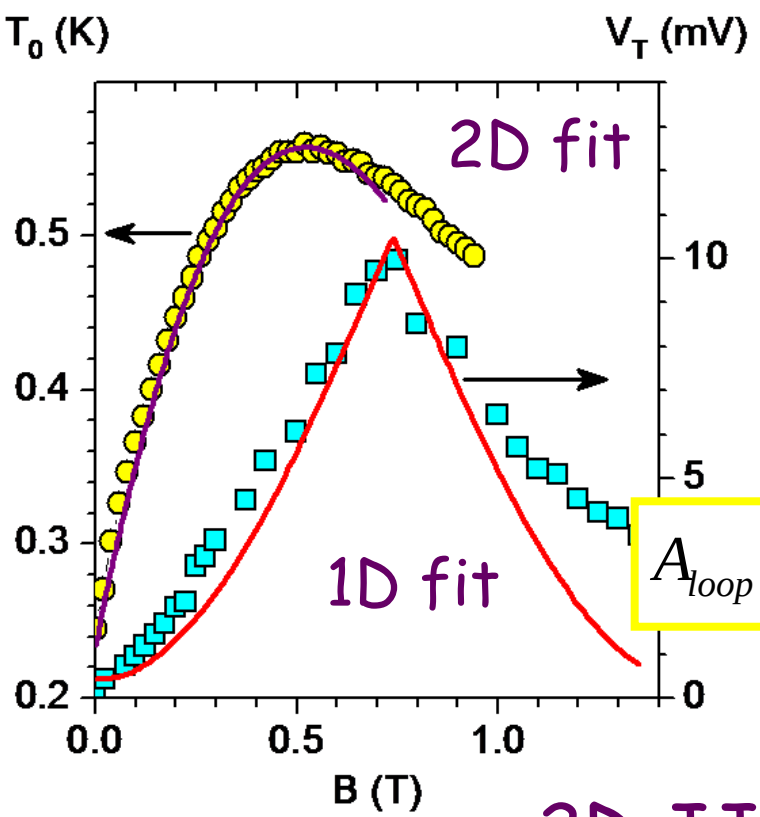

magnetic field dependence:

$$\Delta_c(B) = \Delta_c[1 - \alpha E_J(B)/E_c]$$

correction from Josephson coupling

$$f = eBA_{loop}/\pi h$$

$$A_{loop} = 1.4 \cdot 10^{-3}\ \mu\text{m}^2 \quad \Rightarrow \quad \sqrt{A_{loop}} \approx 40\ \text{nm} \approx 4\xi$$

1D JJA: $E_J^{1D} = E_{J0}|\cos(\pi f)|$

2D JJA: $E_J^{2D} = E_{J0}\{1 - 4f\sin^2[\pi(1-f)/4]\}$

M. Tinkham, D.W. Abraham, and C. J. Lobb, Phys. Rev. B **28**, 6578 (1983)

The film in a critical region of D-SIT can be viewed as

self-organized 2D JJ array!!!

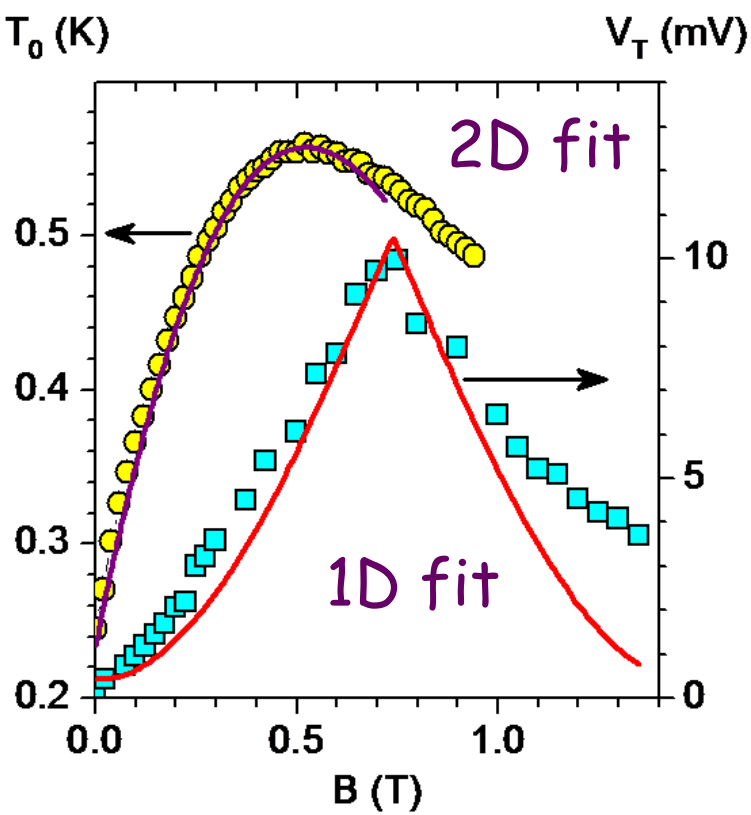

superconducting islands
immersed into an insulating matrix

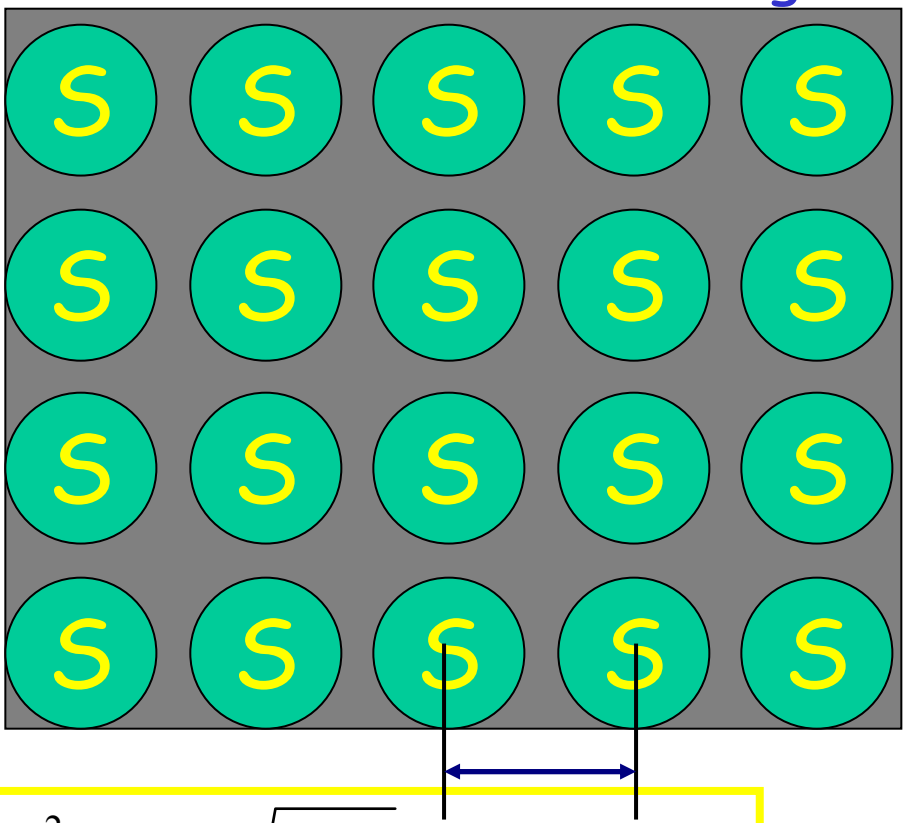

$$A_{loop} = 1.4 \cdot 10^{-3}\ \mu\text{m}^2 \quad \Rightarrow \quad \sqrt{A_{loop}} \approx 40\ \text{nm} \approx 4\xi$$

continuous film

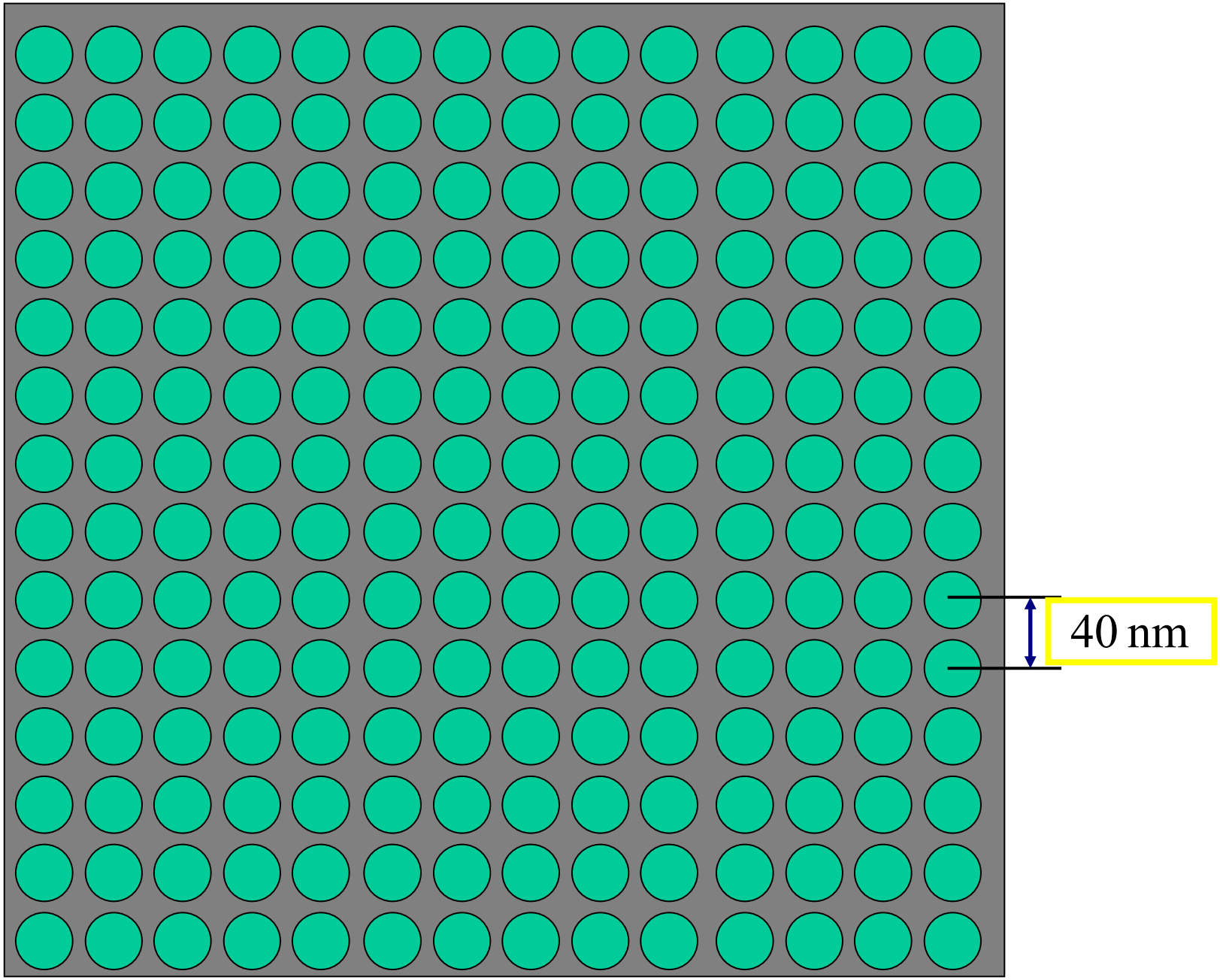

perforated film

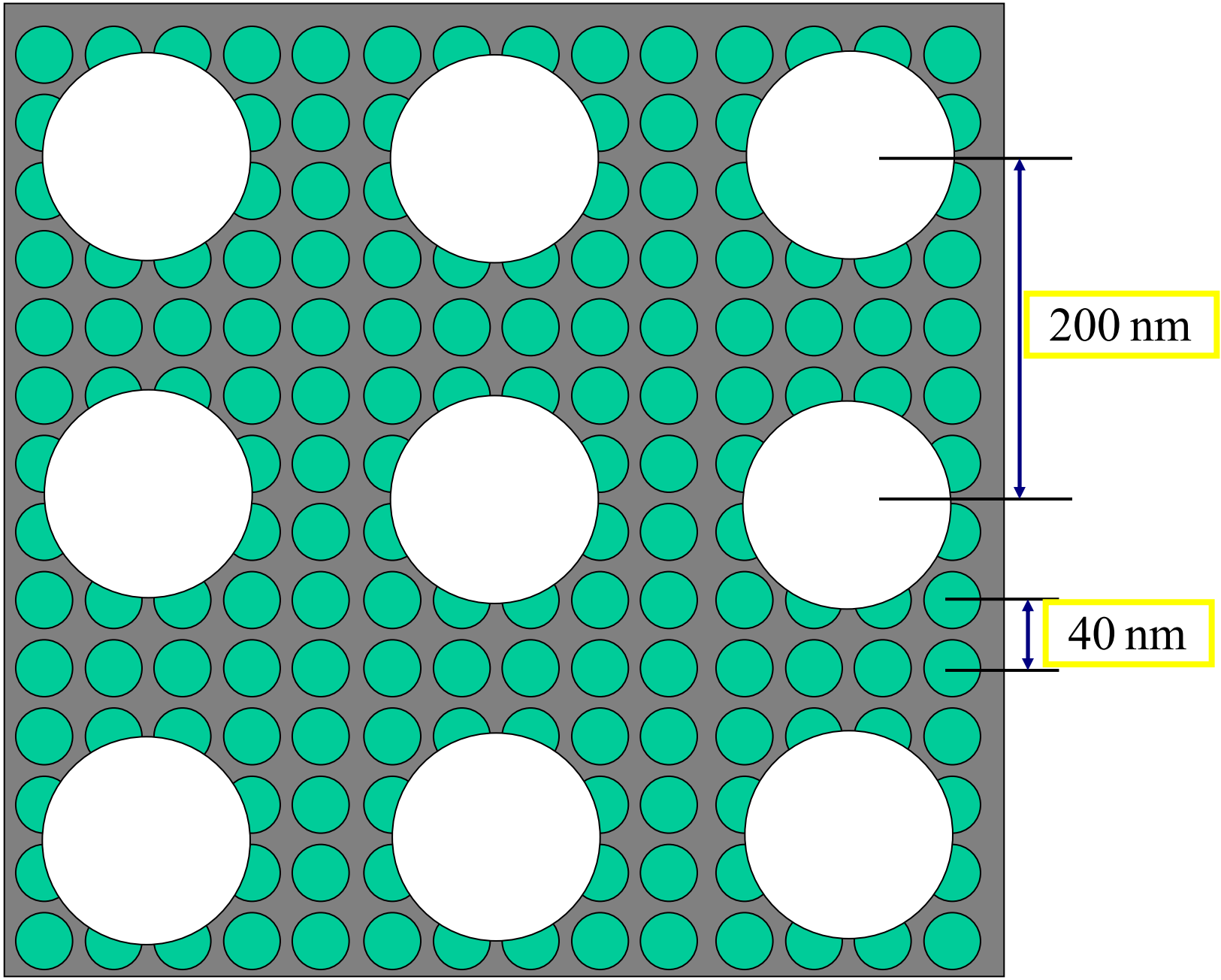

perforated film

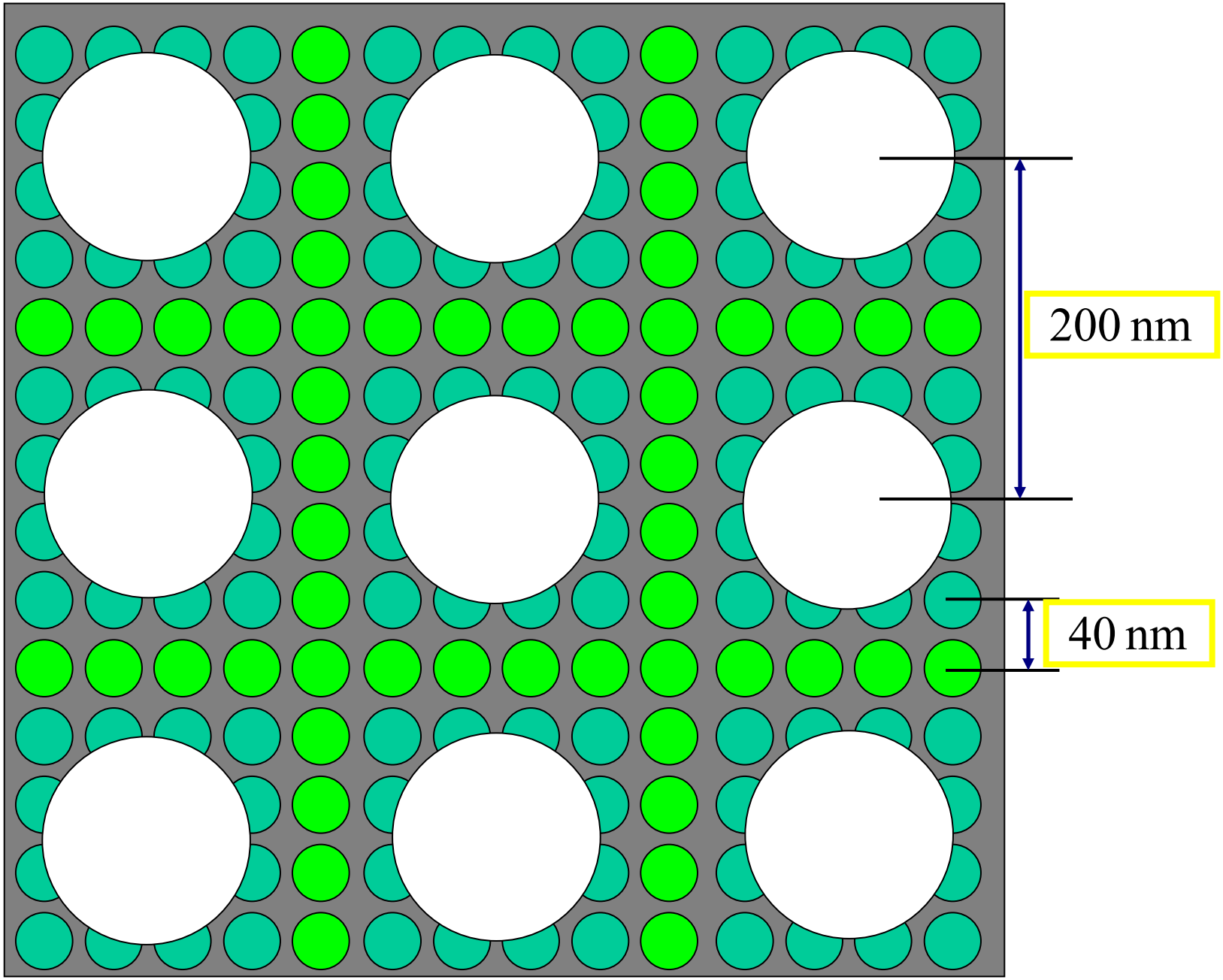

Estimations

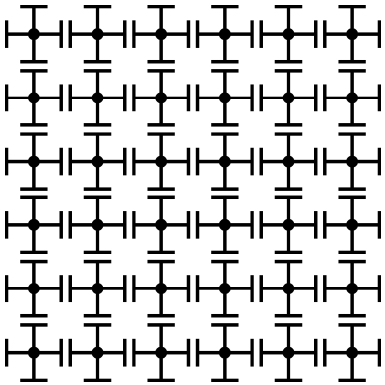

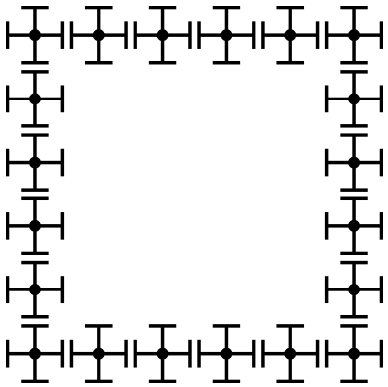

$$\tilde{b} = nb$$

$$\tilde{E}_c = nE_c$$

$$\Delta_c \cong E_c \ln(L/b) \qquad \tilde{\Delta}_c = n\Delta_c - nE_c \ln(n)$$

removing a part of junctions results in increase of Δ_c

$$E_c = ?$$

Journal of the Physical Society of Japan
Vol. 67, No. 3, March, 1998, pp. 729-731

More of experiment…

Two-Dimensional Arrays of Small Josephson Junctions with Regular and Random Defects

Takahide YAMAGUCHI, Ryuta YAGI, Shun-ichi KOBAYASHI and Youiti OOTUKA[1]

We investigated the transport properties of two-dimensional arrays of small Josephson junctions of which a number of junctions are removed. We found that the more the number of removed junctions, the more rapidly the array resistance increases with decreasing temperature. The

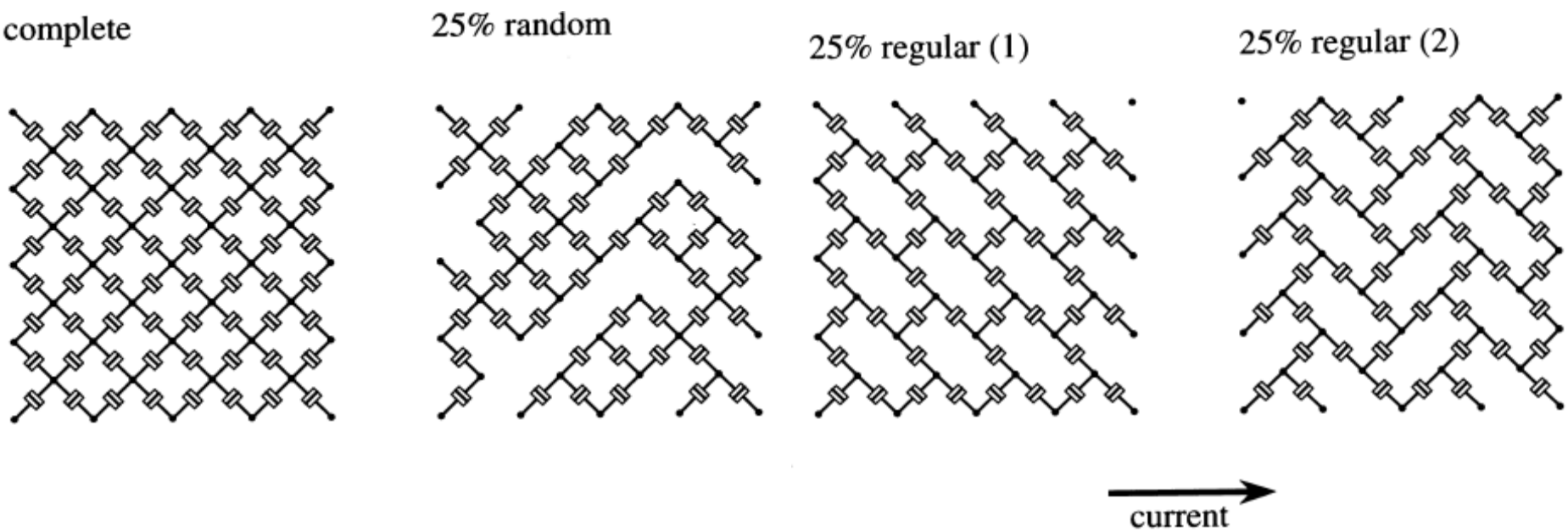

Journal of the Physical Society of Japan
Vol. 67, No. 3, March, 1998, pp. 729-731

More of experiment…

Two-Dimensional Arrays of Small Josephson Junctions with Regular and Random Defects

Takahide YAMAGUCHI, Ryuta YAGI, Shun-ichi KOBAYASHI and Youiti OOTUKA[1]

We investigated the transport properties of two-dimensional arrays of small Josephson junctions of which a number of junctions are removed. We found that the more the number of removed junctions, the more rapidly the array resistance increases with decreasing temperature. The

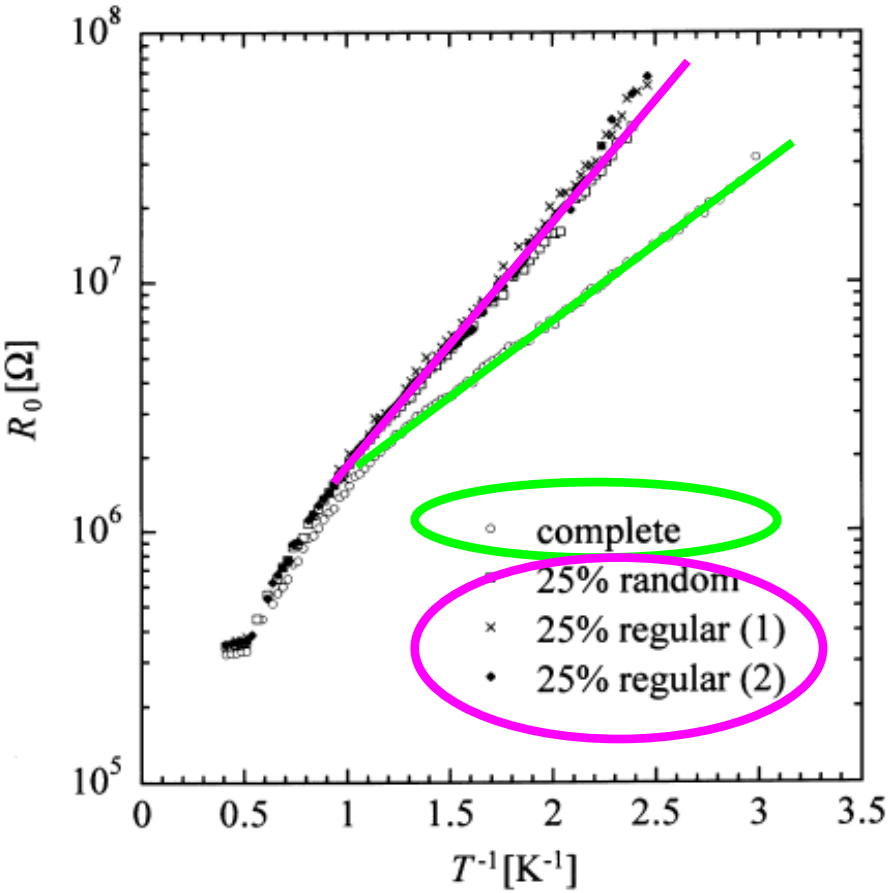

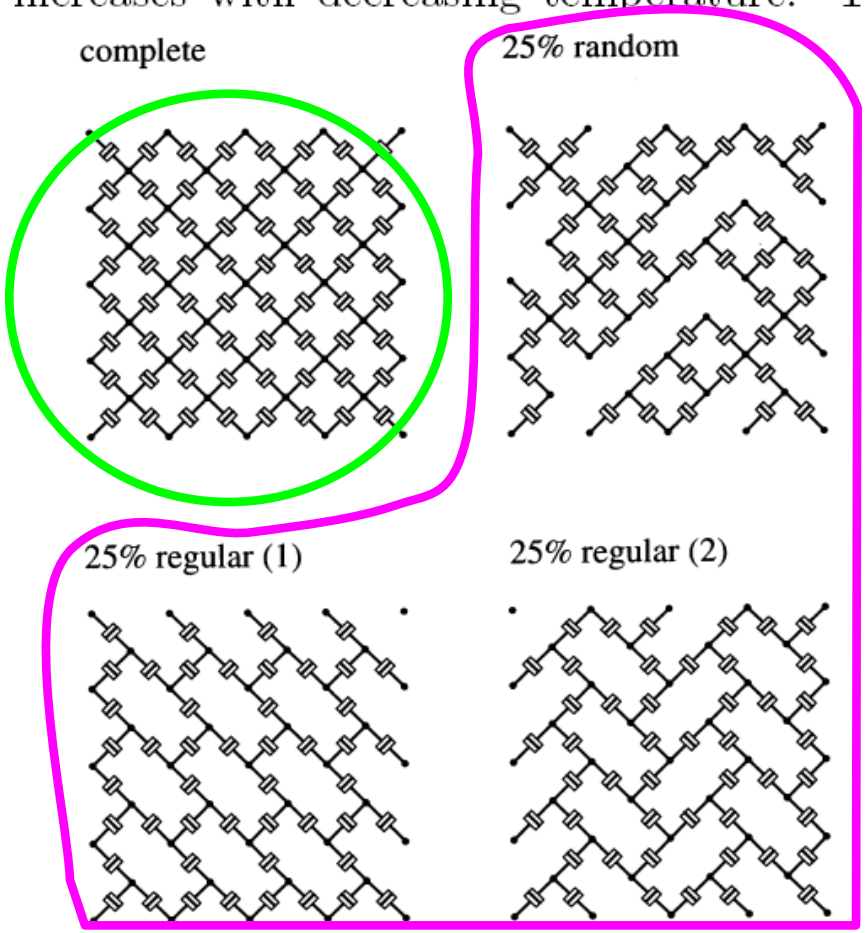

Journal of the Physical Society of Japan
Vol. 67, No. 3, March, 1998, pp. 729-731

More of experiment…

Two-Dimensional Arrays of Small Josephson Junctions with Regular and Random Defects

Takahide YAMAGUCHI, Ryuta YAGI, Shun-ichi KOBAYASHI and Youiti OOTUKA[1]

We investigated the transport properties of two-dimensional arrays of small Josephson junctions of which a number of junctions are removed. We found that the more the number of removed junctions, the more rapidly the array resistance increases with decreasing temperature. The

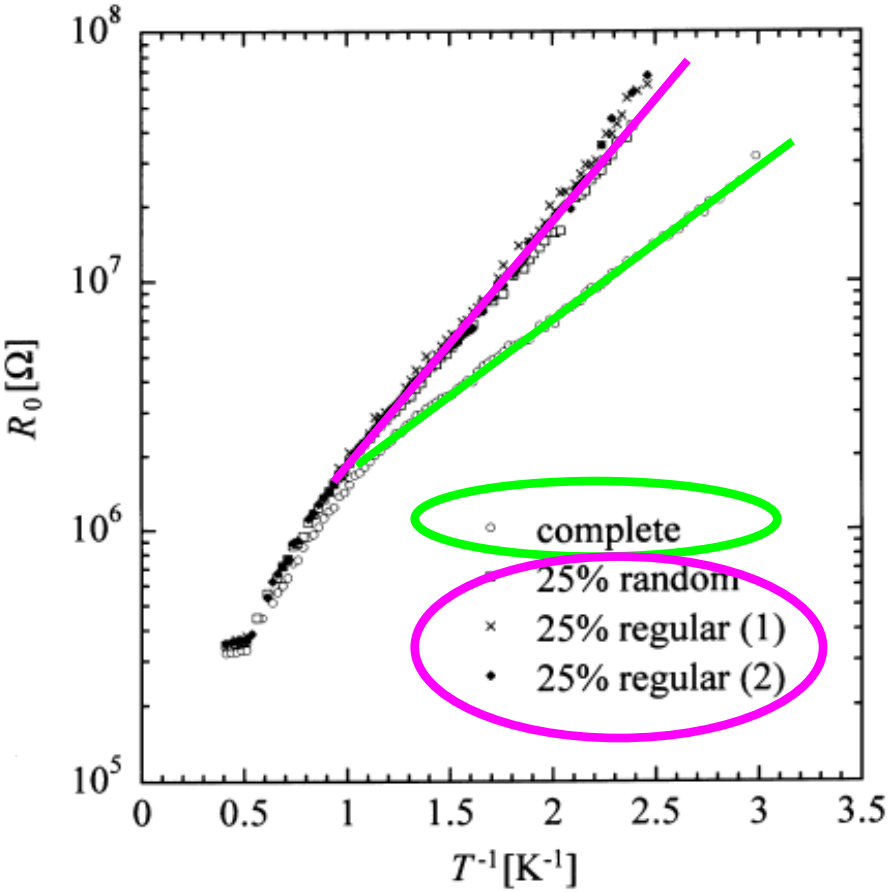

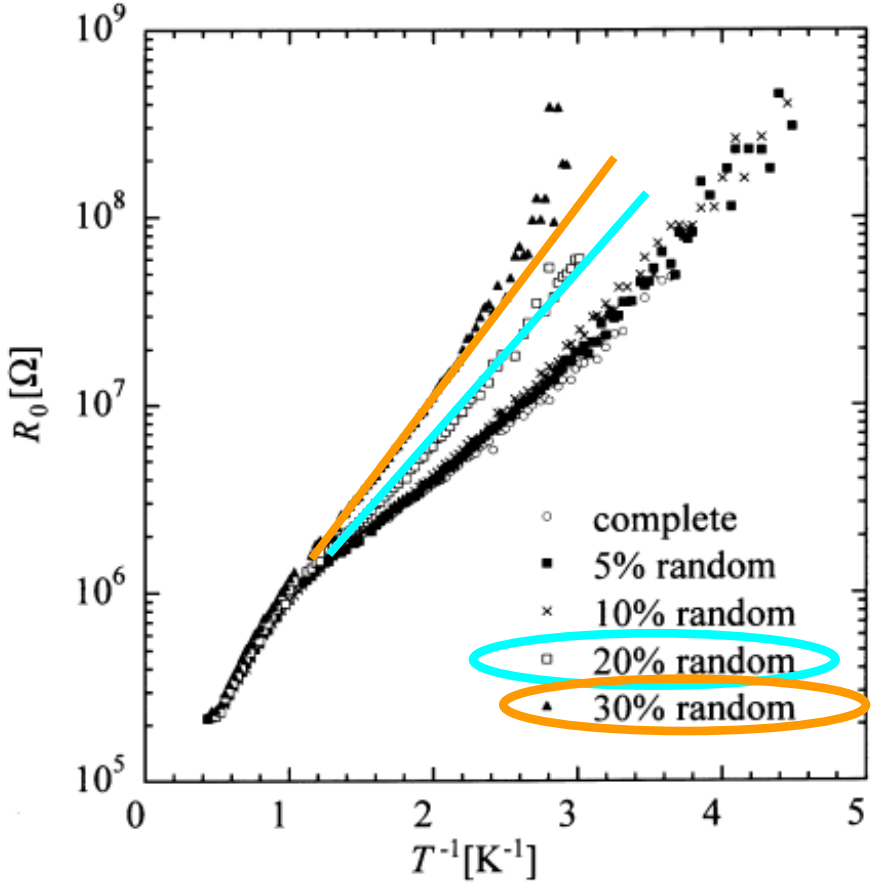

Journal of the Physical Society of Japan
Vol. 64, No. 1, January, 1995, pp. 19–21

More of experiment…

Precursor of Charge KTB Transition in Normal and Superconducting Tunnel Junction Array

Akinobu KANDA and Shun-ichi KOBAYASHI

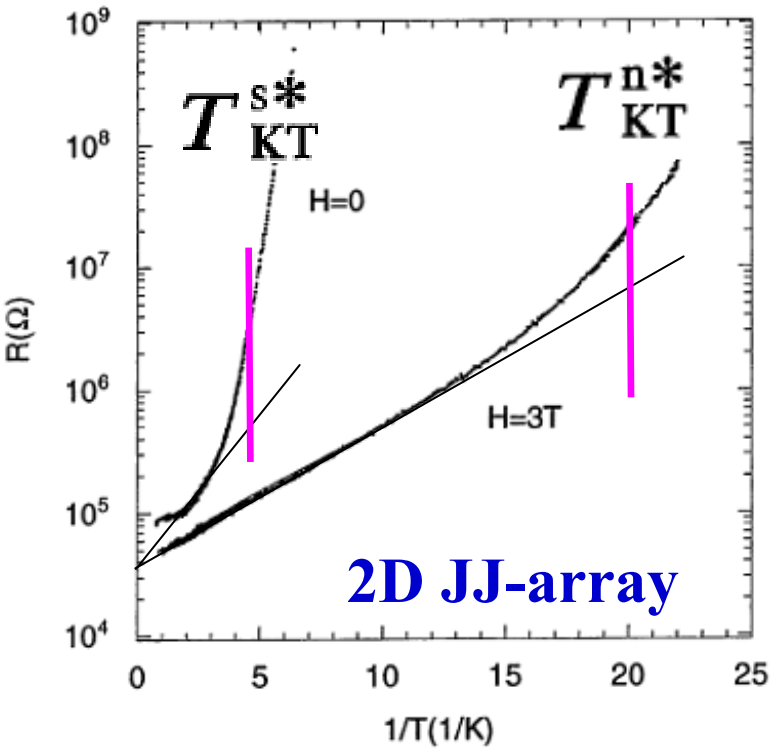

Fig. 1. Resistance at $V=50\,\mu$V as a function of $1/T$ in $H=0$ and 3 T. Solid lines are results of fitting with eq. (1). The values of fitting parameters are $K=1.6$ and $b=1.0$ in $H=0$, and $K=1.6$ and $b=2.2$ in $H=3$ T. For the values of T_{KT}, see the text.

The array was 380 junctions in length and 331 junctions in width. Each junction had an area of 0.0072 $(\mu\text{m})^2$, normal-state tunneling resistance $R_N=32\,\text{k}\Omega$ and the capacitance $C=1.1\times10^{-15}$ F. The self-capacitance of the island electrode was 5.1×10^{-17} F.

$$T_{KT}^{s*}=(0.19\pm0.01)\ \text{K} \qquad e^*=2e$$

$$T_{KT}^{n*}=(0.05\pm0.01)\ \text{K} \qquad e^*=e$$

$$T_{KT}^{s*}/T_{KT}^{n*}\sim4$$

$$k_B T_{C-BKT}=E_c=\frac{e^*}{2C}$$

Estimations

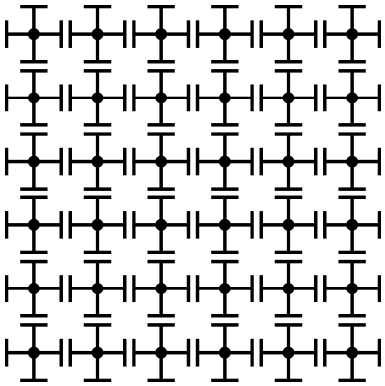

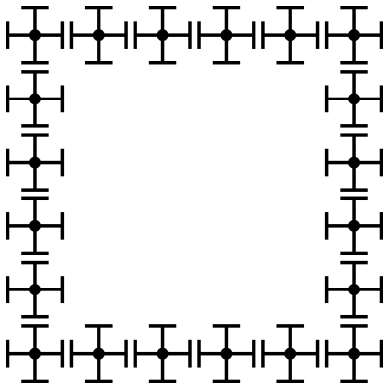

$$\tilde{b} = nb$$

$$\tilde{E}_c = nE_c$$

$$\Delta_c \cong E_c \ln(L/b) \qquad \tilde{\Delta}_c = n\Delta_c - nE_c \ln(n)$$

	T_0
continuous rC	0.63 K
perforated pC	1.9 K

why are T_0's different

$$n = 200\,\text{nm}/40\,\text{nm} = 5$$

$$\tilde{\Delta}_c = 5\Delta_c - 5E_c \ln(5) = 2\,\text{K}$$

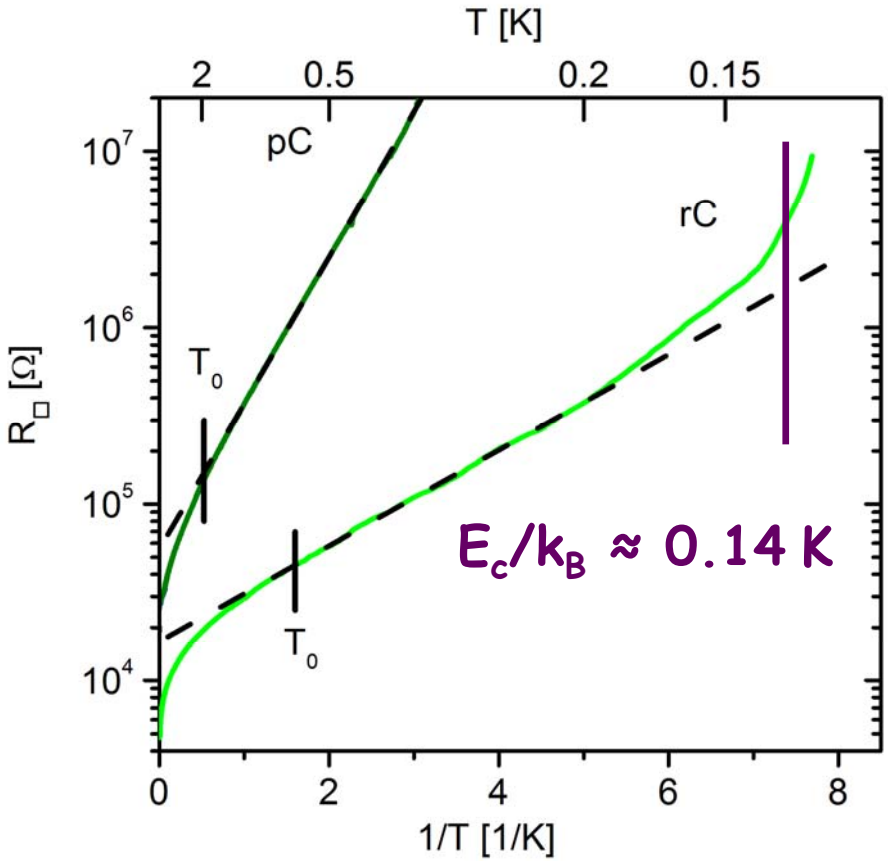

magnetoresistance

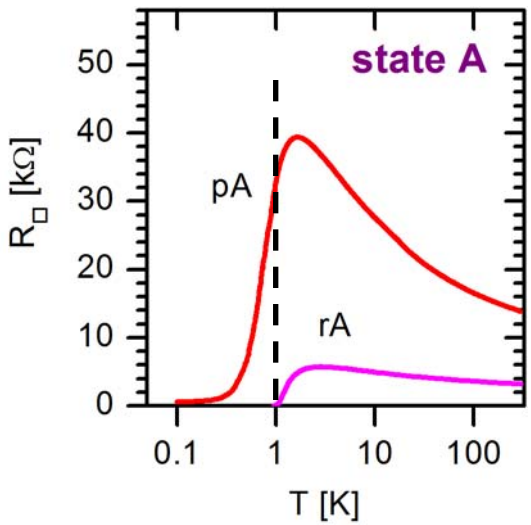

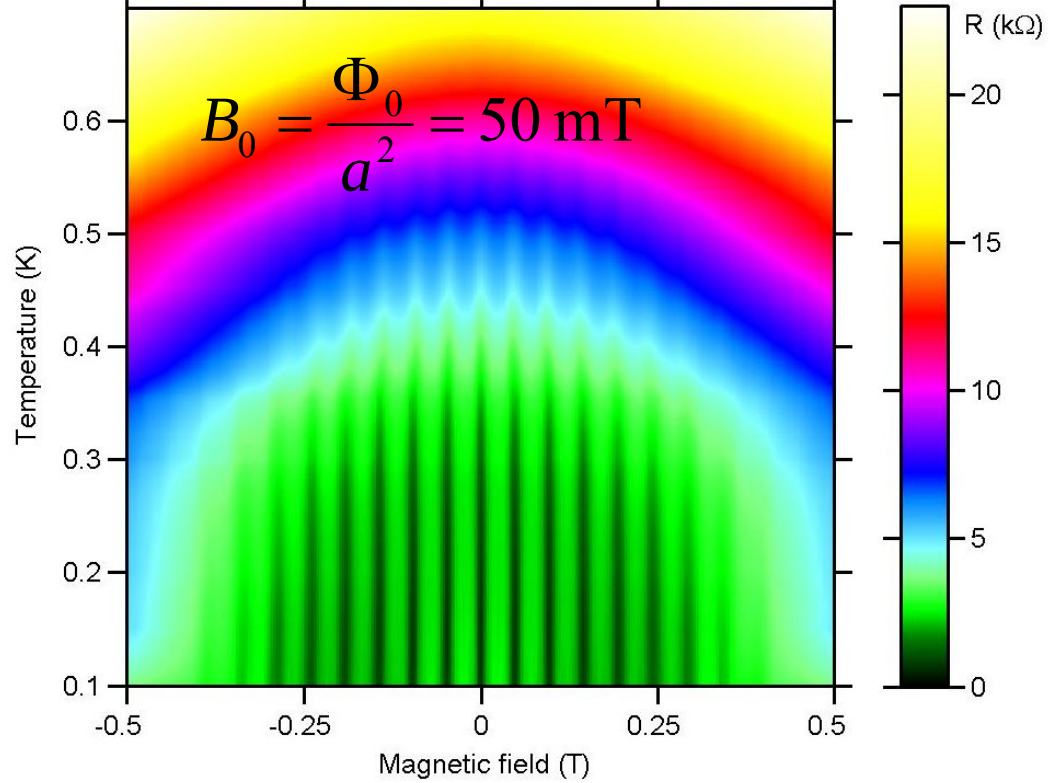

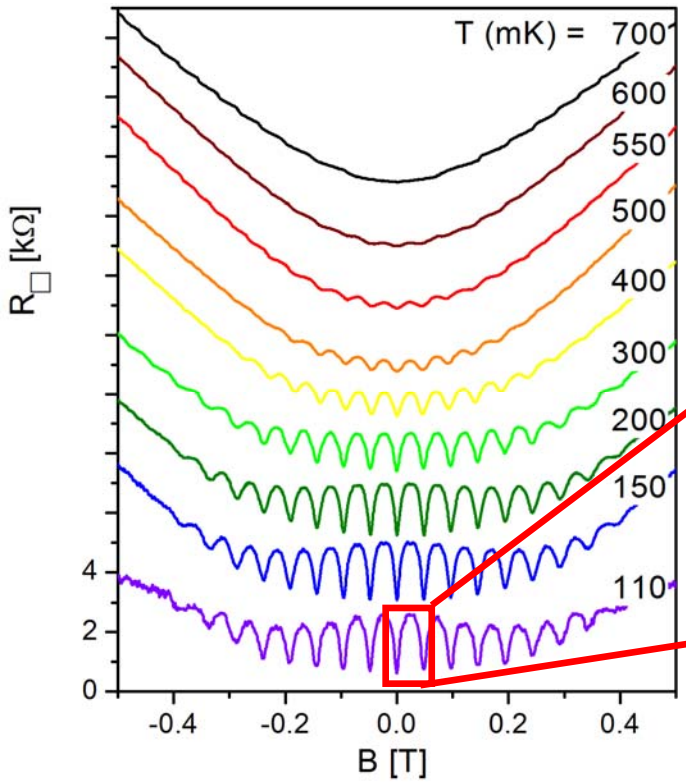

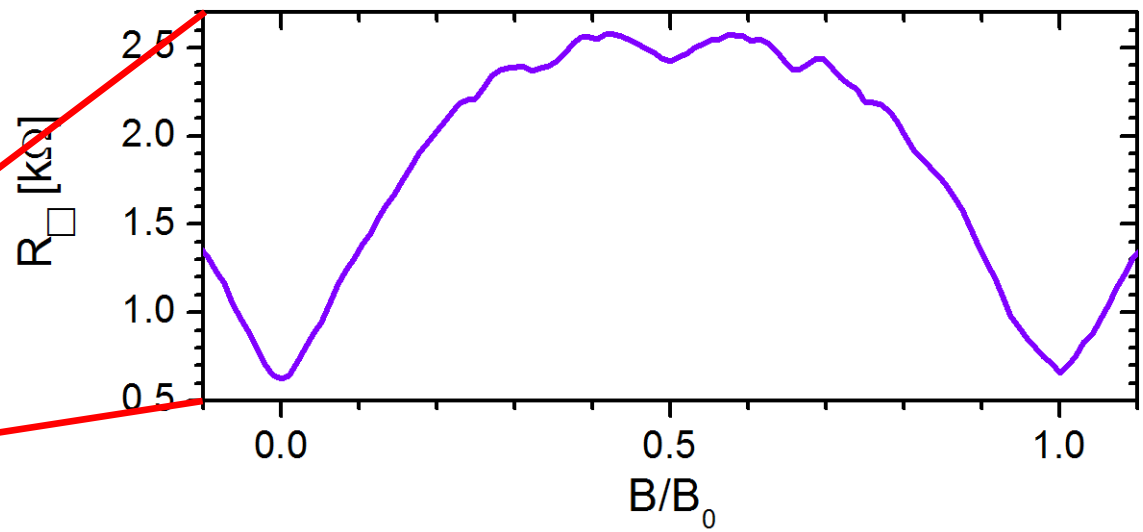

magnetoresistance

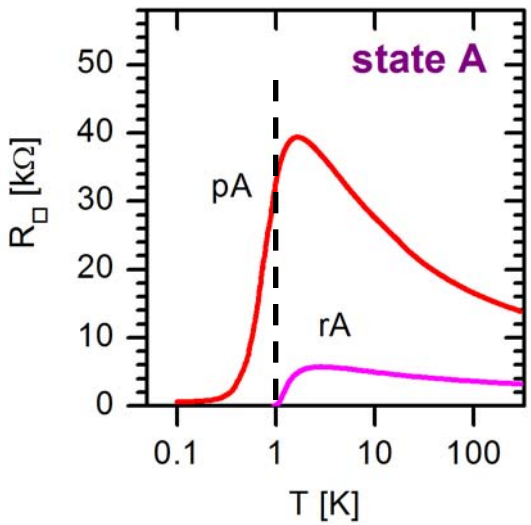

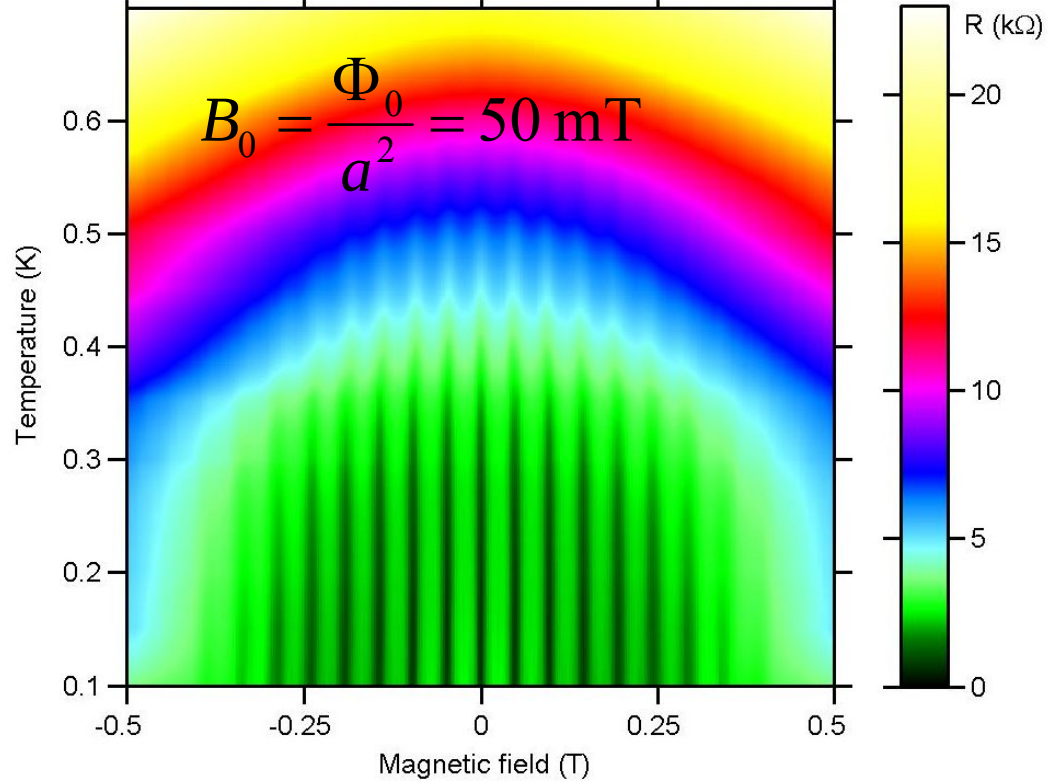

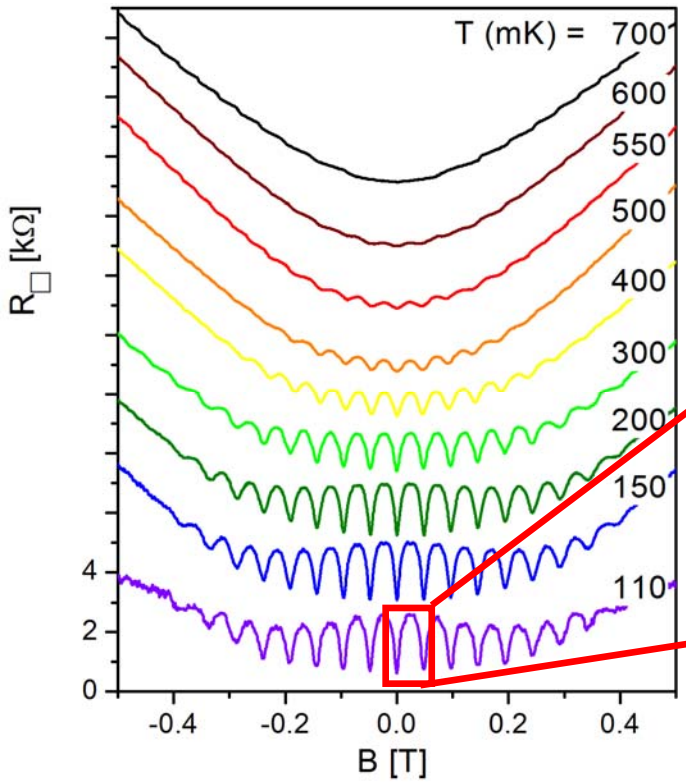

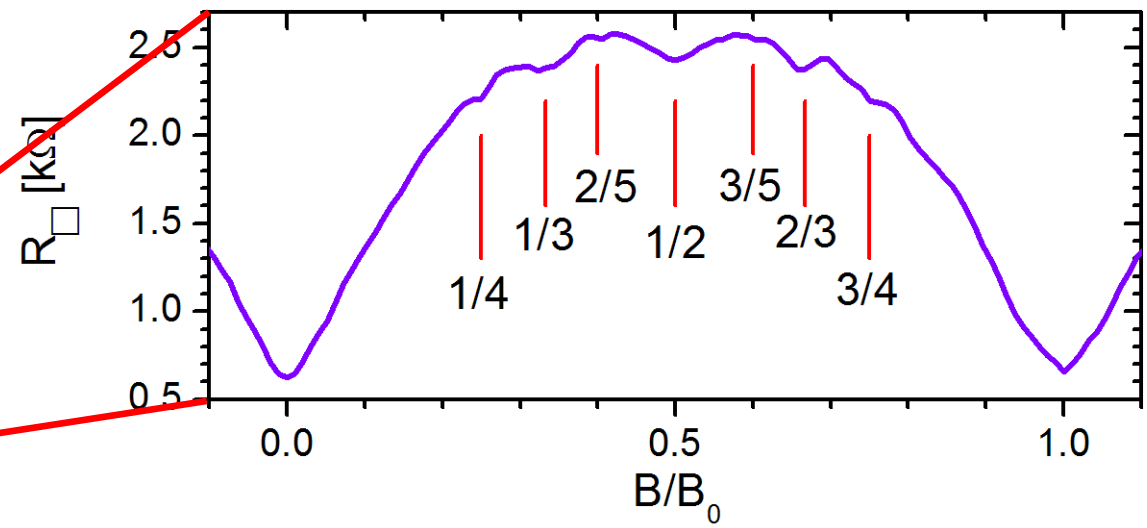

magnetoresistance

Two major features:

- ✓ fine structure of the MR oscillations
- ✓ extremely wide temperature region of the MR oscillations

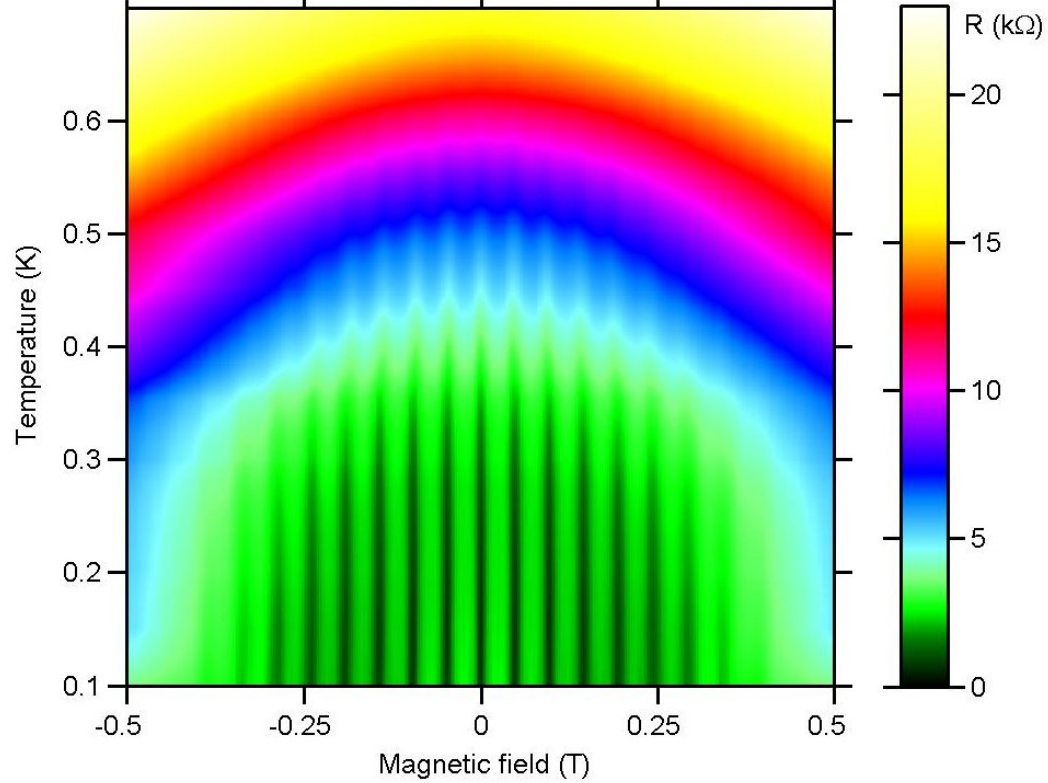

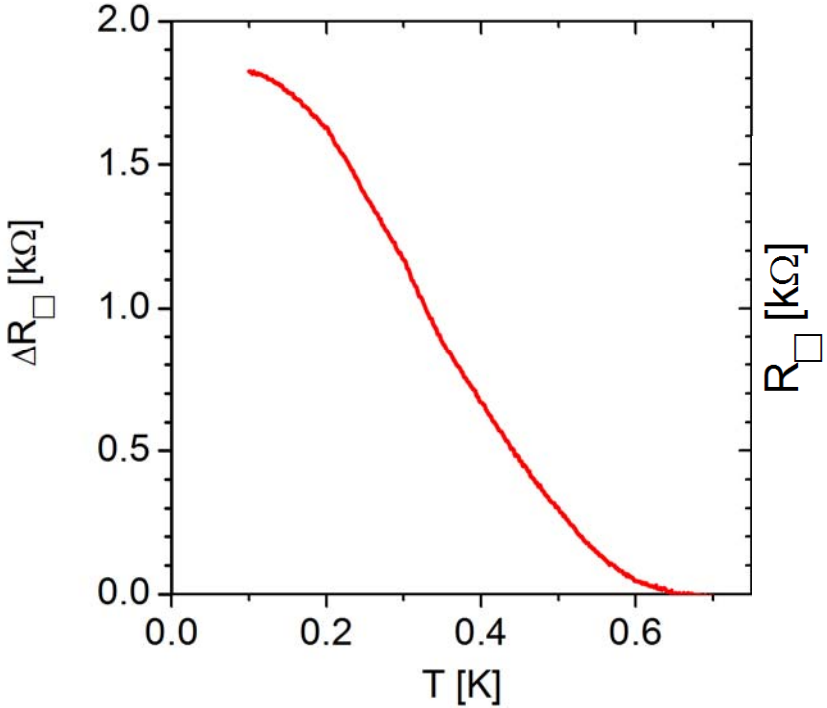

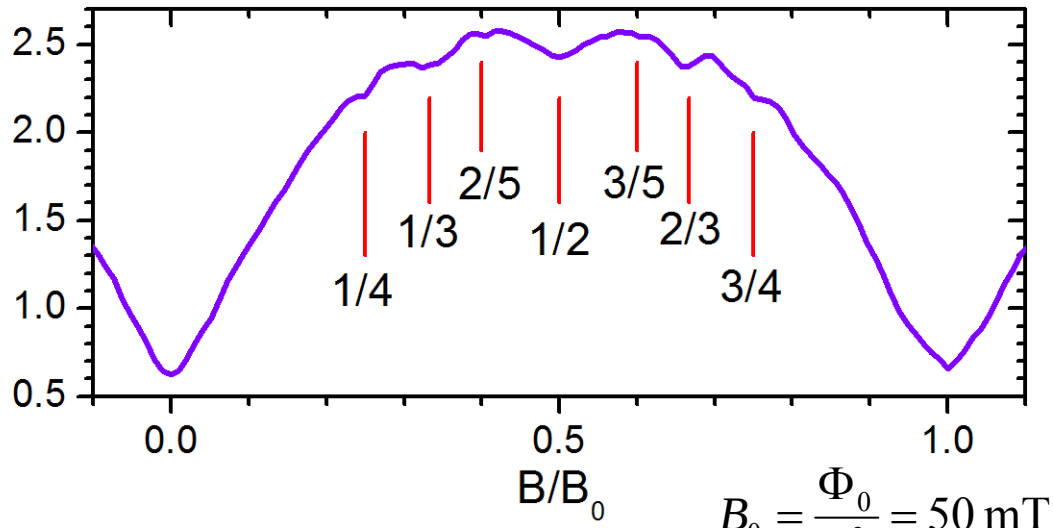

$$B_0 = \frac{\Phi_0}{a^2} = 50\,\mathrm{mT}$$

magnetoresistance

B/B_0=1/4, 1/3, 2/5, 1/2, 3/5, 2/3, 3/4

This fine structure reflects
the collective behavior of the multiconnected
superconducting film
differing it from the behavior of a single
superconducting loop

W. A. Little and R. D. Parks,
PRL 9, 9 (1962).

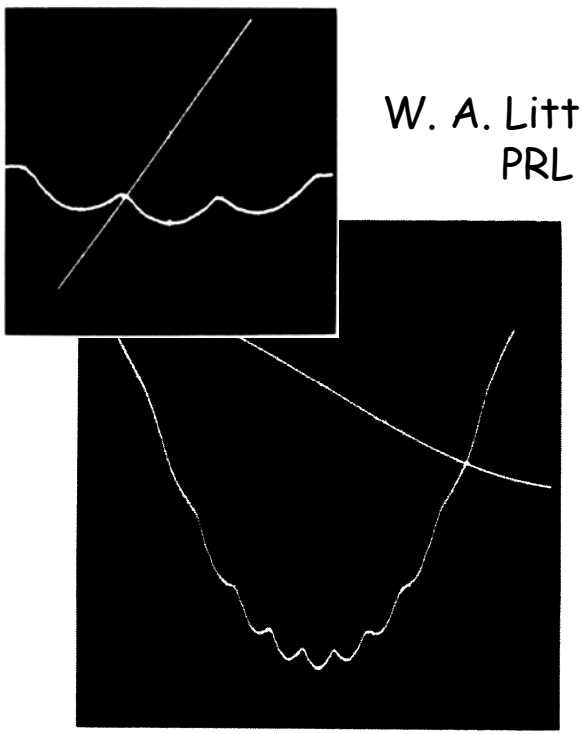

FIG. 2. Lower trace: variation of resistance of tin cylinder at its superconducting transition temperature as a function of magnetic field. Upper trace: magnetic field sweep.

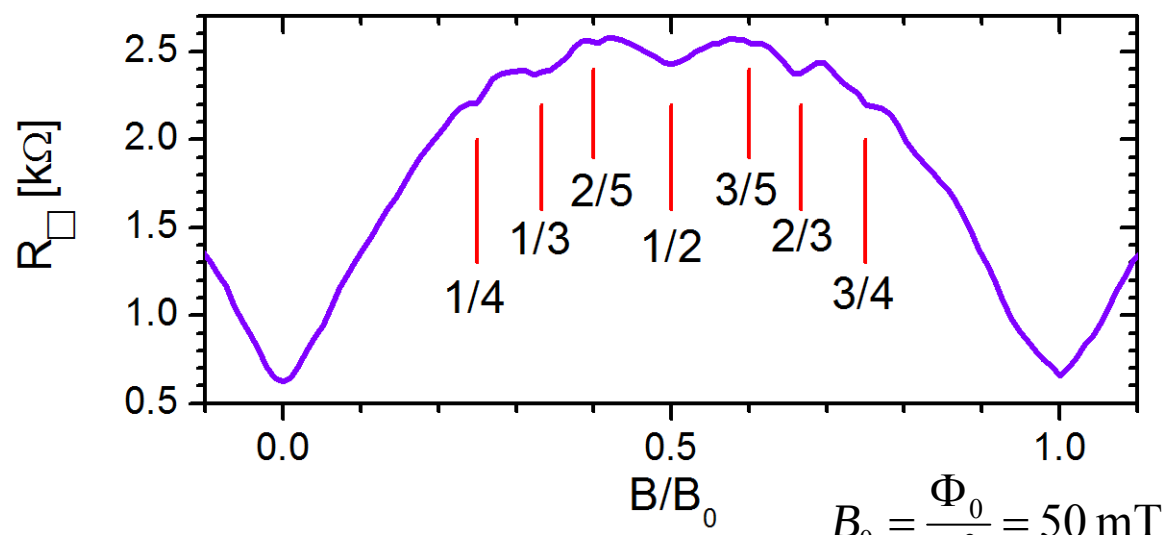

$$B_0 = \frac{\Phi_0}{a^2} = 50\,\mathrm{mT}$$

magnetoresistance

$B/B_0=1/2$ square 2D JJ arrays

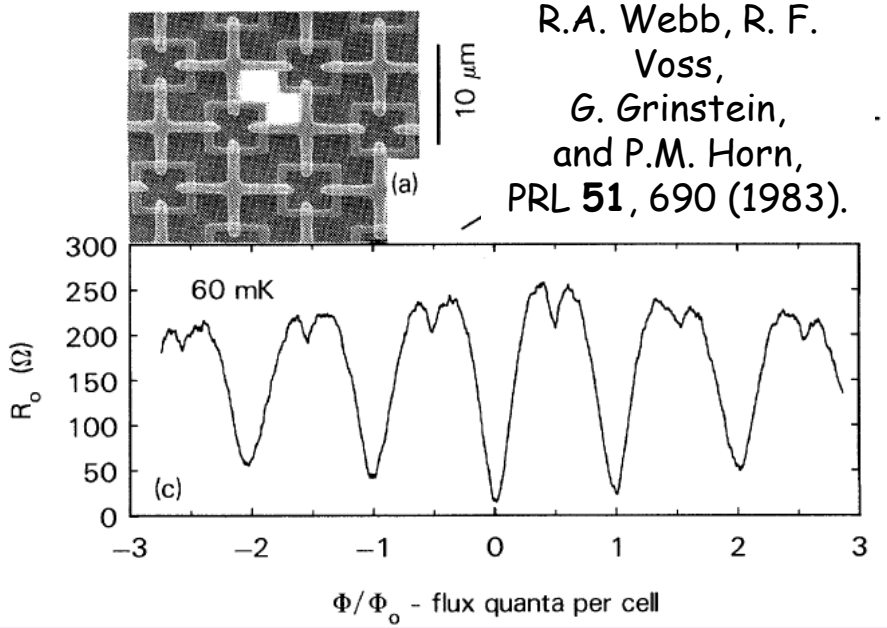

R.A. Webb, R. F. Voss, G. Grinstein, and P.M. Horn, PRL **51**, 690 (1983).

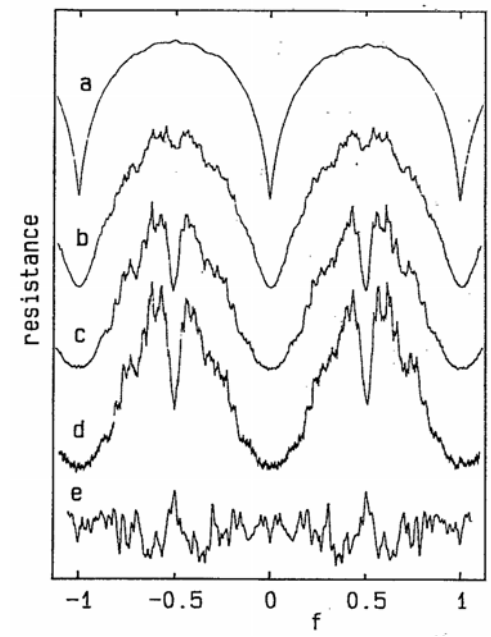

B. J. van Wees, H. S. J. van der Zant, and J. E. Mooij, PRB **35**, 7291 (1987).

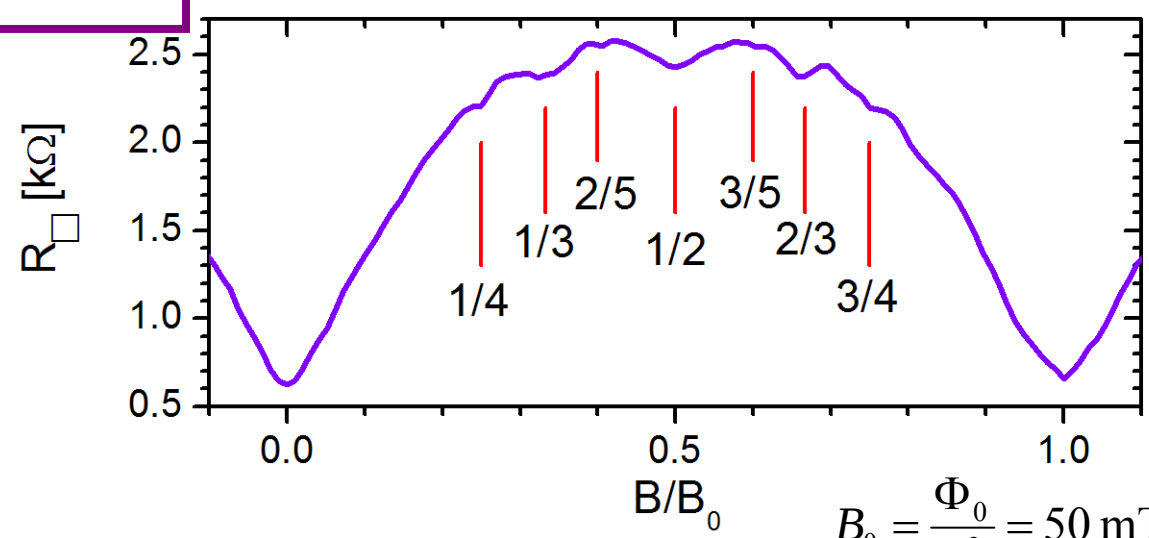

$$B_0 = \frac{\Phi_0}{a^2} = 50\,\mathrm{mT}$$

magnetoresistance

B/B_0=1/4, 1/3, 2/5, 1/2, 3/5, 2/3, 3/4

square 2D JJ arrays

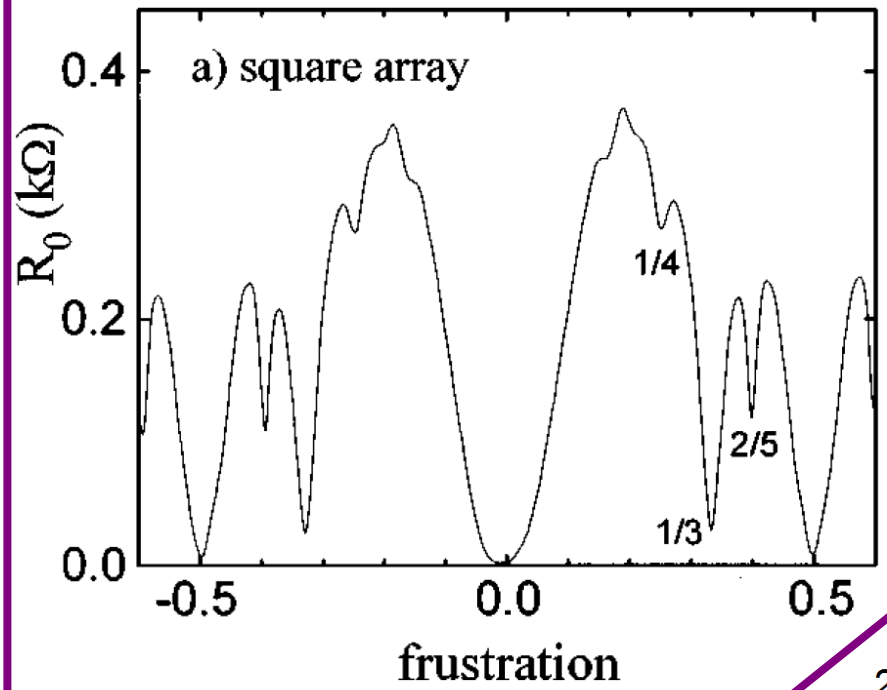

H. S. J. van der Zant, W. J. Elion, L. J. Geerligs, and J. E. Mooij, Phys. Rev. B 54, 10081 (1996).

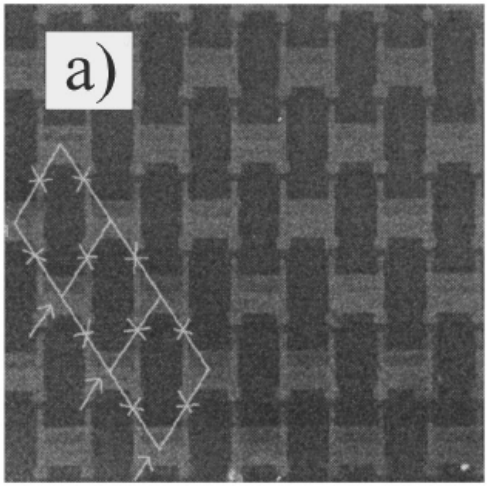

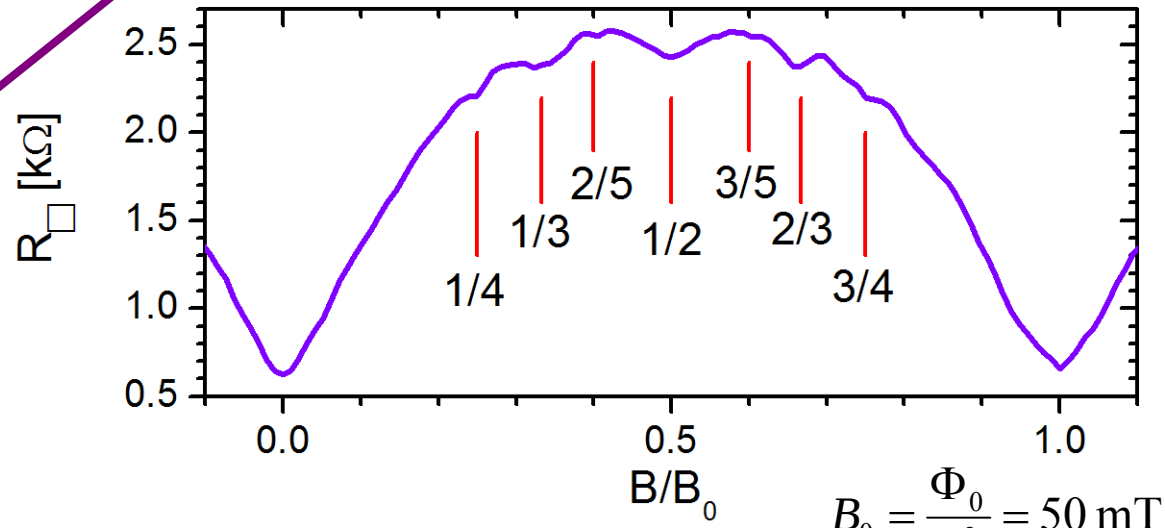

$$B_0 = \frac{\Phi_0}{a^2} = 50\,\mathrm{mT}$$

magnetoresistance

$B/B_0=1/2$

proximity effect
junction arrays

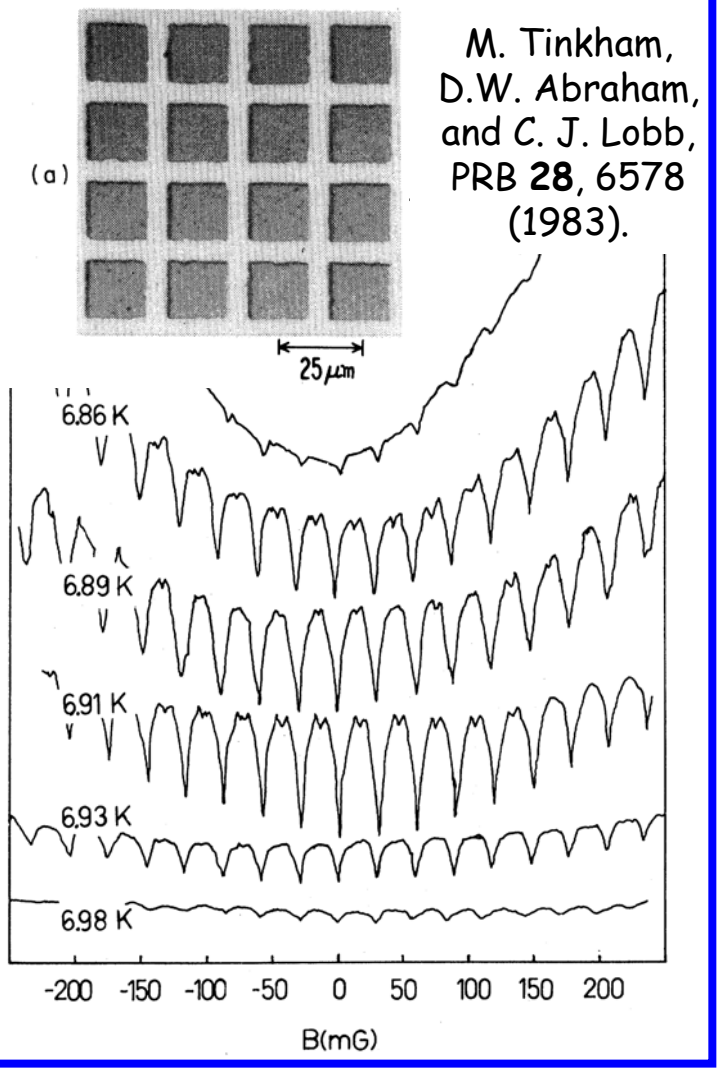

M. Tinkham, D.W. Abraham, and C. J. Lobb, PRB **28**, 6578 (1983).

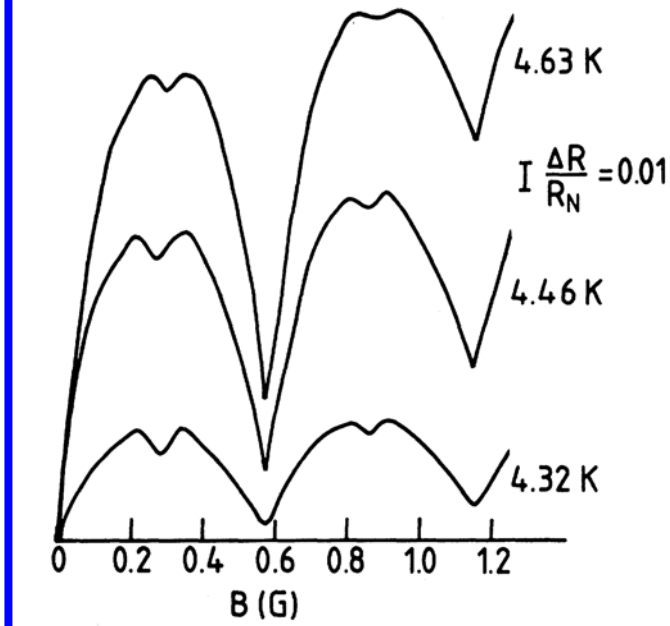

D. Kimhi, F. Leyvras, and D. Ariosa, PRB **29**, 1487 (1984).

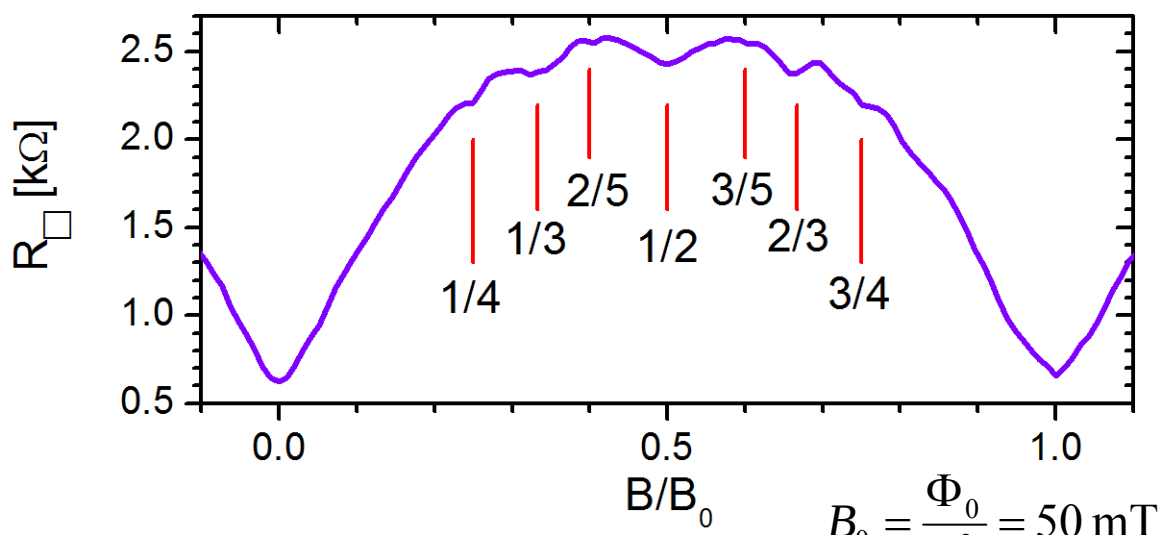

$$B_0=\frac{\Phi_0}{a^2}=50\,\mathrm{mT}$$

magnetoresistance

B/B_0=1/4, 1/3, 2/5, 1/2, 3/5, 2/3, 3/4

proximity effect junction arrays

S.P. Benz, M. S. Rzchowski, M. Tinkham, and C. J. Lobb, Phys. Rev. B **42**, 6165 (1990).

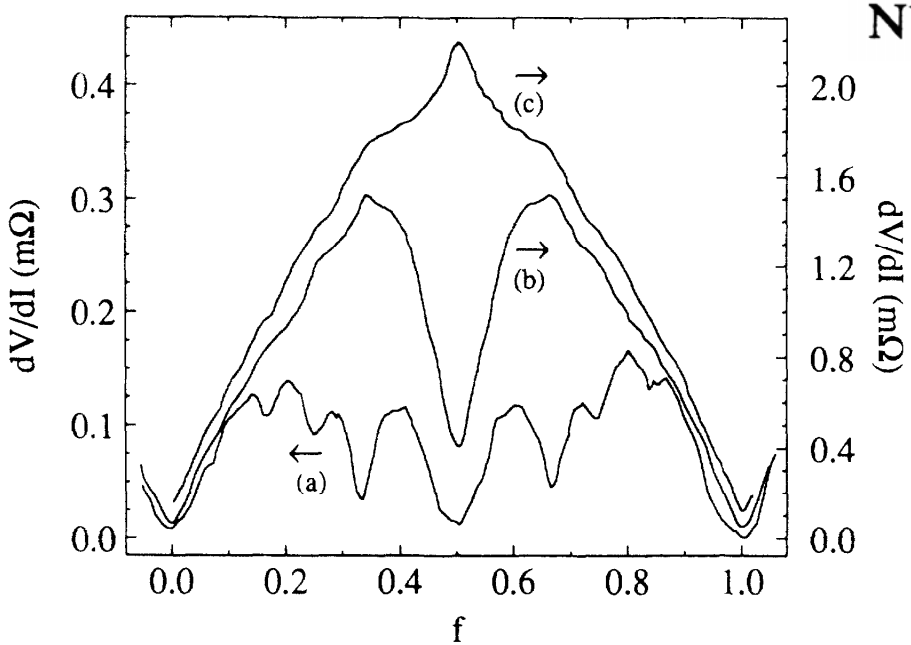

FIG. 2. Magnetoresistance at $T = 2.09$ K for three different dc bias currents: (a) 0.92 mA, (b) 1.84 mA, and (c) 2.79 mA. Note that the left and right vertical scales differ by a factor of 5. Minima in the dynamic resistance coincide with magnetic fields where the vortex superlattice is commensurate with the array of junctions, namely $f = 0, \frac{1}{6}, \frac{1}{4}, \frac{1}{3}, \frac{1}{2}, \frac{2}{3}, \frac{3}{4}, \frac{5}{6}$, and 1.

Nb-Cu-Nb proximity-effect junctions.

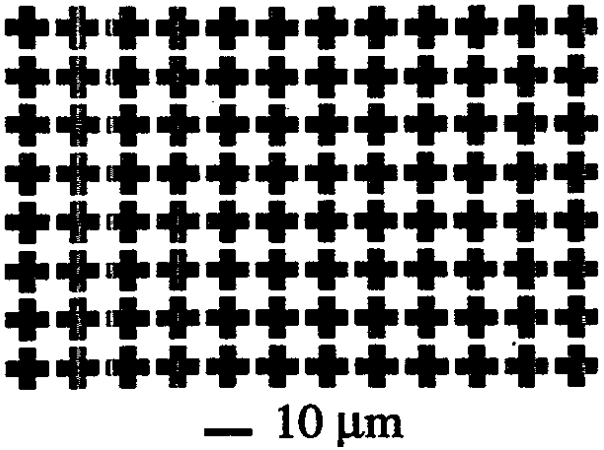

The lower current, the smaller amplitude, the more pronounced fine structure

magnetoresistance

$B/B_0=1/2$ perforated films and superconducting wire networks

B. Pannetier, J. Chaussy, R. Rammal, and J. C. Villegier, PRL **53**, 1845 (1984).

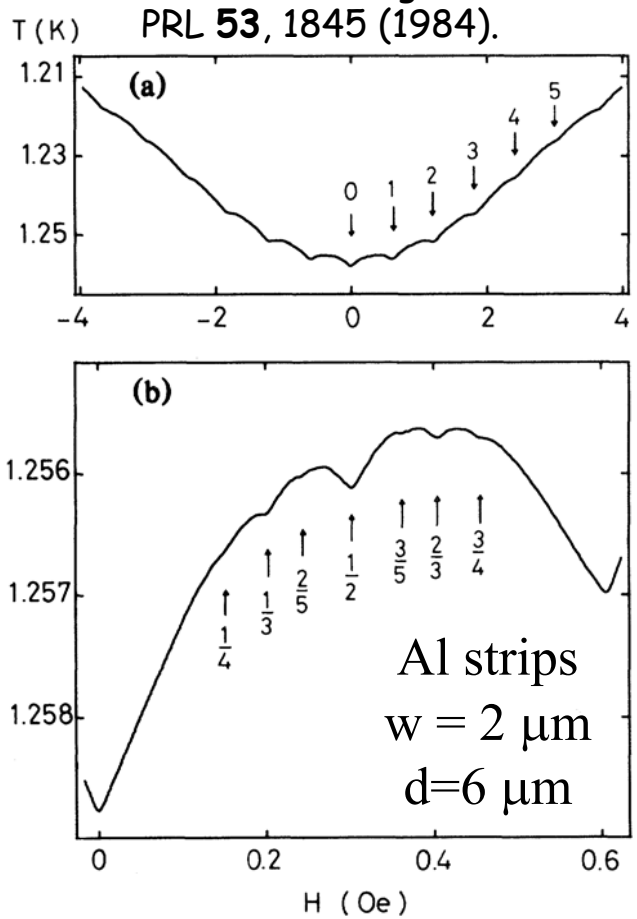

T. I. Baturina et al., Physica B **329**, 1496 (2003).

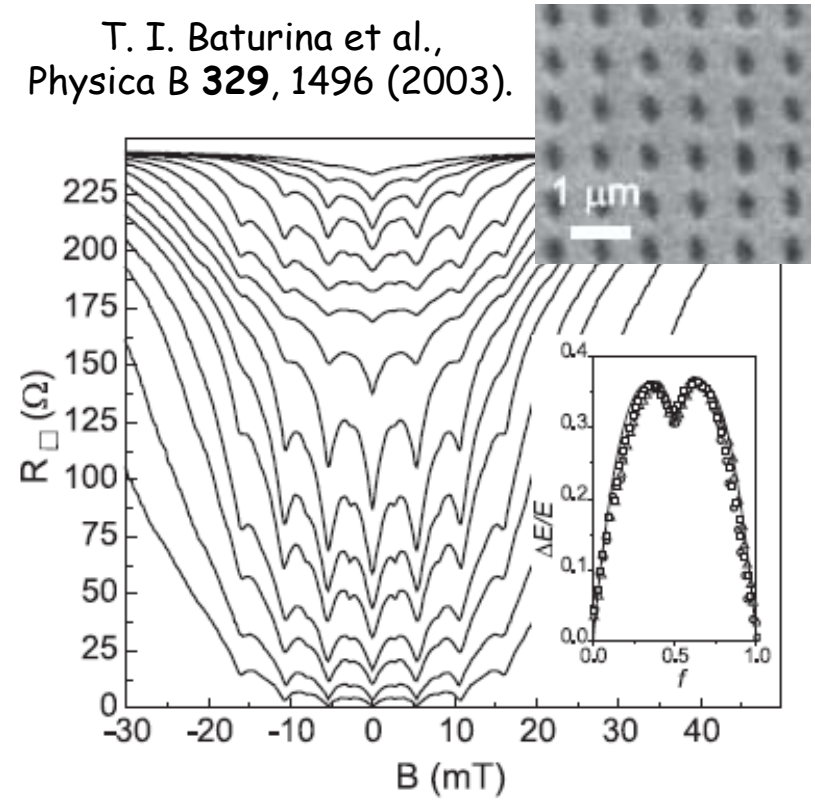

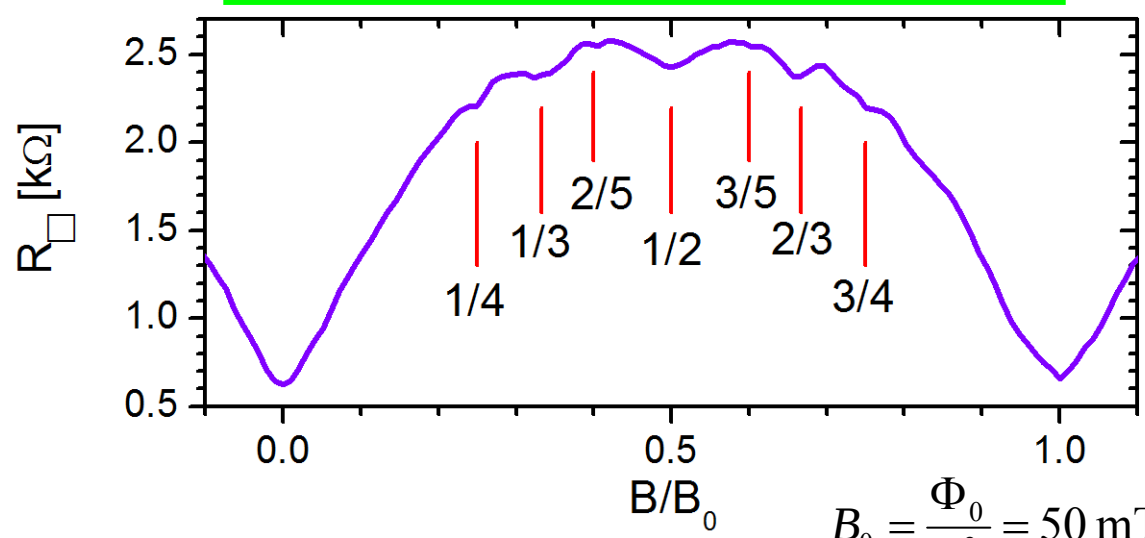

$$B_0 = \frac{\Phi_0}{a^2} = 50\ \mathrm{mT}$$

magnetoresistance

B/B_0=1/4, 1/3, 2/5, 1/2, 3/5, 2/3, 3/4

perforated films and superconducting wire networks

critical temperature variation

B. Pannetier, J. Chaussy, R. Rammal, and J. C. Villegier, PRL **53**, 1845 (1984).

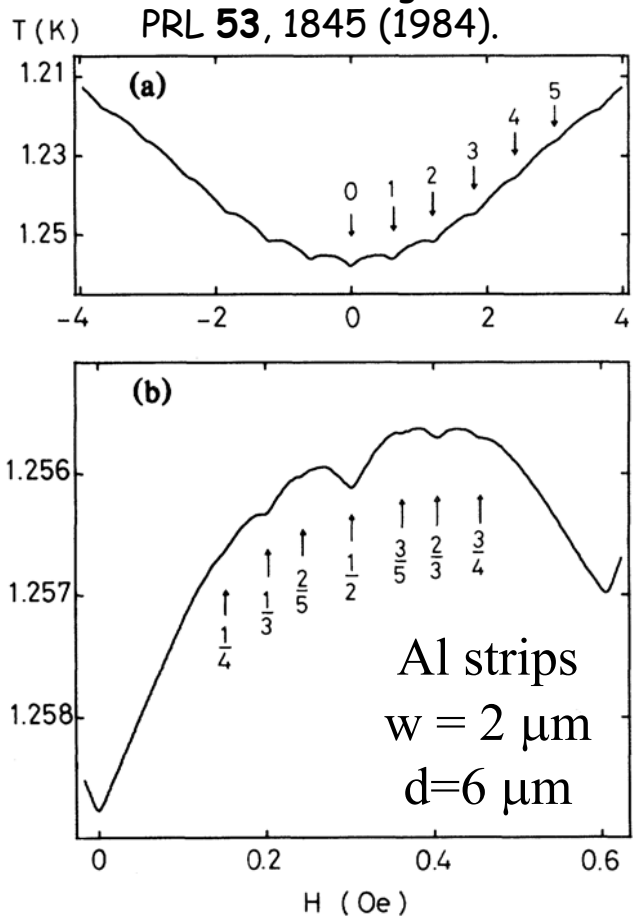

As the magnetic field is increased, the resistance change is fed back to the temperature regulation in order to keep the network at a constant value R_0 ($=0.1\ \Omega$) chosen at the steepest slope in the resistive transition. The field-dependent critical temperature $T_c(H)$ is defined as the temperature for which $R(T)=R_0$. By this method, the network is maintained at $T=T_c(H)$ during the sweep of the field.

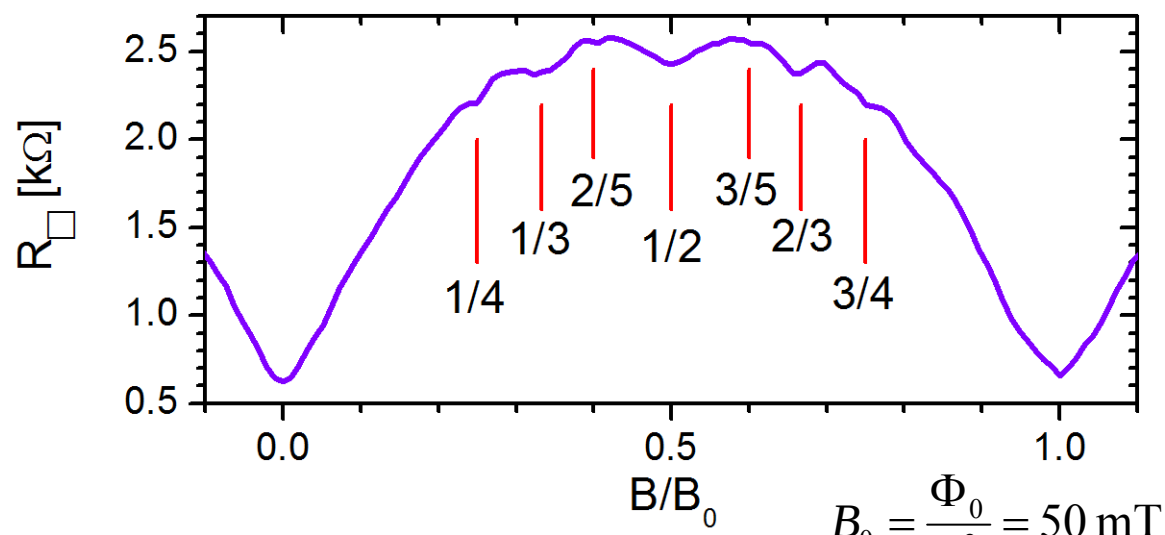

$$B_0 = \frac{\Phi_0}{a^2} = 50\ \mathrm{mT}$$

magnetoresistance

B/B_0=1/4, 1/3, 2/5, 1/2, 3/5, 2/3, 3/4

perforated films and superconducting wire networks

B. Pannetier, J. Chaussy, R. Rammal, and J. C. Villegier, PRL **53**, 1845 (1984).

Harper equation

P.G. Harper, Proc. Phys. Soc. London A 68, 874 (1955).

$$\psi_{n+1} + \psi_{n-1} + 2\cos(2\pi\Phi n + \alpha)\psi_n = \epsilon\psi_n$$

$Ba^2/\Phi_0 \equiv \Phi/\Phi_0 = p/q$, p and q are relative prime numbers

The fields at which resistivity exhibits the dips are defined by the boundaries of the energy spectrum as function of the magnetic field $E(\Phi)$

The change in the magnetoresistance is calculated as

$$\Delta R(B) \propto \arccos^2\left[E(\Phi)/4\right]$$

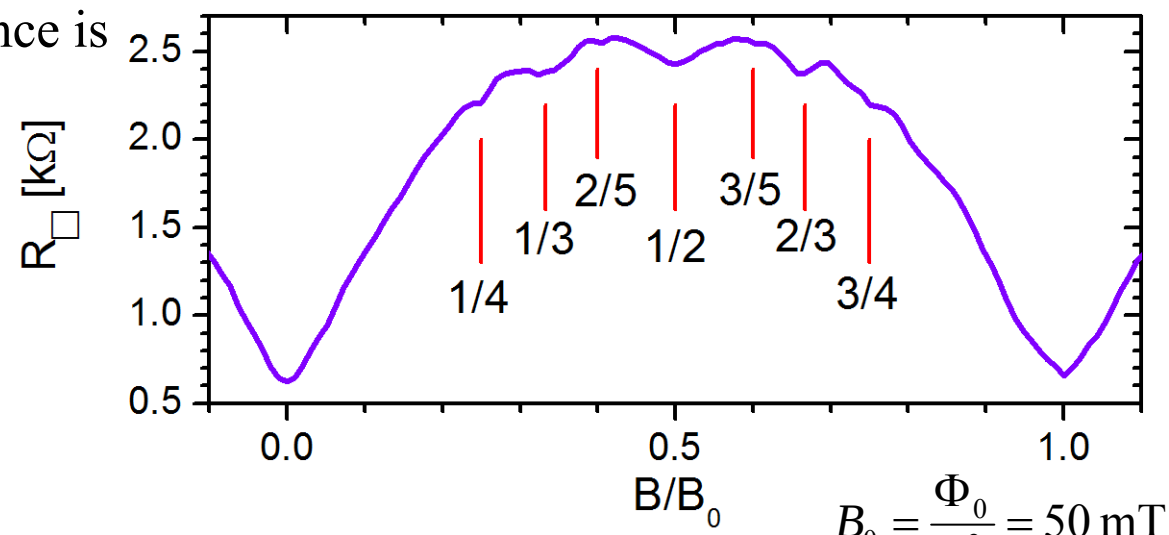

$$B_0 = \frac{\Phi_0}{a^2} = 50\,\mathrm{mT}$$

magnetoresistance

B/B_0=1/4, 1/3, 2/5, 1/2, 3/5, 2/3, 3/4

perforated films and superconducting wire networks

B. Pannetier, J. Chaussy, R. Rammal, and J. C. Villegier, PRL **53**, 1845 (1984).

Harper equation

P.G. Harper, Proc. Phys. Soc. London A 68, 874 (1955).

$$\psi_{n+1} + \psi_{n-1} + 2\cos(2\pi\Phi n + \alpha)\psi_n = \epsilon\psi_n$$

$Ba^2/\Phi_0 \equiv \Phi/\Phi_0 = p/q$, p and q are relative prime numbers

The fields at which resistivity exhibits the dips are defined by the boundaries of the energy spectrum as function of the magnetic field $E(\Phi)$

The change in the magnetoresistance is calculated as

$$\Delta R(B) \propto \arccos^2\left[E(\Phi)/4\right]$$

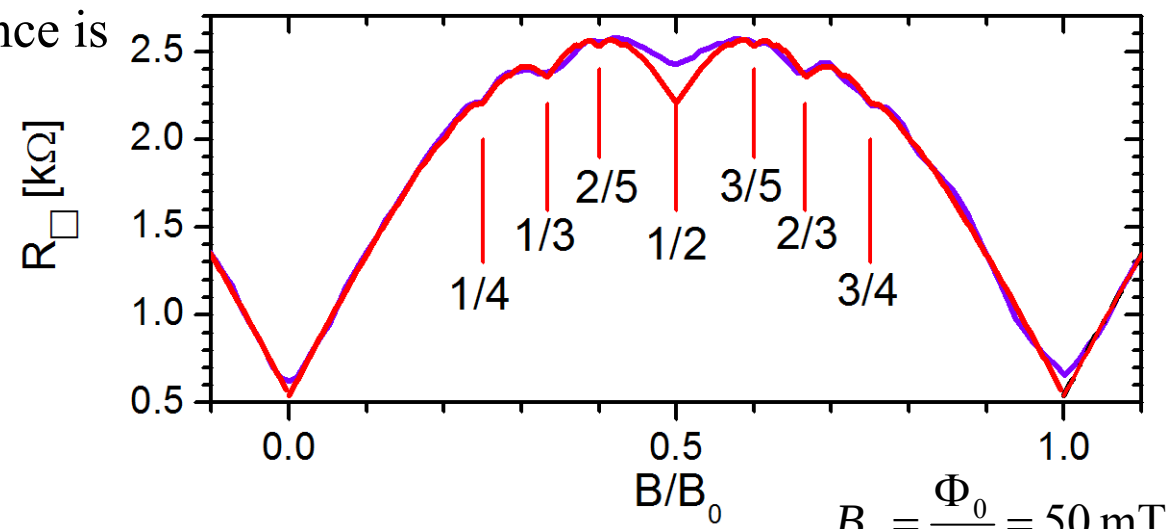

$$B_0 = \frac{\Phi_0}{a^2} = 50\,\mathrm{mT}$$

magnetoresistance

Two major features:

- ✓ fine structure of the MR oscillations
- ✓ extremely wide temperature region of the MR oscillations

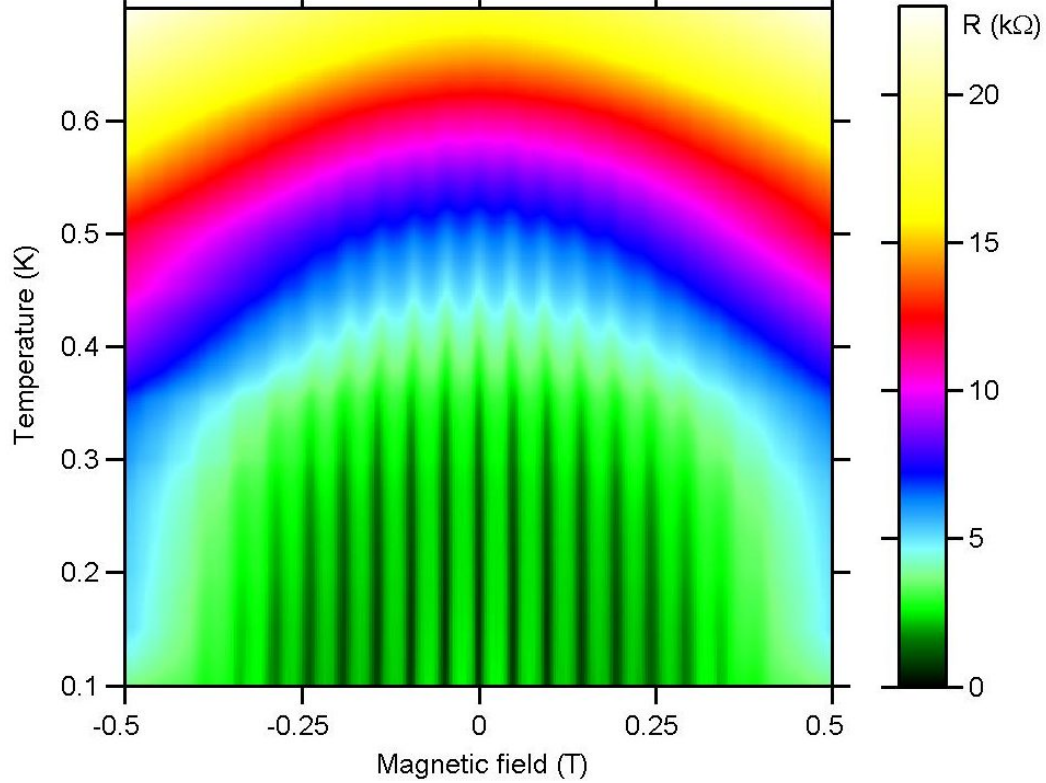

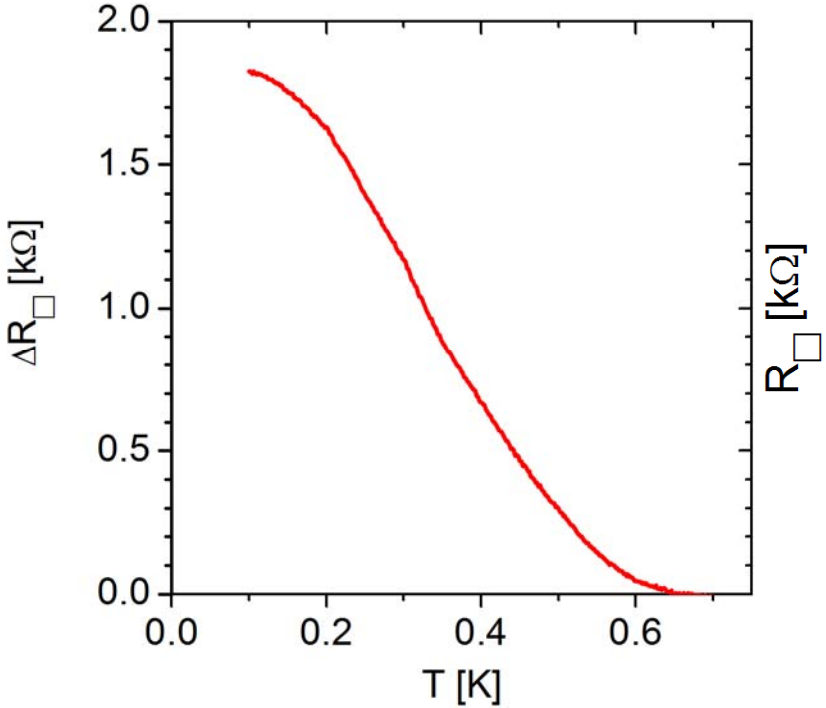

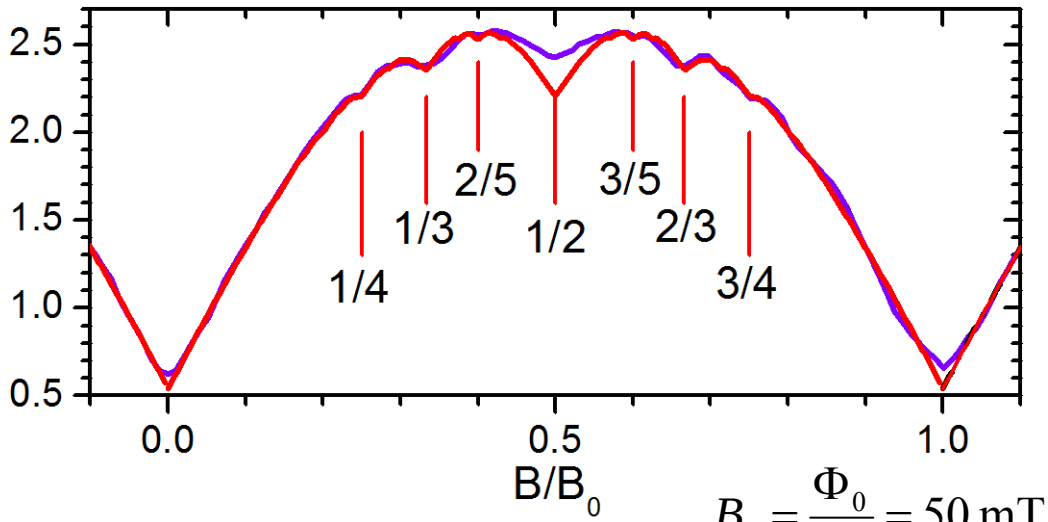

$$B_0 = \frac{\Phi_0}{a^2} = 50\,\mathrm{mT}$$

magnetoresistance

temperature region of the MR oscillations

The MR oscillations in the perforated films and/or superconducting wire networks, were usually found in the close proximity to T_c (if measured in the linear response regime)

A.T. Fiory, A. F. Hebard, and S. Somekh, Appl. Phys. Lett. 32, 73 (1978).

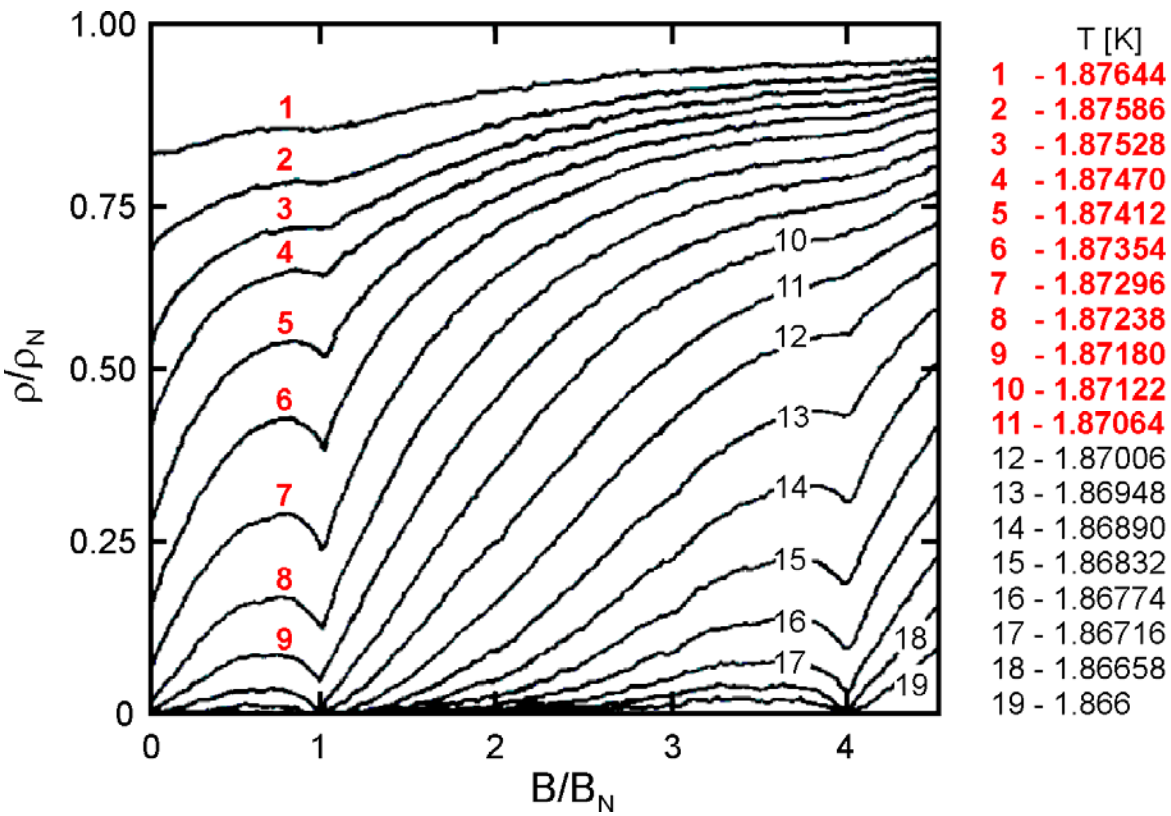

$w = 2\ \mu m$

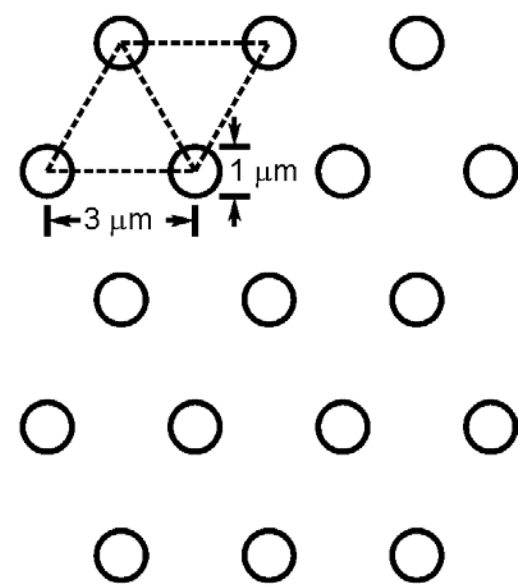

magnetoresistance

temperature region of the MR oscillations

The MR oscillations in the perforated films and/or superconducting wire networks, were usually found in the close proximity to T_c (if measured in the linear response regime)

A.T. Fiory, A. F. Hebard, and S. Somekh, Appl. Phys. Lett. 32, 73 (1978).

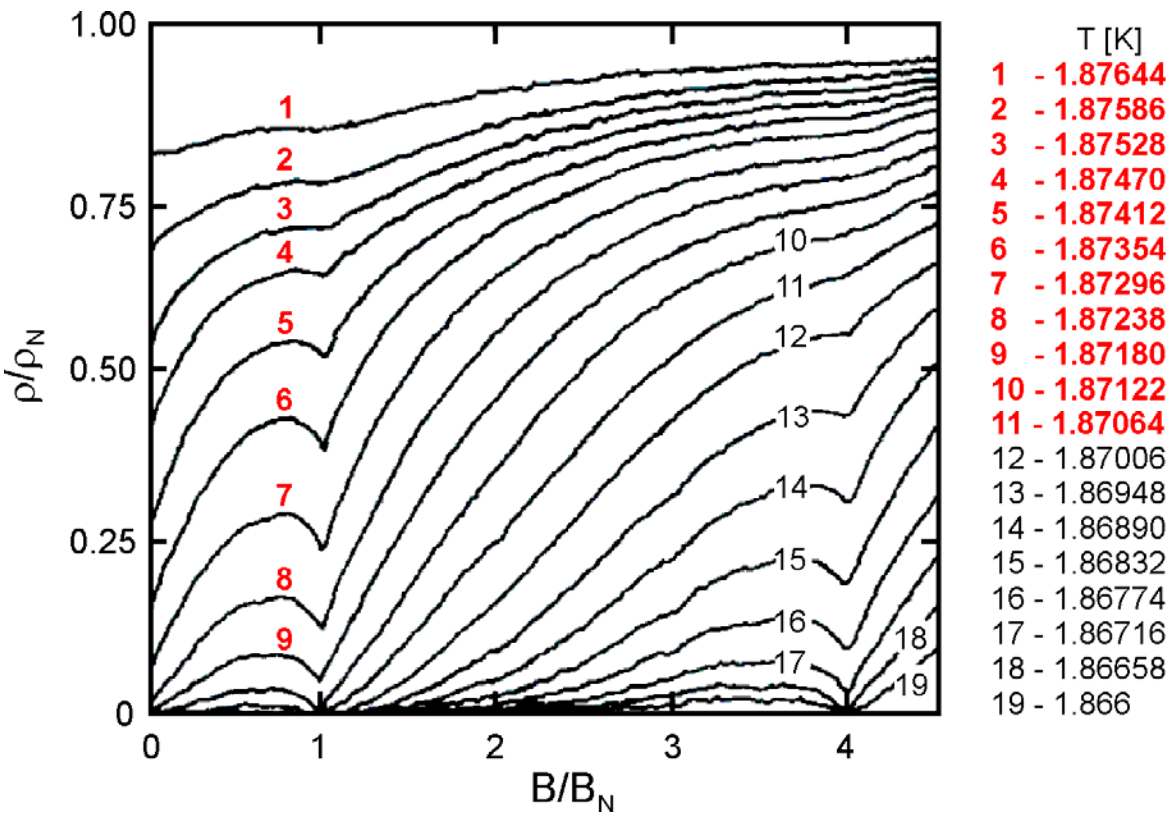

Estimations

$$\xi_d(0) \approx 26\ \text{nm}$$

$$w = 2\ \mu\text{m}$$

$$\xi_d(T) = \xi_d(0)\sqrt{1 - T/T_c}$$

at $T = 1.87$ K

$$w/\xi_d(T) \approx 4.4$$

$$\Delta T \approx 6\ \text{mK}$$

$$\Delta T / T_c \approx 0.003$$

magnetoresistance

temperature region of the MR oscillations

The MR oscillations in the perforated films and/or superconducting wire networks, were usually found in the close proximity to T_c (if measured in the linear response regime)

A.D. Thakur et al.,
Appl. Phys. Lett. 94, 262501 (2009).

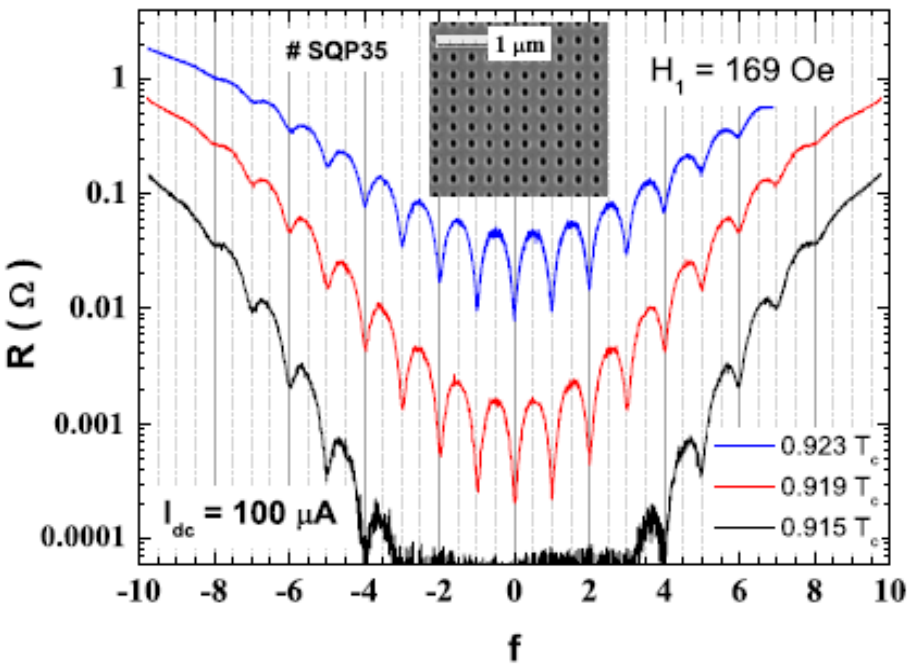

FIG. 3. (Color online) R vs f data obtained with a drive current $I_{dc}=100$ μA for a square antidot lattice observed in the temperature range of $0.915T_c$ and $0.923T_c$. The inset panel shows the SIB image of a portion of the square antidot lattice with a pitch of 350 nm and an average antidot diameter of 180 nm.

A. Hoffmann, P. Prieto, and I. K. Schuller,
PRB 61, 6958(R) (2000).

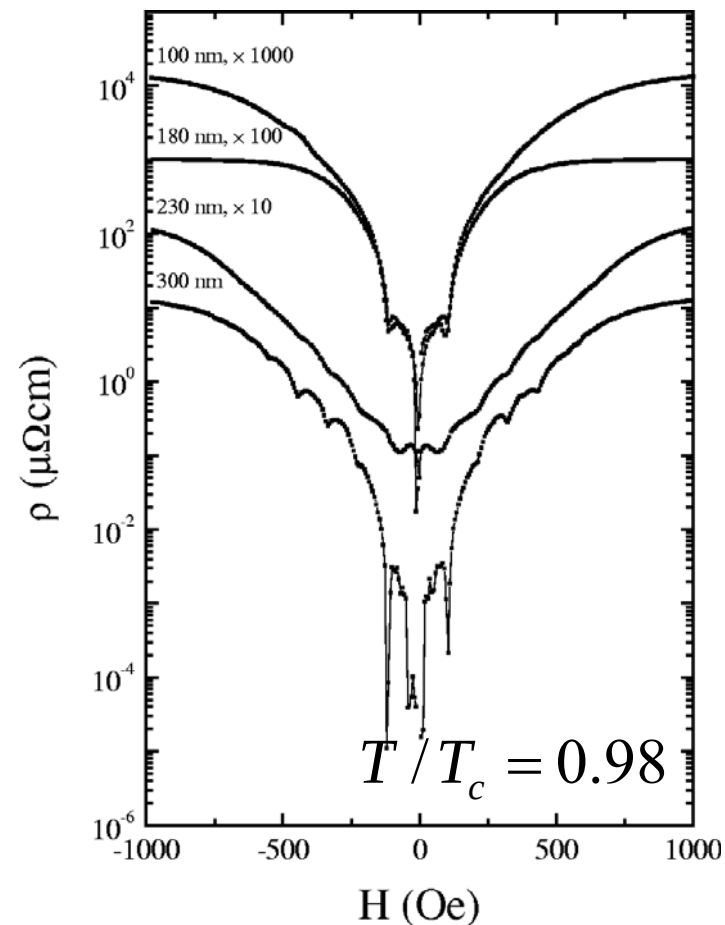

magnetoresistance

temperature region of the MR oscillations

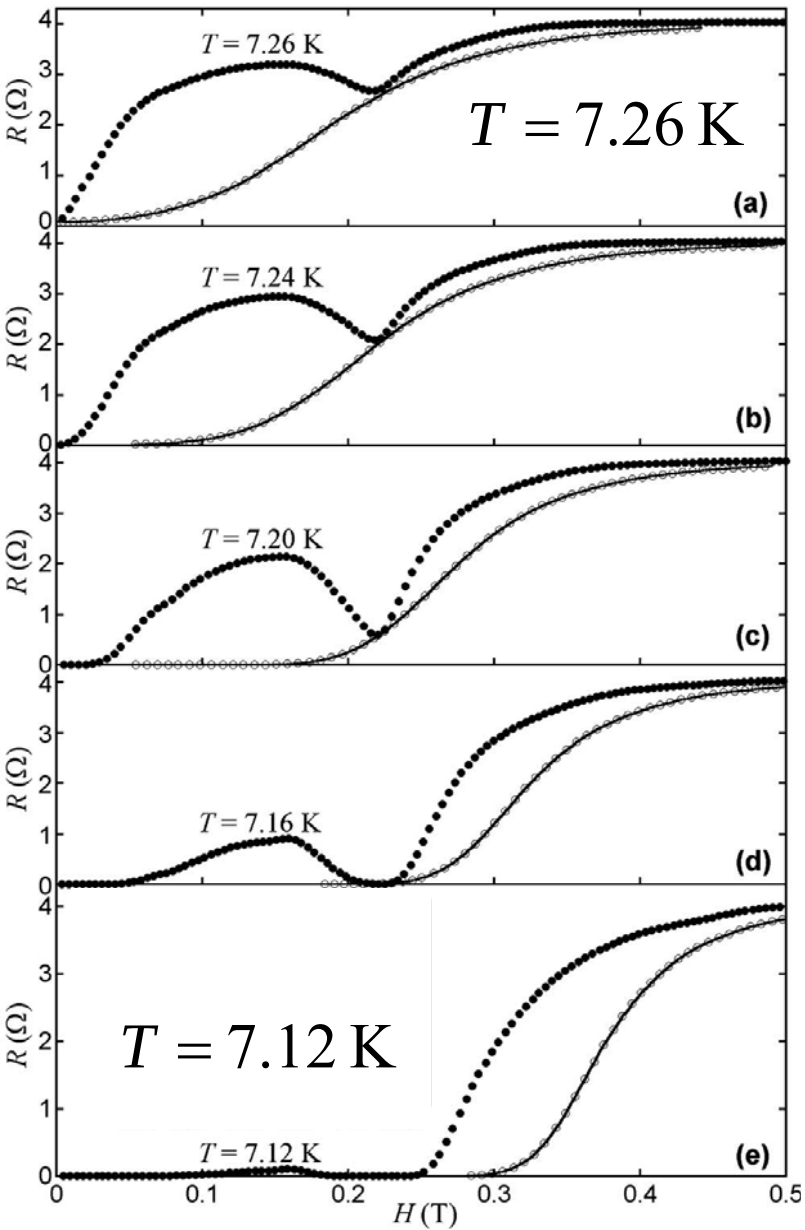

U. Patel, Z. L. Xiao, J. Hua, T. Xu, D. Rosenmann, V. Novosad, J. Pearson, U. Welp, W.K. Kwok, and G.W. Crabtree, Phys. Rev. B 76, 020508(R) (2007).

$$T_c = 7.310\,\mathrm{K}$$

$$\Delta T / T_c \approx 0.026$$

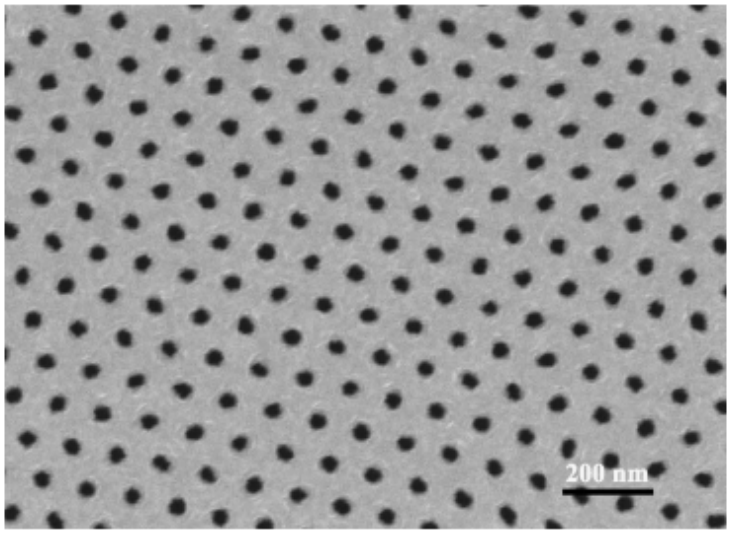

FIG. 2. SEM micrograph of a 60 nm thick Nb film deposited on an AAO substrate containing a triangular channel array (sample A).

magnetoresistance

temperature region of the MR oscillations

The MR oscillations in the perforated films and/or superconducting wire networks, were usually found in the close proximity to T_c (if measured in the linear response regime)

B. Pannetier, J. Chaussy, R. Rammal, and J. C. Villegier, PRL **53**, 1845 (1984).

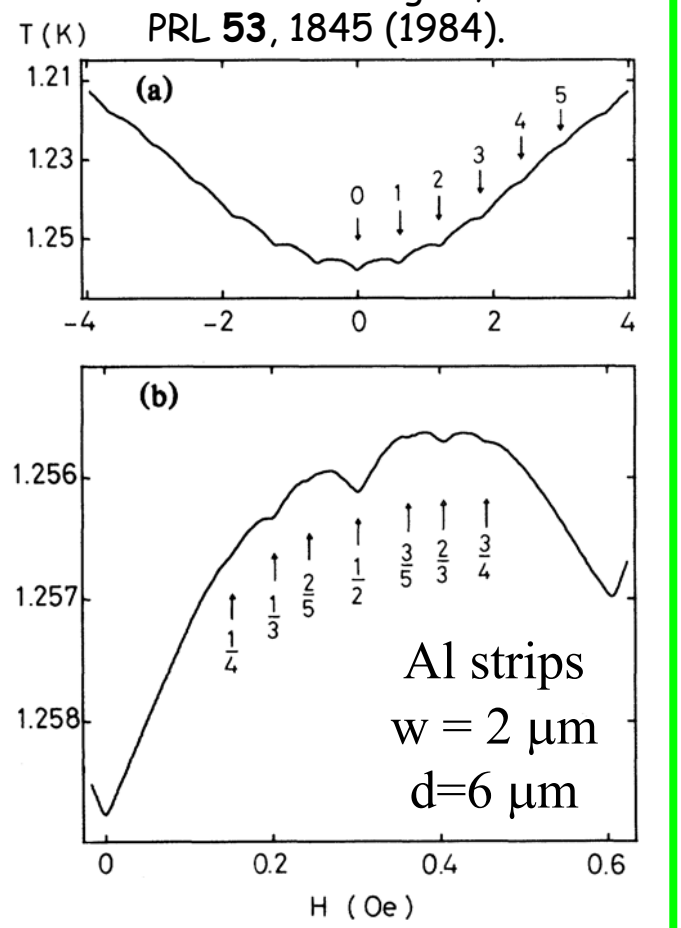

magnetoresistance

temperature region of the MR oscillations

The MR oscillations in the perforated films and/or superconducting wire networks, were usually found in the close proximity to T_c (if measured in the linear response regime)

with few exceptions

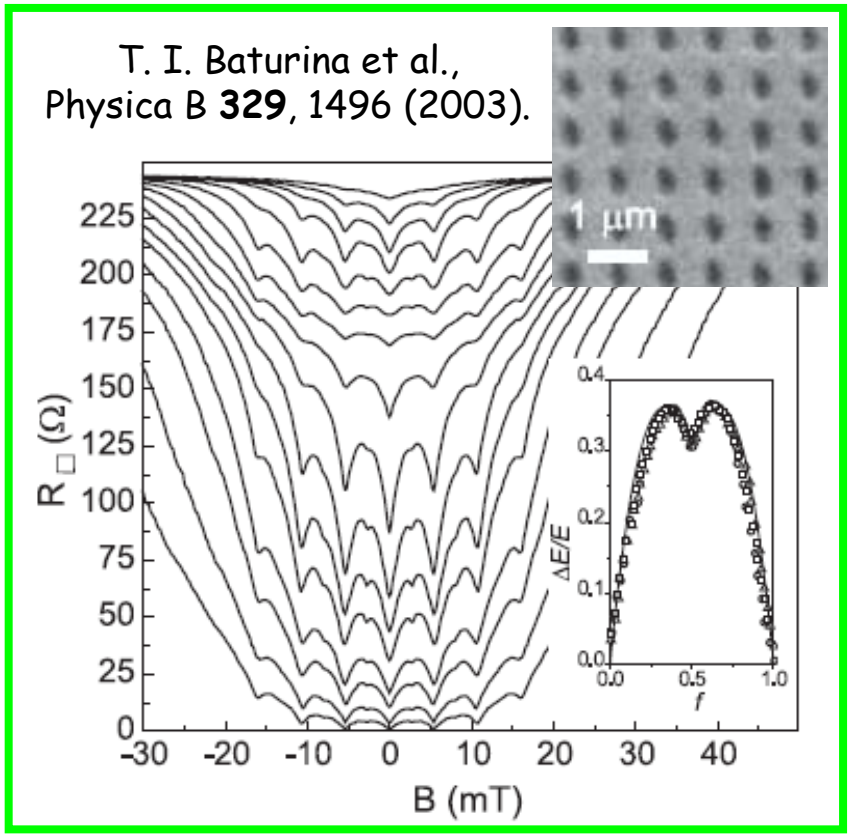

Estimations

$$T_c = 0.56\ \mathrm{K}$$

$$a = 600\ \mathrm{nm} \qquad d = 200\ \mathrm{nm}$$

$$w = 400\ \mathrm{nm}$$

$$\xi_d(0) \approx 56\ \mathrm{nm}$$

$$\xi_d(T) = \xi_d(0)\sqrt{1 - T/T_c}$$

at $T = 0.1\ \mathrm{K}$

$$w/\xi_d(T) \approx 5.9$$

$$\Delta T / T_c > 0.7$$

magnetoresistance

temperature region of the MR oscillations

The MR oscillations in the perforated films and/or superconducting wire networks, were usually found in the close proximity to T_c (if measured in the linear response regime)

with few exceptions

H.Q. Nguyen, S.M. Hollen, M.D. Stewart, Jr., J. Shainline, Aijun Yin, J.M. Xu, and J. M. Valles, Jr., Phys. Rev. Lett. 103, 157001 (2009).

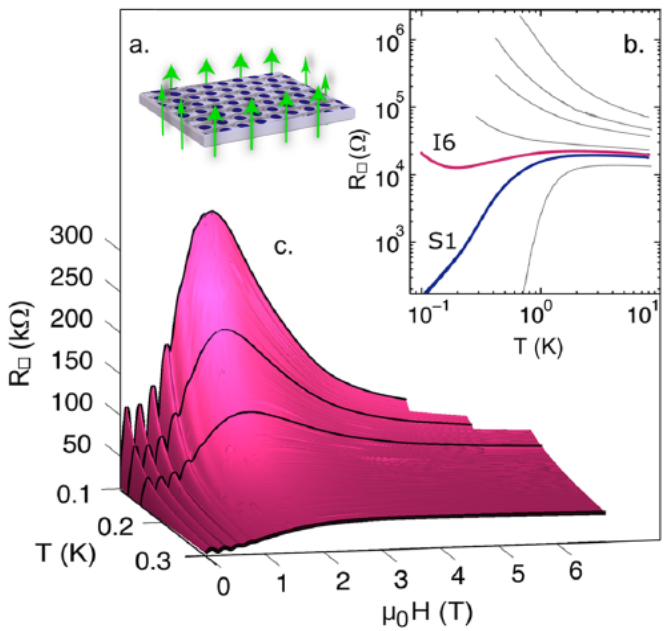

FIG. 1 (color online). (a) SEM image of the nanohoneycomb substrate. The hole center to center spacing and radii are 100 ± 5 and 27 ± 3 nm, respectively. Arrows denote $\vec{H}$. (b) Sheet resistance as a function of temperature, $R_\square(T)$, of NHC films produced through a series of Bi evaporations. The film I6 is the last insulating film and S1 is the first superconducting film in the series. (c) Surface plot of $R_\square(T, H)$ for film I6, which has a normal state sheet resistance of 19.6 kΩ and 1.1 nm Bi thickness. The solid lines are isotherms.

Estimations

$$a = 100 \pm 5 \text{ nm} \qquad d = 54 \pm 6 \text{ nm}$$

$$w \approx 50 \text{ nm}$$

$$\xi_d(0) \approx 10 \text{ nm}$$

$$\xi_d(T) = \xi_d(0)\sqrt{1 - T/T_c}$$

at lowest $T = 0.1$ K

$$T_{osc} \leq 0.7 \text{ K}$$

$$w/\xi_d(T) \approx 5$$

magnetoresistance

temperature region of the MR oscillations

The MR oscillations in the perforated films and/or superconducting wire networks, were usually found in the close proximity to T_c (if measured in the linear response regime)

with few exceptions

This study: arXiv:1011.1592

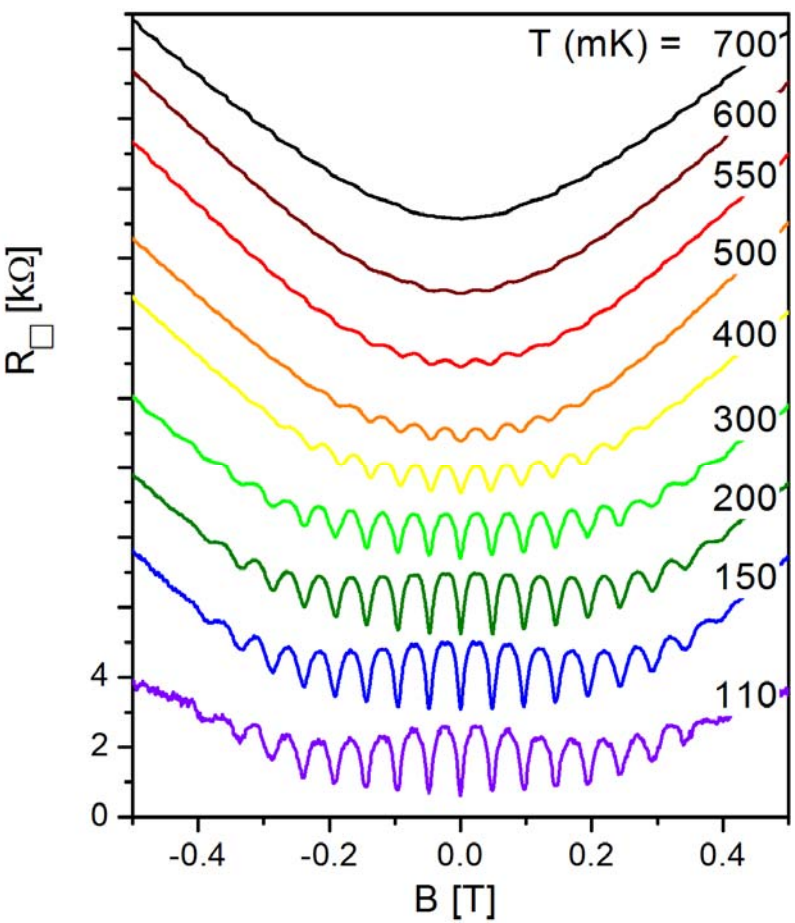

Estimations

$$a = 200\ \text{nm} \qquad d = 120\ \text{nm}$$

$$w \approx 80\ \text{nm}$$

$$\xi_d(0) \approx 9.3\ \text{nm}$$

$$\xi_d(T) = \xi_d(0)\sqrt{1 - T/T_c}$$

$$w/\xi_d(T) \approx 8$$

at lowest $T = 0.1$ K

$$T_{osc} \leq 0.7\ \text{K}$$

magnetoresistance

temperature region of the MR oscillations

The MR oscillations in the perforated films and/or superconducting wire networks, were usually found in the close proximity to T_c (if measured in the linear response regime)

with few exceptions

This raises a question about the parameters that govern manifestations of quantization of the magnetic flux in dissipative characteristics of two-dimensional superconducting wire networks

K.K. Likharev, Rev. Mod. Phys. 51, 101 (1979).

Critical length versus link width

Abricosov vortices in weak links

"Explosion" of core

dissipation due to vortex motion

T close to T_c

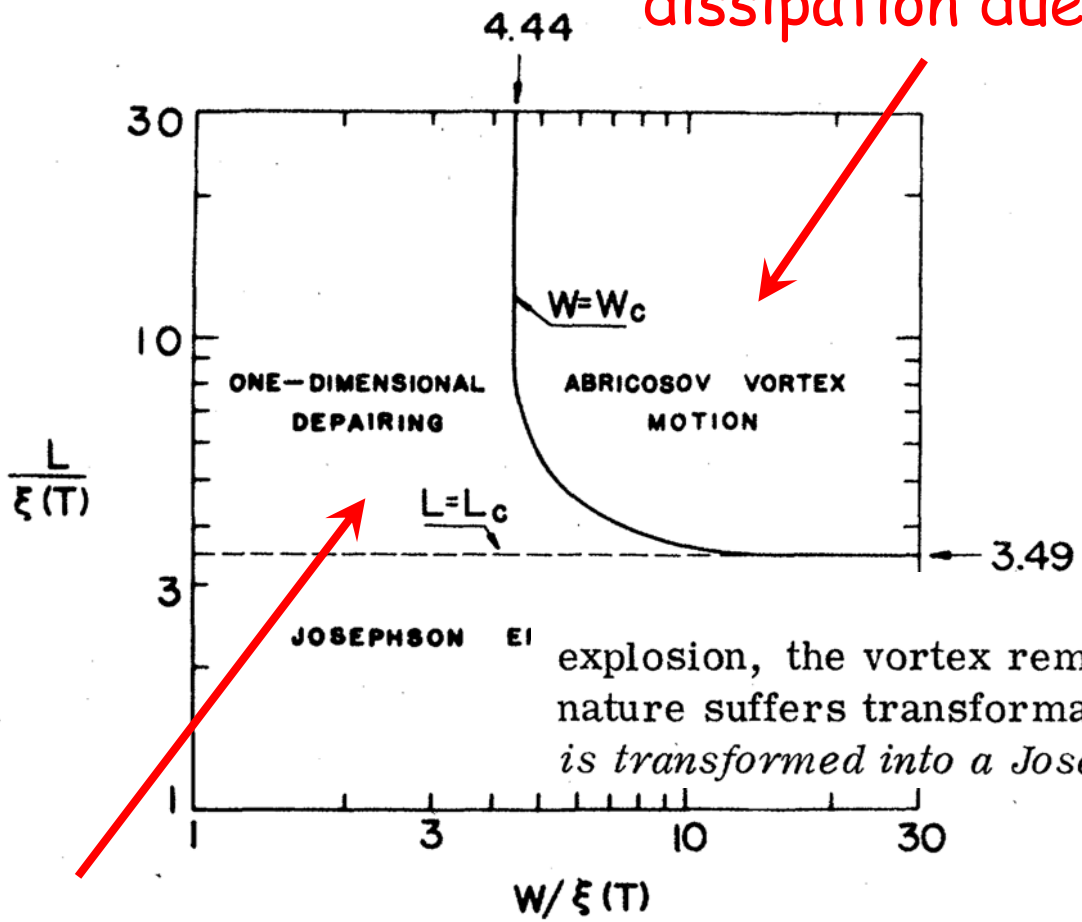

Thus, after core explosion, the vortex remains where it was, but its nature suffers transformation, i.e., an *Abricosov vortex is transformed into a Josephson vortex.*

dissipation due to phase slips

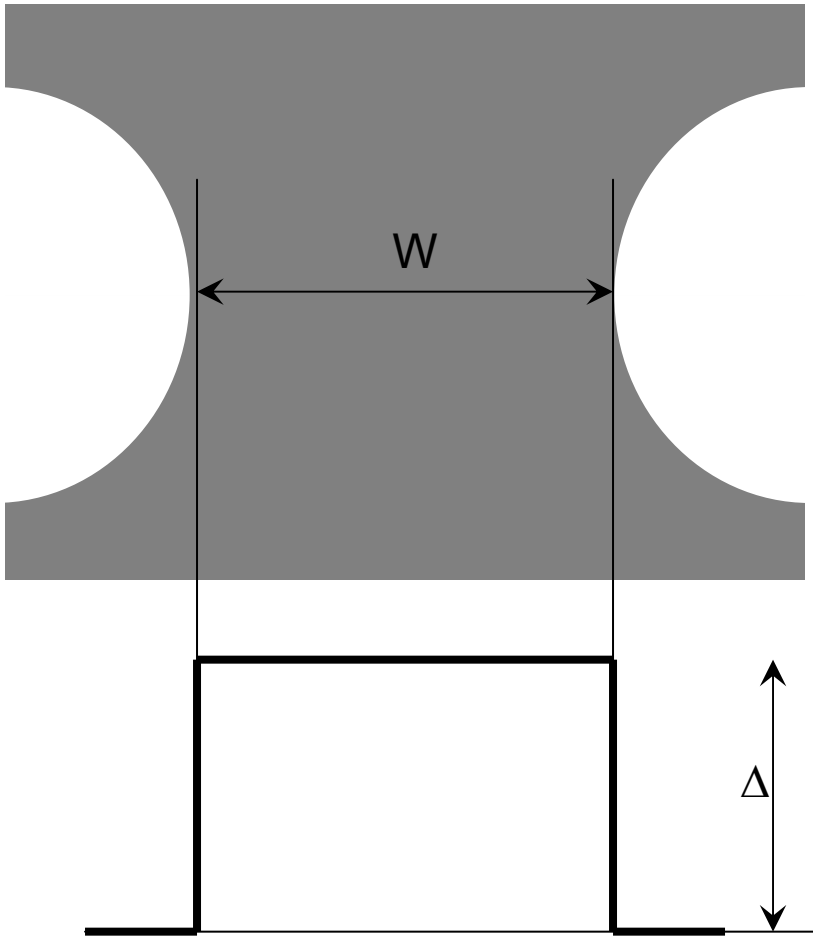

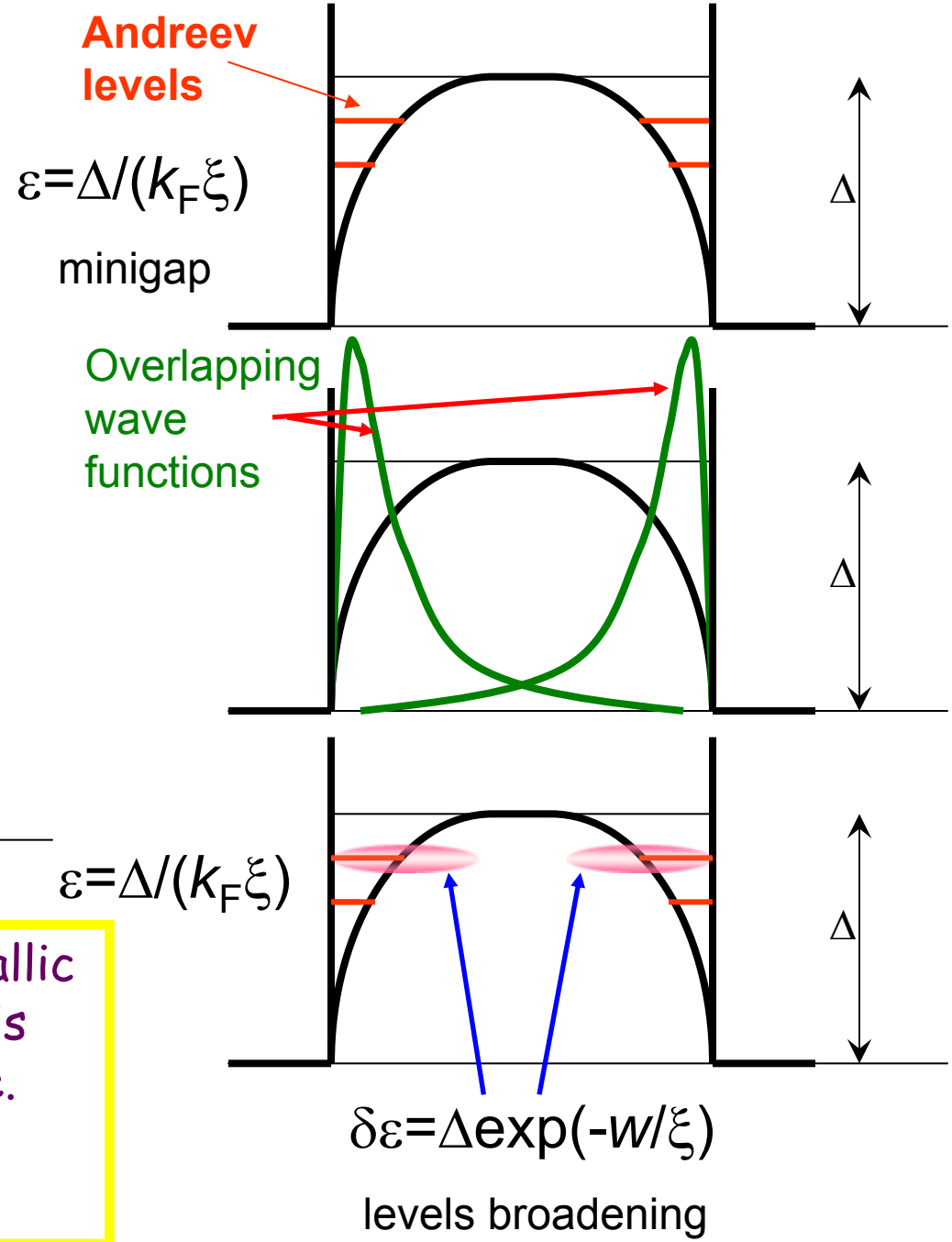

The constriction becomes metallic when broadening of the levels is on the order of the minigap, i.e.

$\delta\varepsilon \sim \varepsilon$ or $w = \xi \ln(k_F \xi)$

next observation…

in order to exhibit oscillations in the magntoresistance,
the SWN should be in a resistive state

Thus the second condition determining the 'range of observability' of the oscillations is that the temperature should be higher than the temperature of the vortex BKT transition in the SWN

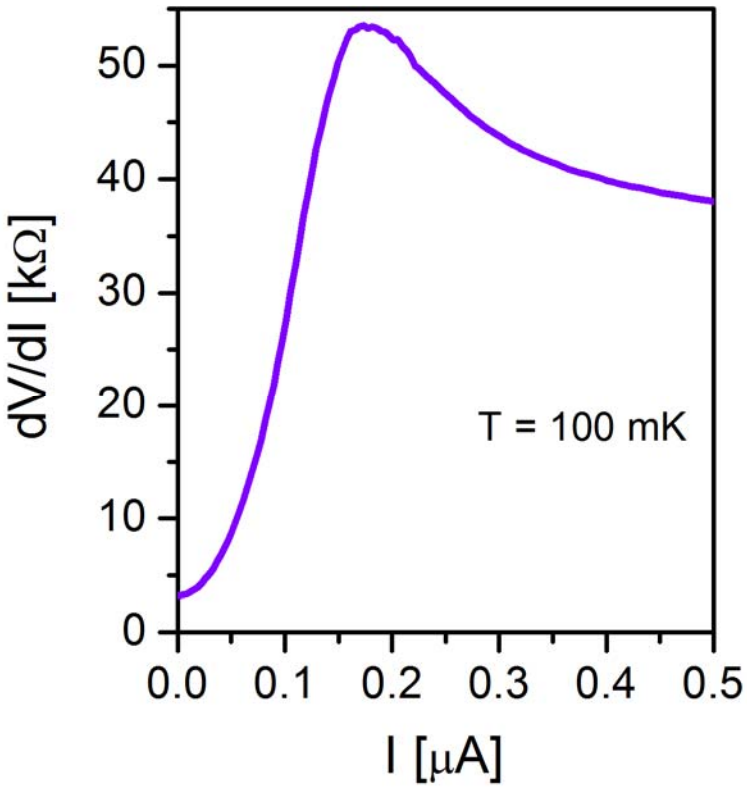

$$I_c = 0.17\,\mu\mathrm{A}$$

$$I_{c(i)} = 0.68\,\mathrm{nA}$$

$$E_\mathrm{J}/k_\mathrm{B} = 0.016\,\mathrm{K}$$

magnetoresistance

pA sample

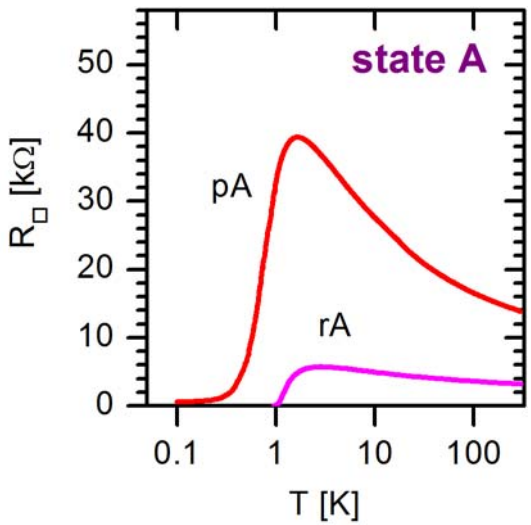

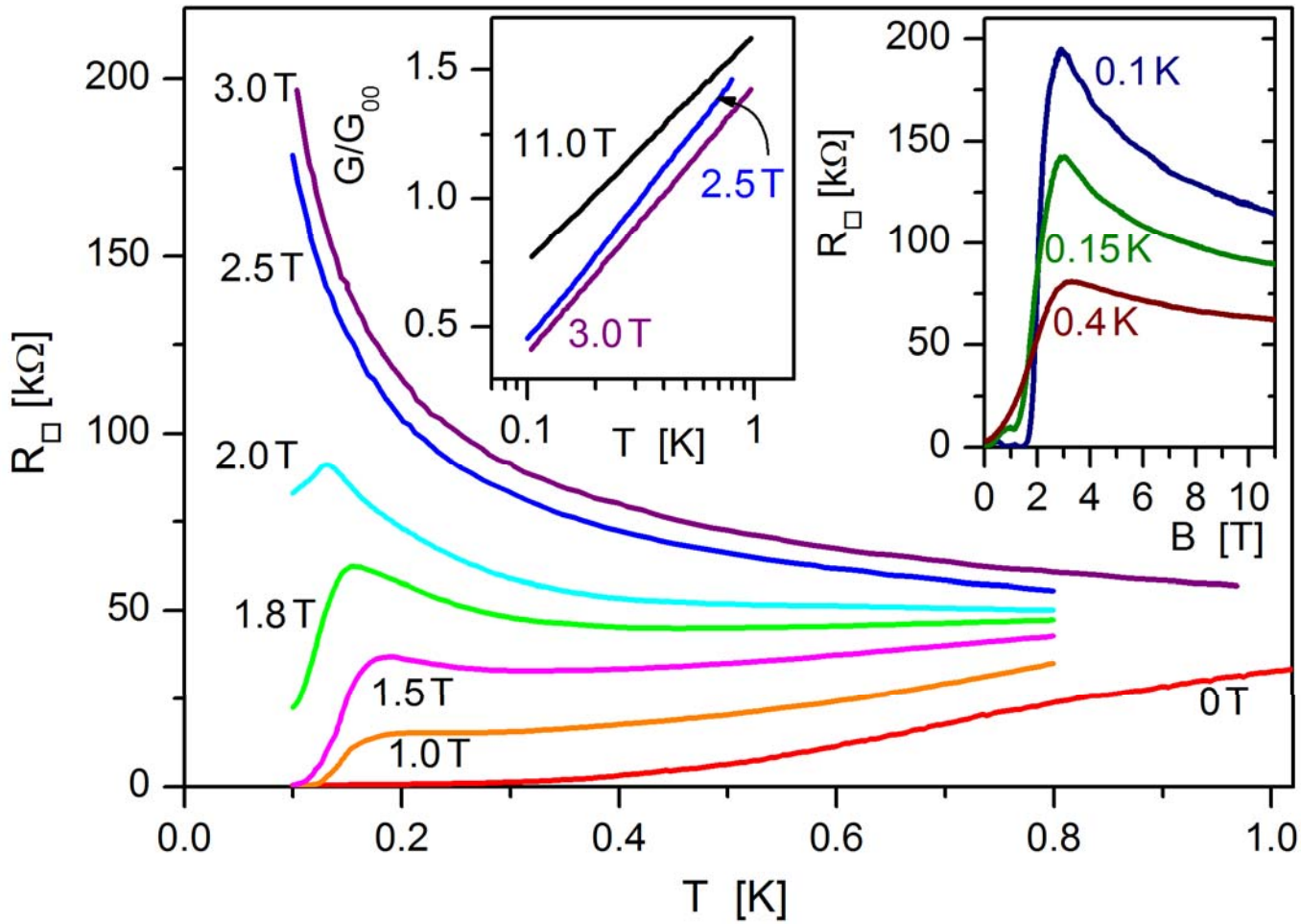

magnetoresistance

pA sample

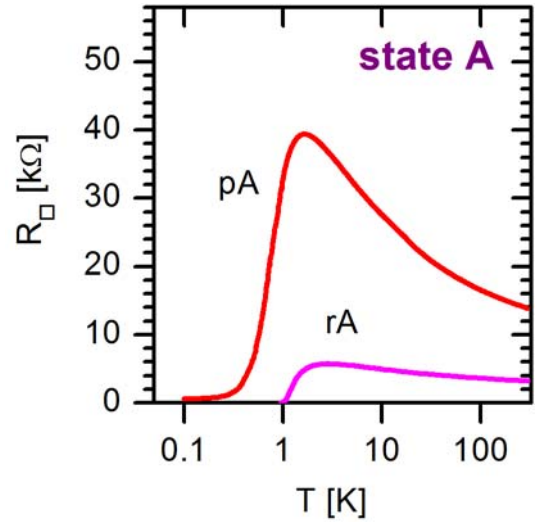

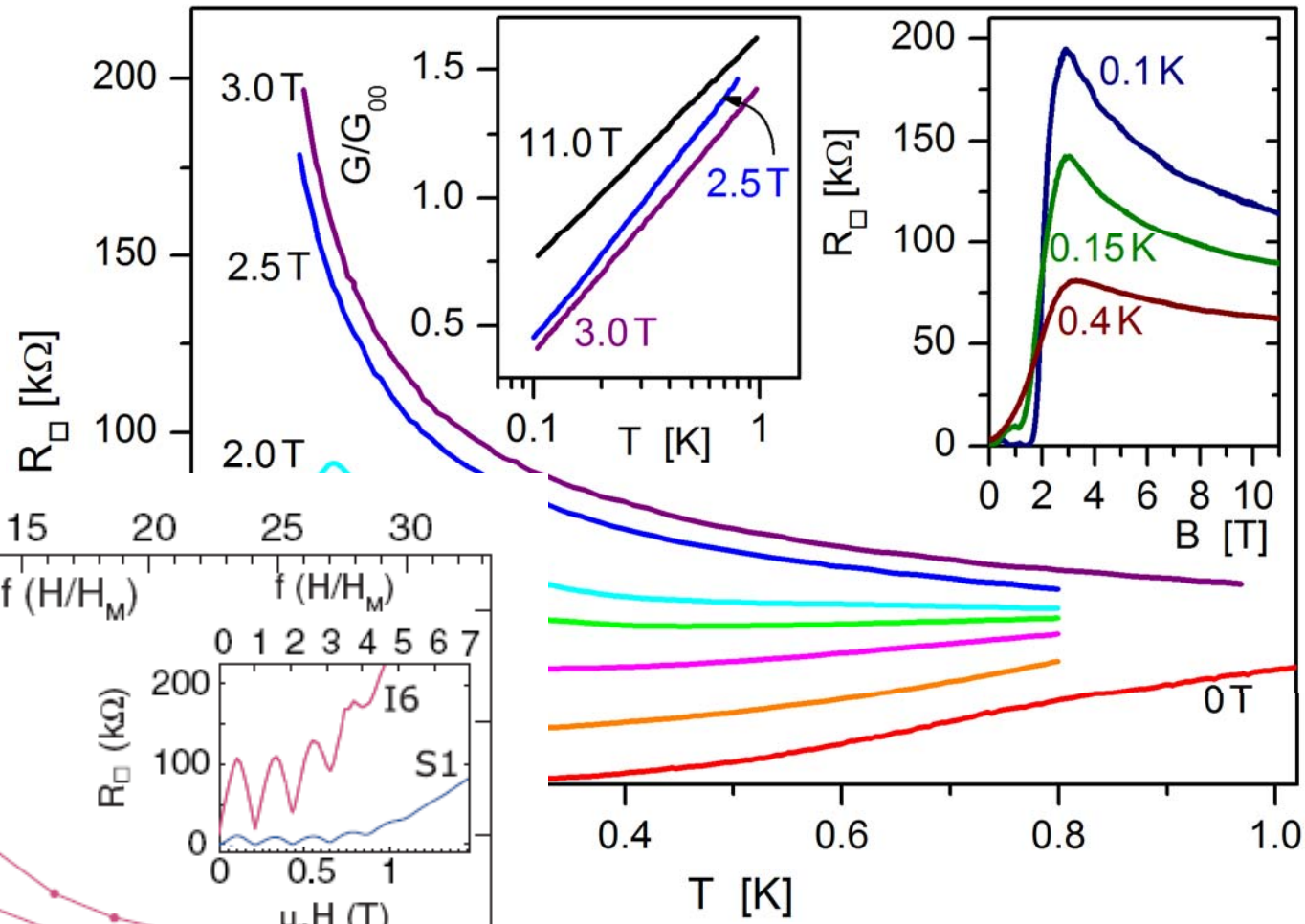

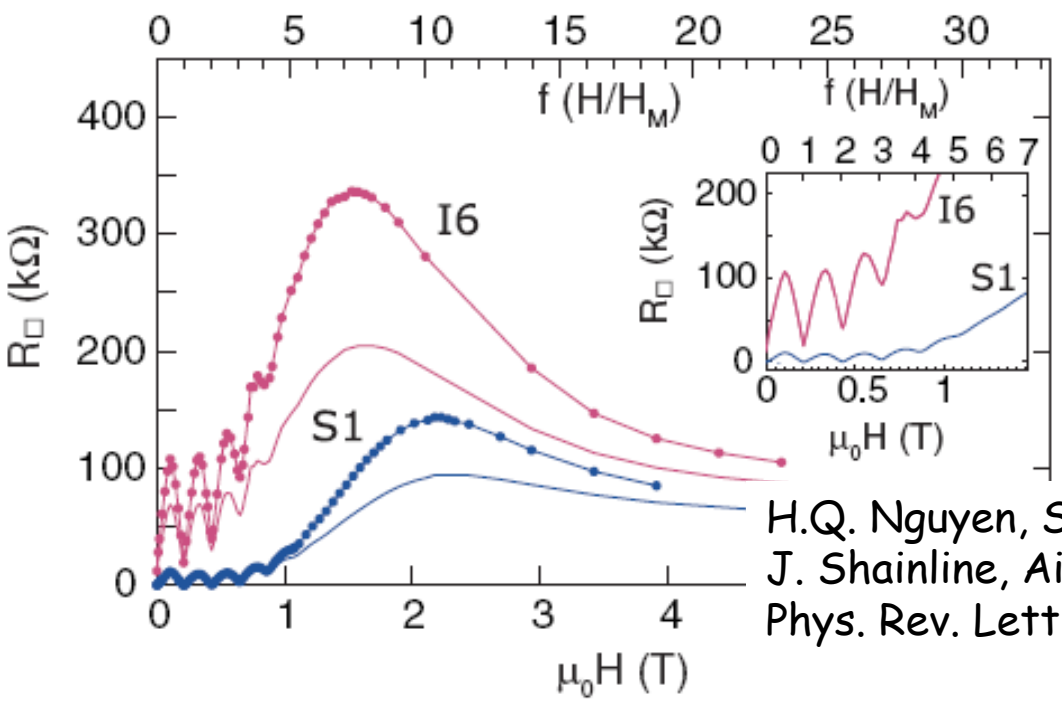

H.Q. Nguyen, S.M. Hollen, M.D. Stewart, Jr., J. Shainline, Aijun Yin, J.M. Xu, and J. M. Valles, Jr., Phys. Rev. Lett. 103, 157001 (2009).

magnetoresistance

pA sample

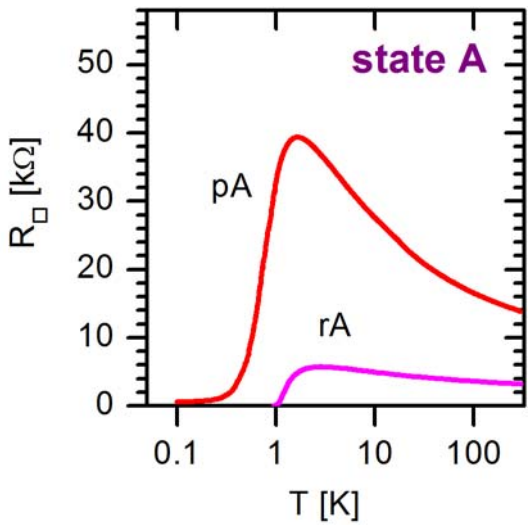

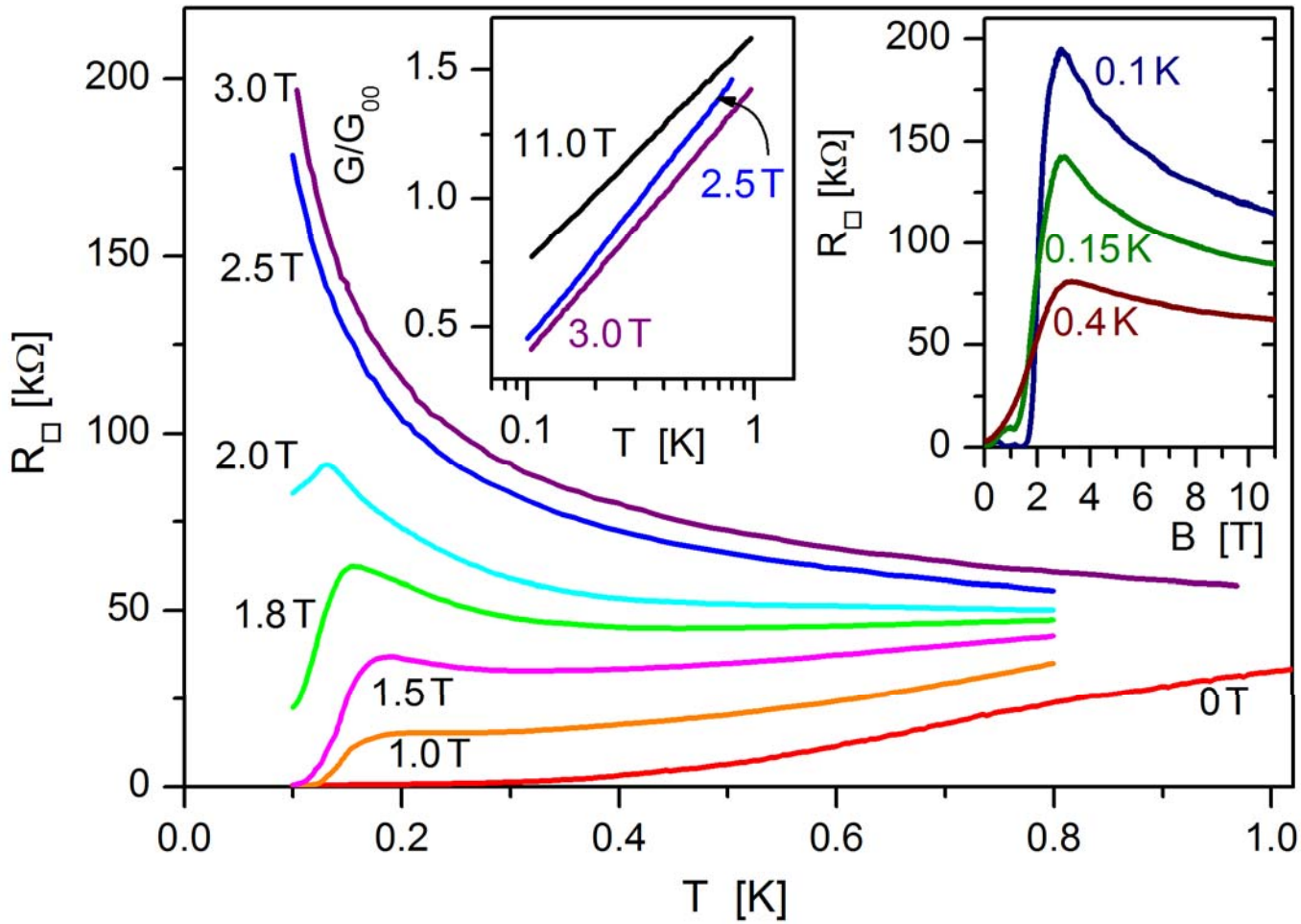

B	A
2.5 T	0.49
3.0 T	0.45
11.0 T	0.38 * 3 = 1.14

$$G = (R_\square)^{-1} = G_0 + G_{00} A \ln(T)$$

$$G_{00} = e^2/(\pi h)$$

magnetoresistance

pA sample

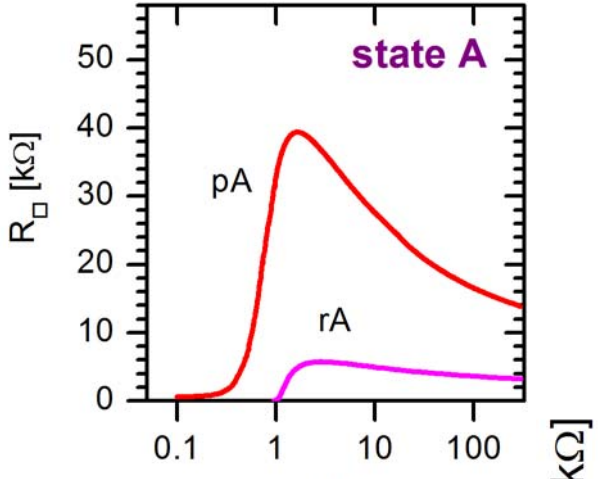

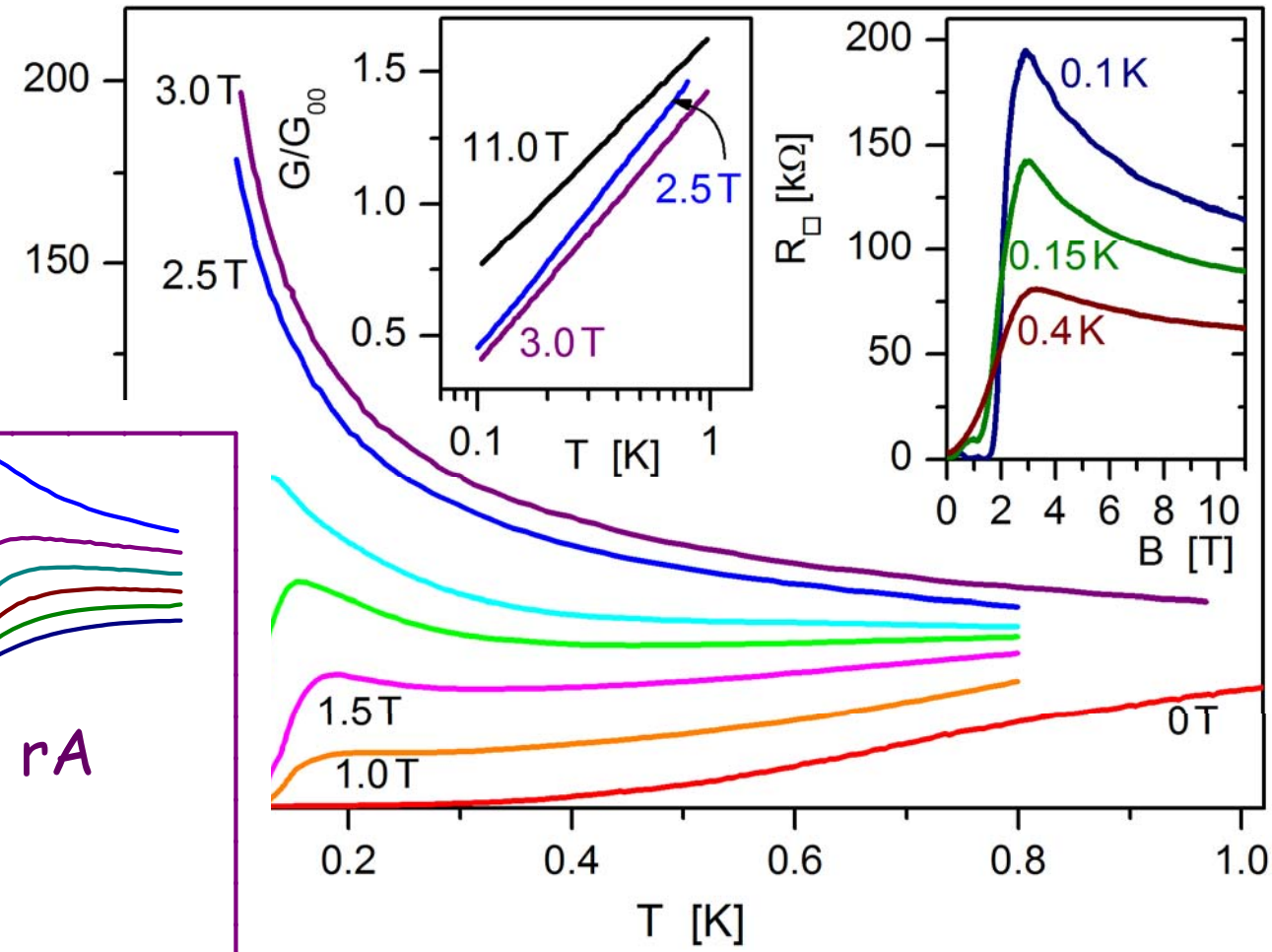

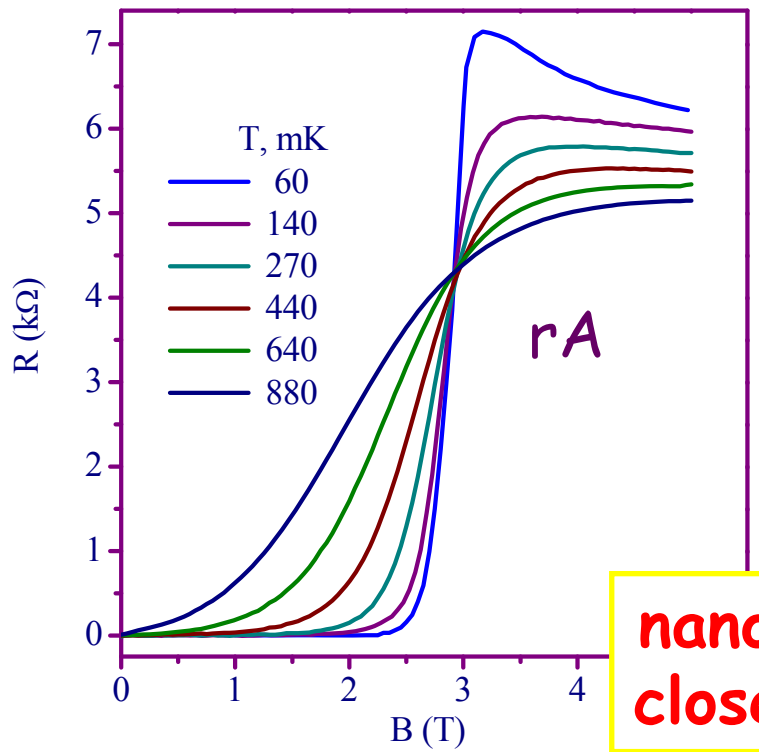

nanopatterning pushes the system closer to the localization threshold

Summary

nanopatterning disordered superconducting films pushes
the superconductor-to-insulator transition to the lower degree
of microscopic disorder opening the route to control the position
of the SIT on the phase diagram

a noticeable increase in the activation energy at the insulating side
of the transition in the perforated samples supports
the notion of the macroscopic origin of the activation barrier

oscillations of the magnetoresistance in a wide temeperature range
due to fractal Josephson effect in the superconducting wire network